VILNIUS UNIVERSITY

AGATA MLYNSKA

THE ROLE OF SYSTEMIC AND LOCAL IMMUNITY IN TUMOR DEVELOPMENT AND RESPONSE TO TREATMENT

Doctoral dissertation
Physical sciences, biochemistry (04 P)

Vilnius, 2018

This doctoral dissertation was prepared in Vilnius University, National Cancer Institute, and Swiss Federal Institute of Technology in Lausanne in 2013-2018.

Scientific supervisor - Dr. Vita Pašukonienė (National Cancer Institute, Physical sciences, Biochemistry – 04P).

VILNIAUS UNIVERSITETAS

AGATA MLYNSKA

SISTEMINIO IR VIETINIO IMUNITETO REIKŠMĖ VĖŽIO VYSTYMUISI IR ATSAKUI Į GYDYMĄ

Daktaro disertacija

Fiziniai mokslai, biochemija (04 P)

Vilnius, 2018

Daktaro disertacija rengta 2013-2018 m. Vilniaus universitete, Nacionaliniame vėžio institute bei Šveicarijos federaliniame tyrimų institute Lozanoje.

Mokslinė vadovė - dr. Vita Pašukonienė (Nacionalinis vėžio institutas, fiziniai mokslai, biochemija – 04P).

Table of Contents

ABBREVIATIONS

ACT – adoptive cell therapy
ADCC – antibody-dependent cellular cytotoxicity
APC – antigen presenting cell
AUC – area under the curve
BRAF – gene coding for B-Raf oncogene
Breg – regulatory B lymphocyte
CAF – cancer-associated fibroblast
CAR – chimeric antigen receptor
CC – cancer cell
CFSE – carboxyfluorescein succinimidyl ester
CIN – chromosome instability
Cis - cisplatin
CM - conditioned medium
CP – anti-CTLA-4 + anti-PD-1 combination treatment
CSC – cancer stem cell
CTL – cytotoxic T lymphocyte
CTLA-4 – cytotoxic T lymphocyte antigen 4
CUI – clinical utility index
DC – dendritic cell
EC – endothelial cell
ECM – extracellular matrix
EMT – epithelial-mesenchymal transition
FBS – fetal bovine serum
FDA – Food and Drug Administration
FDR – false discovery rate
GMP – good manufacturing practice
H&E – hematoxylin and eosin staining
HPV – human papillomavirus
HR – hazard ratio
iBIP2 – inducible BRAF Ink/Arf Pten driven mouse model of melanoma
IC_{50} – half maximal inhibitory concentration
ICD – immunogenic cell death
IgG – immunoglobulin G
LPS - lipopolysaccharide
MAPK - mitogen-activated protein kinase
MDR – multidrug resistance
MDSC – myeloid-derived suppressor cell
MEK – mitogen-activated protein kinase kinase

MHC – major histocompatibility complex
MMR – mismatch repair
MSC – mesenchymal stem cell
NK – natural killer
NR – not reached
OC – ovarian cancer
OS – overall survival
PBMC – peripheral blood mononuclear cells
PD-1 – programmed cell death protein 1
PMA – phorbol 12-myristate 13-acetate
qPCR – quantitative polymerase chain reaction
RFS – recurrence-free survival
ROC – receiver operating characteristic
SE – sensitivity
SP – specificity
TAM – tumor-associated macrophage
TCGA – The Cancer Genome Atlas
TCR – T lymphocyte receptor
TF – transcription factor
Th – T helper lymphocyte
TIL – tumor infiltrating lymphocyte
TLR – Toll-like receptor
TLS – tertiary lymphoid structure
TME – tumor microenvironment
TP – total protein
Treg – regulatory T lymphocyte

INTRODUCTION

MOTIVATION

The tumor microenvironment is shaped by a variety of a heterotypic and heterogeneous collection of cell types. Their interactions and signaling contribute to the processes of tumor development, invasion, and response to treatment [1,2]. The acquired mutations and phenotypic plasticity create a pool of cells of various differentiation and stemness levels [3,4], which able to recruit and reprogram normal stromal cells (fibroblasts, endothelial cells, pericytes, immune system cells) to serve the needs of the tumor [5].

Mutational load and emergence of neoantigens make cancer cells recognizable by the immune system [6]. The cancer-immunity cycle summarizes the pivotal steps that are essential for the generation of successful specific antitumor response [7]. However, cancer employs various strategies of escape from the surveillance by the immune system [8–10]. Depending on the evasion strategy, several immune phenotypes are defined [7,11]. The immune contexture, determined by the density, composition, and functional state of the immune infiltrate in the tumor, is associated with disease prognosis and can predict a treatment response [12–14]. More, based on the immune phenotype, tumors can be targeted with several types of immune-based therapies that are currently under preclinical or clinical evaluation [7,15].

Over the past decades, the tumor immunology and immunotherapy have revolutionized the clinical oncology. However, there are still challenges to overcome in understanding and targeting the immune elements of the tumor. First, the distinct genomic and cellular landscapes shaping the tumor heterogeneity impede the efficacy of conventional and immune therapies. Second, the lack of clinically significant biomarkers for patient stratification weakens the ratio of successful response to treatment. Third, multiple active targets as well as resistance development urge for combinatorial trials and improving the treatment efficacy.

Addressing these challenges on the molecular, cellular, tissue and organism level creates opportunities for improved cancer management. In this study, we attempted to provide the new insights into the contribution of immune tumor microenvironment to the processes of tumor development and response to treatment, as well as propose the new predictive biomarkers.

AIM

The overall aim of this study was the elucidation of local and systemic crosstalk between cancer and immune cells for a better understanding of the immune system role in tumor development and response to treatment.

OBJECTIVES

1. Evaluate the effect of cancer cell lysate on dendritic cell maturation and immunostimulatory capacity.
2. Determine the macrophage polarization ability in colon cancer cell lines with varying levels of stemness traits.
3. Study the bidirectional interplay between macrophages and ovarian cancer cell lines of varying chemotherapy resistance level.
4. Characterize the formation of immune tumor microenvironment during melanoma development in the iBIP2 mouse model.
5. Address the mechanisms of response and resistance to checkpoint blockade with anti-CTLA-4 and anti-PD-1 in the iBIP2 mouse model.
6. Examine the immune phenotype of ovarian tumors and select the potential systemic markers reflecting their immune infiltration.
7. Evaluate the potential of systemic cytokines as predictive markers of ovarian cancer recurrence.

NOVELTY

This study is based on an original research and encompasses several levels of crosstalk between immunity and cancer.

We approached the interactions between cancer cells and monocyte-derived cells of tumor microenvironment: dendritic cells and macrophages. Our findings emphasize the potential immunosuppressive impact of selected cancer cells on dendritic cells, resulting in the emergence of their tolerogenic properties. This effect is often overlooked in studies describing the design of the therapeutic dendritic cell-based cancer vaccines.

Also, studies comparing the macrophage polarizing potential of cells with different features are scarce. Here, for the first time, we demonstrate how stemness potential and drug resistance status of cancer cells influence their ability to induce macrophage polarization. More, we also describe the bidirectional interplay between cancer cells and macrophages in the presence of a chemotherapeutic agent cisplatin. By investigating the interplay of cancer cell and macrophages against the background of stemness and drug resistance, we provided the primary evidence for collaboration of both cell types towards developing the tumor-promoting microenvironment.

The iBIP2 model is a newly generated mouse model of melanoma. So far, this model was mostly serving for testing MAPK pathway inhibitors or single-agent checkpoint blockade. We were the first ones to demonstrate the dynamics of the immune tumor microenvironment development and conduct the preclinical trials using double checkpoint inhibition with anti-CTLA-4 and anti-PD-1 in this model. Also, we introduced a ratio between immunosuppressive and antitumor myeloid cells as a novel biomarker of response to double checkpoint blockade as well as a co-target for enhancing the effect of T lymphocyte-based immunotherapies.

Cancer-immunity cycle and immune tumor phenotypes are relatively new concepts, therefore, there are still very few published studies employing this classification. We were the first ones to subtype ovarian tumors based on their immune-related gene expression as well as assign the phenotype-specific chemokine expression pattern. We also proposed two novel circulating serum biomarker combinations: CXCL9+CXCL10 for distinguishing immune-infiltrated tumors, and CCL4+CCL20+CXCL1 for distinguishing recurrence-

prone patients. These markers could prove useful in the stratification of patients for clinical trials, as well as in making second-line treatment decisions.

Together, our novel findings substantiate the relevance of the immune system in tumor development and response to therapy and suggest novel biomarkers and targets for cancer immunotherapy.

HYPOTHESES

1. Maturation with cancer cell lysate induces tolerogenic properties in dendritic cells.
2. The colon cancer cells ability to polarize macrophages is associated with their stemness properties.
3. Bidirectional interplay exists between macrophages and ovarian cancer cells of different chemotherapy resistance status.
4. The melanoma tumor growth in the iBIP2 mouse model is accompanied by the development of immunosuppressive microenvironment.
5. The response to checkpoint blockade in the iBIP2 mouse model of melanoma is reflected by the level of the tumor-infiltrating immunosuppressive myeloid cells.
6. Specific tumor and serum chemokine expression patterns reflect the immune infiltration in ovarian tumors.
7. Preoperative level of circulating chemokines can predict the recurrence of ovarian cancer.

BACKGROUND AND STATE-OF-THE-ART

1.1. The hallmarks of cancer

The term 'cancer' covers a plethora of heterogeneous neoplastic diseases, characterized with the dysregulation of cell's molecular machinery and manifestation of the outgrowing mass of literally any tissue-specific cells. For decades, research has focused on the cancer cell itself, trying to understand the transformations leading to uncontrolled cell division and formation of the tumor mass. In the early seventies, first tumor suppressor genes and oncogenes were discovered, beginning the era of cancer research. Today, accumulated fundamental knowledge about cancer etiology and development advances the diagnostics and treatment of tumors, which are still one of the leading causes of mortality worldwide [16].

The hallmarks of cancer (Figure 1) comprise ten biological features acquired during the tumor development, as summarized by Hanahan and Weinberg in 2011. **Genome instability and mutations** create the genetic diversity of cancer cell clones. Increased expression of growth factors and their receptors **sustain proliferative signaling**. Disrupted tumor suppressors signaling pathways allow for **evading growth suppressors**. Maintaining length of telomeres and quiescence of cell senescence **enable replicative immortality**. Antiapoptotic oncogenes and loss of proapoptotic regulators help to **resist cell death**. Upregulation of factors responsible for blood vessel formation **induces chaotic tumor angiogenesis**. **Tumor-promoting inflammation** mirrors the inflammatory conditions arising in non-neoplastic tissues. Various immune evasion mechanisms help tumors to **avoid destruction by the antitumor immune response.** Hypoxia and aerobic glycolysis **deregulate cellular energetics**. Loss of cell junctions and extracellular matrix remodeling **activate invasion and metastasis** [1].

Particular genetic lesions may result in activation of several hallmarks, e.g. loss of function of the p53 tumor suppressor is simultaneously an example of genomic instability as well as an inducer of both angiogenesis and resistance

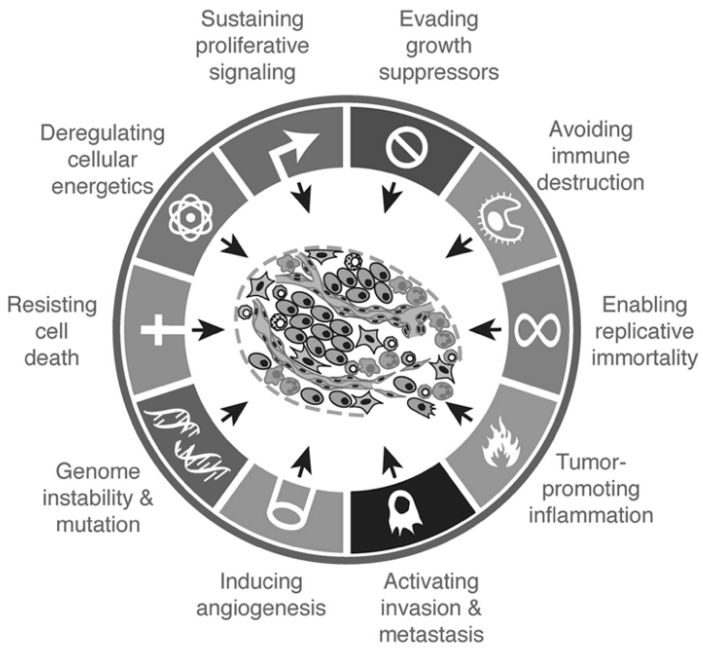

Figure 1. The hallmarks of cancer. Accumulating findings of cancer research field resulted in coining the concept of „hallmarks of cancer" by Hanahan and Weinberg. These hallmarks encompass biological characteristics acquired during the tumor initiation and development. Adapted from [1].

to apoptosis [17]. Each hallmark presents a possibility for targeted treatment. However, as tumors are usually distinguished by the presence of all or at least the majority of the above hallmarks, and their order of appearance during the tumor development is not fixed, the effective eradication of tumors remains a challenge, recently approached by combination cancer therapy [18,19].

1.2. Cancer heterogeneity

The complexity of tumors, often named cancer heterogeneity, is an important clinical determinant of highly variable response to treatment. Molecular profiling of tumors revealed that cancer heterogeneity is usually defined by the intra-tumoral diversity of cancer cell clones (genetic level), as well as the variety of non-cancerous cells in tumors stroma (cellular level). The genetic and cellular landscapes of tumors are dynamic and may change during the response to therapy, tumor recurrence, and metastasis. A rapid increase in the global understanding of cancer genome and tumor microenvironment is currently refining the molecular classification of different cancers. However,

translating this knowledge into clinical practice and fully executing the idea of precision medicine is still a challenge. We will next discuss the molecular and cellular determinants of cancer heterogeneity.

1.2.1. Clonal evolution model

Molecular tumor heterogeneity refers to the existence of subpopulations of genetically and phenotypically distinct cancer cells within a single tumor. Although the early model of clonal evolution in cancer development was first proposed in 1976 [20], the primary evidence for the presence of multiple sub-clones was provided in the late nineties by the observation of discrete patterns of copy number alterations and chromosomal rearrangements [21]. The contemporary model of clonal evolution encompasses the concept of 'driver' and 'passenger' mutations. The driver mutations are central to the originating of cancerous lineage. The passenger mutations might be neutral or deleterious, but they result in budding of the lateral cancerous clones. Branch models reflecting the mutational landscape evolution of individual patients are now translated into prospective clinical studies [22–24].

1.2.2. Cancer stem cell model

The cancer stem cell (CSC) model provides another explanation for the phenotypical and functional heterogeneity of cancer cells in tumors. This theory, conceived four decades ago, states that the growth of a solid tumor is similar to a renewal of healthy tissues, and is driven by the small number of cells with features similar to those of stem cells: self-renewal by asymmetric division, long-term clonal growth, plasticity, and low level of differentiation. Altogether, molecular programs that govern and maintain the stem cell state in CSCs are referred to as "stemness" [3,28,29]. There is an inconsistency of opinions on the origin of CSC *per se*. However, many authors agree that stemness can also be a transient state acquired by cancer cells and affected by environmental factors. By applying strategies typically exploited by stem cells, cancer cells may employ some aspects of stemness to induce growth and metastasis [27]. CSCs

are often characterized by the dependence on typical stem cell signaling cascades - Notch, Wnt, Hedgehog - and the upregulation of key pluripotency inducing transcription factors Oct3/4 (POU5F1), Sox2, Nanog [3,28–30]. Recent studies have confirmed that many tumors harbor stem cells in dedicated niches [31,32] and provided the rationale for targeting CSCs by inhibition of key signaling pathways, ablation of CSCs, or epigenetic therapy [33].

1.2.3. Epithelial-mesenchymal transition as a link between two models

Epithelial-mesenchymal transition (EMT) is a process first studied in embryonic morphogenesis. Its activation induces profound changes in cell-cell junctions, cytoskeletal composition, cellular interactions with ECM, and cell polarity. These tissue remodeling features were also found to be characteristic to wound healing, tissue fibrosis, or cancer, and thus highlighted the role of EMT in the above processes. In cancer, EMT plays a crucial role in cancer cell invasion and metastasis [34]. EMT can be triggered by the intrinsic oncogenic activation or various microenvironmental stimuli [35]. In response to these impulses, EMT regulators transform the cancer cells from epithelial-like to mesenchymal-like, simultaneously inducing the expression of specific markers (Figure 2).

The level of activation of the EMT program determines its effect. During weak activation, multicellular migration predominates. The migration of individual cells requires strong activation of EMT. The intermediate EMT activation level is shown to induce the tumor-initiating ability of carcinoma cells [34,36,37]. The link between EMT and tumor initiation, as well as common pathways shared with stem cells (Notch, Wnt-β-catenin), provide an evidence for the emergence of transient EMT-induced plastic cancer stem cells in various tumors, although EMT is not necessary to sustain the CSC phenotype and is not coupled to stemness [33,38,39].

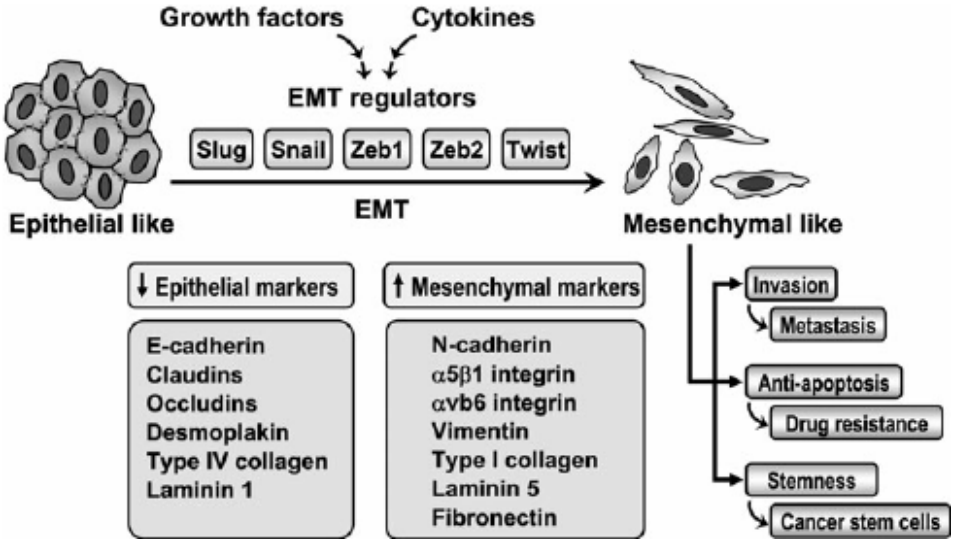

Figure 2. An overview of epithelial-mesenchymal transition. The EMT regulators transform the epithelial-like cancer cells into mesenchymal-like cells, which acquire the set of specific markers. Adapted from [35].

EMT is proposed as a component that merges the clonal evolution (non-CSC based) and CSC models into a phenotypic plasticity model (Figure 3).

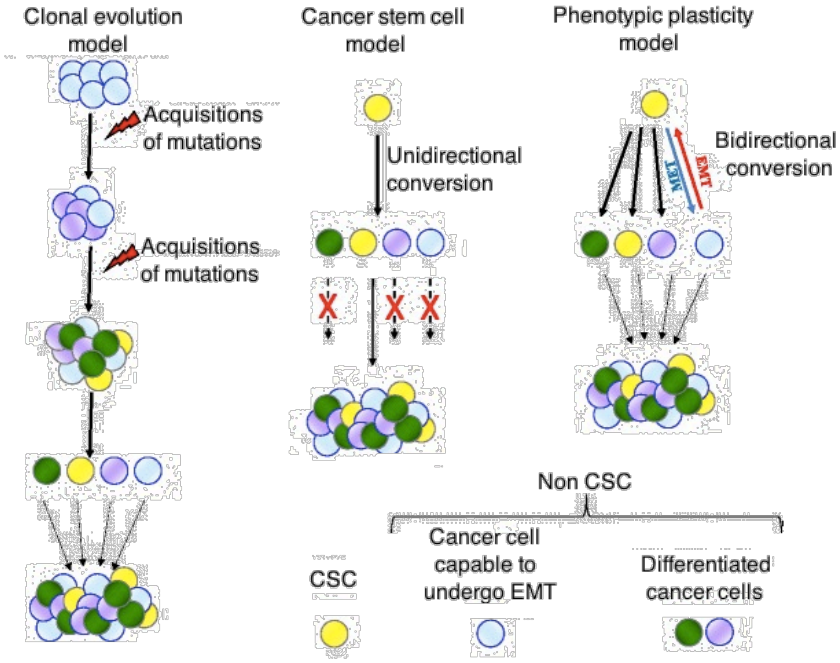

Figure 3. Models of tumor heterogeneity. Clonal evolution model suggests that tumor heterogeneity is generated by the serial acquisition of mutations, and all cells are capable of renewal and tumorigenesis. Cancer stem cell (CSC) model implies the existence of only a small subset of cancer-sustaining cells in the tumor. Phenotype plasticity model posits that irreversibly differentiated cells can be converted back to an undifferentiated state given the appropriate stimulus. Adapted from [4].

The phenotypic plasticity model implies that the irreversibly differentiated cells can be converted back to the undifferentiated state or stem-like state given the appropriate stimulus. This dynamic bidirectional conversion between CSC and non-CSC can result in tumor heterogeneity [3,4,40].

1.3. Tumor microenvironment

Tumor microenvironment (TME) is composed of a heterotypic and heterogeneous collection of cell and sub-cell types, including (but not restricted to) the mutated cancer cells, which, through their various interactions, functionally manifest the growth, progression, and dissemination of malignant tumors [1,2]. Both the parenchyma and stroma of tumors contain distinct cell types, creating a unique cellular landscape of individual tumors. Notably, the tumor stroma can make up to as much as 90% of the tumor mass. Apart of the pre-existence of stromal cell types in the invaded tissue, cancer cells can also recruit all range of cells and convert them to the executors of tumor-promoting functions [5]. The crosstalk between genetically altered carcinoma cells and genetically stable stromal cells also manifests in cancer hallmarks [2], as seen in the example of the CSC interplay with other cell types in TME in Figure 4.

We will next discuss the cell types within TME, as well as supporting extracellular matrix, and relevant signaling networks.

1.3.1. Cancer-associated fibroblasts

CAFs are functionally and morphologically distinct from normal fibroblasts and likely arise via the reprogramming of healthy fibroblasts or the recruitment of bone marrow-derived cells. Cancer-induced transformation of normal fibroblasts deprives them of tumor-suppressing function. Their pro-tumorigenic phenotype reminds of wound-activated fibroblasts with tissue-repair functions. By secreting growth factors (EGF, HGF) and promoting EMT through TGFβ secretion, they help to sustain the cancer cell proliferation. CAFs also secrete pro-angiogenic factors (VEGF, FGF, IL-8), immunosuppressive

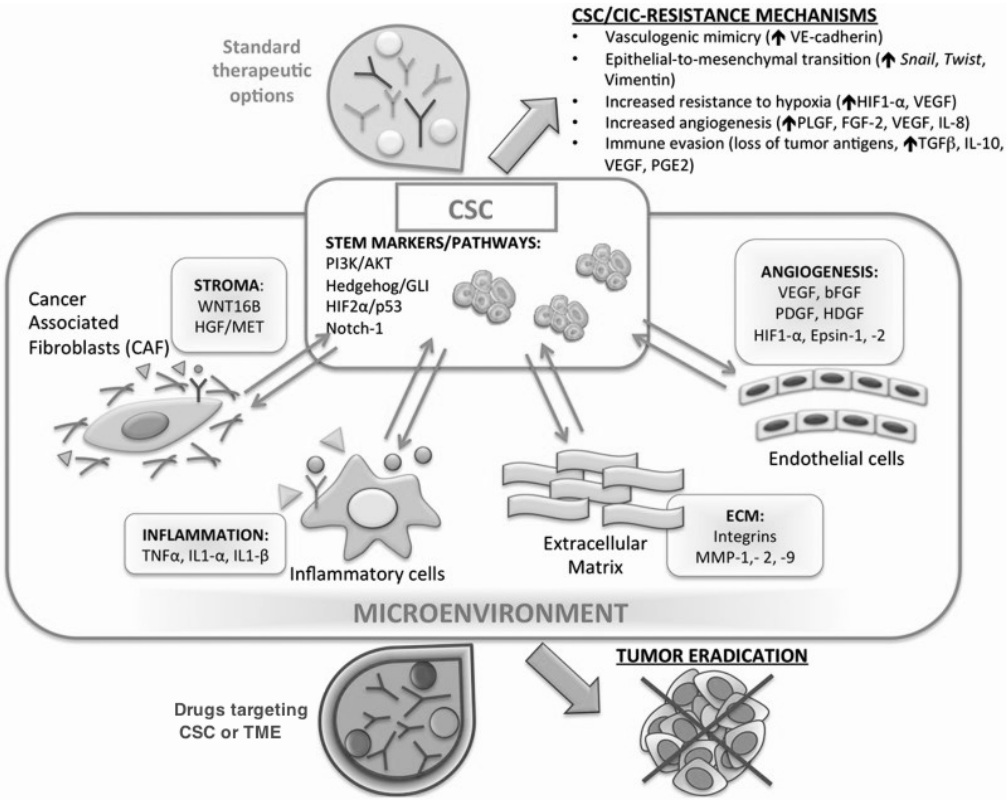

Figure 4. Interaction of cancer stem cells (CSC) and the surrounding microenvironment. CSCs interaction with the surrounding tumor microenvironment (TME), mediated by stem cell- and self-renewal-associated pathways, contribute to the development of cancer hallmarks. Conventional therapies mainly target bulk tumor cells, but not CSCs, that are responsible for disease recurrence by activating resistance mechanisms. Targeting both TME and CSCs would potentiate the tumor eradication without disease recurrence. Adapted from [41].

factors (TGFβ), myeloid-attracting chemokines, as well as matrix-remodeling enzymes, which promote tumor invasion and metastasis. More, they are often found at the invasive margin of a tumor. CAFs play an important role in regulating tumor energetics, as they mimic the tumor metabolism. They promote the aerobic glycolysis and sustain the glucose/lactate balance in the tumor. Also, CAFs contribute to tumor chemoresistance by creating physical barriers and activating epigenetic plasticity in neighboring cells [2,42,43].

1.3.2. Endothelial cells and pericytes

Tumors cannot grow or metastasize without developing the vasculature network. Evidence shows that angiogenesis is induced unusually early during

the tumor development [44]. Angiogenesis, triggered by hypoxia and the balance of pro- and anti-angiogenic factors, is the process of sprouting, cell division, and assembly of endothelial cells (ECs) from pre-existing vessels. Pericytes, representing a specialized mesenchymal cell type, are commonly located on the microvessel walls, within the basement membrane. Oppositely to healthy vasculature, ECs usually do not form regular monolayers, and pericyte coverage is loose and incomplete, all leading to vessel leakiness. An overexpression of VEGF and hypoxic regions around tumor microvessels promote invasion and metastasis. The chaotic blood flow may result in lowering therapeutic effectiveness and allowing resistant clones expansion [1,45,46].

Tumor-associated ECs were shown to have a distinctive gene expression profile and cell surface markers in comparison to normal tumor ECs. More, ECs are also forming tumor-associated lymphatic vessels, that are usually collapsed and non-functional at the tumor core, whereas at the periphery they serve as channels for the seeding of metastases [47,48].

1.3.3. Dendritic cells

Dendritic cells (DCs) originate from common myeloid progenitor, which can further differentiate into monocytes and give rise to monocytic DCs under inflammatory conditions, or it becomes a common dendritic cell progenitor. The conventional type 1 DCs, conventional type 2 DCs and plasmacytoid DCs arise from the common dendritic cell progenitor, during the multistep processes that include the expression of critical transcription factors (TFs) [49].

In cancer, conventional and monocyte-derived DCs foster tumor control, in contrast to other myeloid cell types that often promote cancer. DCs are the major antigen presenting cells (APCs) initiating the antitumor immune response by priming naïve T cells in the lymph nodes. High levels of DCs infiltration in tumor lesions are usually associated with prolonged survival. DCs are abundant in well-differentiated and less invasive tumors. The presence of tertiary lymphoid structures (TLS) was confirmed in tumors vastly infiltrated with DCs [50]. TLS are lymph node-like structures that include a T cell zone with mature

DCs, a germinal center with follicular DCs and proliferating B cells, and high endothelial venules [51]. Data demonstrating the T cell activation in the tumor site, independently of secondary lymphoid organs, suggest an important function of DCs and explains the clinical significance of tumor infiltration with DCs [50]. More, tumor-associated DCs are the major source of CXCL9 and CXCL10, chemokines that promote tumor-reactive effector T cell recruitment [52].

However, tumors can develop the ways to impair differentiation and activation of DCs, resulting in accumulation of functionally deficient immature DCs that have low levels of costimulatory molecules. They are unable to neither induce activation of antigen-specific or allogeneic T cells nor suppress the proliferation of pre-activated T cells. However, in specific TME conditions, the loss of function in DCs may be associated with the acquisition of tolerogenic and/or immunosuppressive activities, such as the expression of IDO or PD-L1 [50,53].

1.3.4. T lymphocytes

T lymphocytes are substantial components of the TME. They involve two main classes of CD4+ and CD8+ T lymphocytes.

Among all tumor infiltrating lymphocytes (TIL), only cytotoxic CD8+ bearing T lymphocytes exhibit direct anticancer activity. **Naïve** CD8+ T cells differentiate into effector T cells upon antigen recognition and co-stimulation by APCs. In case of cancer, this T cell priming can occur both in tumor-draining lymph nodes as well as in TLS within the tumor. Terminally differentiated **effector** T cells, also called cytotoxic T lymphocytes (CTL), are able to destroy tumor cells with the help of IFNγ, perforin, and granzyme B. A subset of antigen-experienced T cells remain as persistent **memory** T cells, which can be further subdivided into central and effector memory cells. Central memory cells are less differentiated and do not exert rapid effector functions upon antigen re-challenge, opposite to effector memory cells. In growing tumors, CD8+ T cells are often functionally impaired by the immunosuppressive cells and signals in

the TME, resulting in T cell exhaustion, anergy or senescence - the states that are characterized with reduced proliferation and cytotoxicity [54].

Another class, CD4+ T lymphocytes, act as helper cells and modulators of antitumor immune response. CD4+ lymphocytes can be subdivided into Th1, Th2, Th9, Th17, Th22 and Tregs. Differentiation of Th0, a precursor of CD4+ T cells, into one of the subtypes is mediated by the amount and type of cytokines in TME.

Exposure of Th0 to IL-12 can facilitate their differentiation into **Th1** and further production of IFNγ, TNFα, IL-12, and IL-2. Collectively, these cytokines promote macrophage polarization towards the M1 phenotype, activate CTL, NK cells, DCs, and therefore play a tumor-suppressing role in TME [55,56].

IL-4 and IL-13 promote the **Th2** differentiation. Th2 cells produce IL-4, IL-5, IL-6, IL-10, they help B cell proliferation and antibody production, educate M2-type macrophages and inhibit CTL-mediated cytotoxicity. Therefore, their role in cancer is tumor-promoting. More, Th1 and Th2 cells are terminally differentiated cells and their populations seem to be stable in tumors [55,56].

Th9 cells secrete IL-9 and originate from naïve T lymphocyte stimulation with IL-4 and TGFβ. Although their role in tumor is not fully known, elevated IL-9 production and Th9 differentiation have been demonstrated in melanoma [57].

Th17 exhibit a controversial behavior in the TME. In cancer conditions, they are able to differentiate into Th1 cells, facilitating the antitumor immune response, or to Tregs, that inhibit the immune response. Therefore, Th17 cells can act as both effectors and regulators, and their role is determined by the local cytokine milieu. The conversion into Th1 is facilitated by the presence of IL-1β, IL-6, IL-12, whereas transition into Tregs is supported by TGFβ, which promotes the FoxP3 TF expression in cells [55].

The combination of TNFα, IL-6 and IL-1β differentiates naïve T cells into **Th22** type of T lymphocytes, that express IL-22, but not IL-17 or IFNγ.

Th22 cells can influence the EMT and play a role in development of skin inflammation. The increased levels of Th22 cells and IL-22 were found in various tumors, and therefore they can be regarded as a potential therapy target [57].

In TME, **Tregs**, regulatory T lymphocytes, play a role of immunosuppressive cells. Tregs are controlled by master TF FoxP3. The natural Tregs are derived from the thymus and are a stable subset. Inducible Tregs develop in the periphery from naïve T cells in response to TGFβ and IL-6 by increasing the expression of Treg-specific TFs, and start producing the IL-17 and IL-10 without production of IFNγ. Tregs interfere with T cell priming and suppress the antitumor immune response. Tregs can be further subdivided into memory-like (generated upon antigen encounter) and naïve-like [55,58,57].

1.3.5. Macrophages

Macrophages, as such, are the primary danger sensors and form an essential part of the first-line defense. Also, they are important in tissue homeostasis and wound healing via secretion of growth factors, cytokines, and proteolytic enzymes. Their ability to respond to various environmental stimuli is reflected in their plasticity and ability to adopt distinct functional states. The M1/M2 paradigm, similarly as Th1/Th2 nomenclature for T cells, represent the two opposite poles of the macrophage polarization spectrum. **M1-like** macrophages are induced by IFNγ and exposure to Toll-like receptor (TLR) ligands, such as lipopolysaccharide (LPS), and are characterized by high phagocytic capacity and antigen presentation abilities, expression of activation molecules (CD80, CD86), and production of pro-inflammatory cytokines. Conversely, **M2-like** macrophages are induced by IL-4 and IL-13, are active during wound healing, upregulate the expression of CD206, and are associated with anti-inflammatory cytokine signature. Between M1 and M2 extremes, there are some intermediate phenotypes, skewed by microenvironmental cues [59].

Tumor-associated macrophages (TAM) make up a great amount of the infiltrating immune cells. Tumors take advantage of the fact that the macrophage

polarization is highly microenvironment-dependent. Therefore, TAMs are often described to acquire an M2-like phenotype. However, different TAM populations may co-exist in the same tumor, depending on the local microenvironment ant the tumor stage [60]. This is confirmed by the correlation of TAMs density in tumor and poor prognosis in a majority of published studies [61].

The inflammatory properties of macrophages (representing M1-like phenotype) are substantial during the tumor initiation, especially the production of DNA-damaging mutagenic reactive oxygen and nitric species [62]. However, during progression, tumors create a microenvironment that causes macrophages to suppress immune functions and polarize them into M2-like type, supporting tumor progression via promoting angiogenesis and enhancing tumor cell invasion [63]. The M1 to M2 transition is associated with decreased expression of proinflammatory cytokines (TNFα, IL-12) and increased expression of immunosuppressive cytokines (IL-10) that further help in maintaining the immunosuppressive microenvironment [64].

1.3.6. Myeloid-derived suppressor cells

Myeloid-derived suppressor cells (MDSC) represent a heterogeneous population of immature myeloid cells consisting of precursors for granulocytes, macrophages or DCs, and are accumulated during the chronic inflammation and tumor progression. Granulocytic- and monocytic-origin MDSCs are distinguished in both human and mouse tumors. MDSCs are potent immunosuppressors that not only inhibit anti-tumor reactions but also directly stimulate tumor growth and metastasis. They act through several mechanisms. Secretory mechanisms include the intensive production of angiogenic factors and immunosuppressive cytokines (IL-10, TGFβ) that skew the immune reactions towards Th2 type and Treg activation. Metabolic mechanisms include nitration of TCR and T cell-recruiting chemokines as well as deprivation of essential amino acids, arginine, and cysteine. MDSCs can also upregulate their

own expression of programmed death ligand 1 (PD-L1) that can downregulate T cell reactivity [65].

Accumulation of MDSCs in the tumor depends on the two-signal model. First, tumor-derived growth factors inhibit the terminal differentiation of immature myeloid cells and promote their accumulation in the tumor site. Second, tumor stroma-derived pro-inflammatory cytokines convert immature myeloid cells into MDSCs, manifesting the pathological activation of these cells. Therefore, MDSCs represent a relatively stable, distinct state of functional activity of neutrophils and monocytes [66].

1.3.7. Natural killer cells

Natural killer (NK) cells are classically considered innate immune effector cells. Their activity depends on the balance of activating and inhibitory signals on target cells. Acquisition of activating ligands on cancer cells, together with reduced expression of major histocompatibility complex (MHC) class I molecules, activates NK cytotoxicity via perforin and granzyme, as well as immunostimulatory cytokine release (TNFα, FasL, IFNγ), which inhibit the proliferation of tumors by inducing anti-angiogenetic factors and maintaining crosstalk with other immune cells. In addition, NK cells can kill antibody-coated tumor cells via antibody-dependent cellular cytotoxicity (ADCC) mechanism. Also, NK cells enhance the expression of costimulatory molecules on DCs, as well as their IL-12 production. However, in the TME NK cells become functionally impaired by the inhibitory ligands on tumor cells. Also, soluble activating ligands shed from tumor cells impair NK cell receptors, favoring tumor cell escape from NK cell immunosurveillance [67].

1.3.8. B lymphocytes

B lymphocytes, adaptive immunity cells, specialize in antibody production. Antibodies made by B cells can alter the antigenic targets on cancer cells, opsonize tumor cells for the presentation and cross-presentation of tumor antigens to DCs, activate the complement cascade, or contribute to NK mediated

tumor killing via ADCC. B cells account for up to 25% of all cells in some tumors, e.g. breast or ovarian carcinomas [68]. Aside from antitumor effects, the pro-tumorigenic activity of B cells is now recognized. Regulatory B cells (Bregs) are a newly designated subset of B cells that regulate the immune response in cancer. Bregs can suppress diverse cell subtypes, including T lymphocytes, through the secretion of anti-inflammatory cytokines (IL-10), and can attenuate the immune response by converting T cells into Tregs [69].

As described, B cells have a strong immunomodulatory role. Interestingly, therapeutic immune checkpoint blockade may also target activated B cells, as they express PD-1, PD-L1, CLTA-4, B7. Blockade of PD-1 or CTLA-4 enhances the proliferation of memory B cells and the production of antibodies [68].

1.3.9. Extracellular matrix

Extracellular matrix (ECM) is composed of a large variety of collagens, laminins, proteoglycans, and hyaluronans. Structurally, ECM comprises both basement membrane and interstitial matrix. Depending on its rigidity, porosity, insolubility, and spatial orientation, ECM determines the tissue architecture. Biochemical properties of ECM refer to its direct and indirect signaling capabilities, as it contains cytokines and growth factors secreted by stromal and tumor cells [70].

ECM is highly dynamic and constantly being remodeled in different tissues. Although this process is strictly controlled during development, tumor-associated cells (CAFs and immune cells) may alter this regulation and lead to the disorganization and changes in the essential properties of ECM. Abnormal ECM dynamics upon tumor development serves towards potentiating the oncogenic effects of growth factors and deregulating the cell behavior. Not only ECM may form the CSC niche and serve as a scaffold for cell differentiation and invasion, it also can alter the phenotype of the cells of the microenvironment. ECM provides a hypoxic or acidic environment that promotes lymphangiogenesis and inflammation [71].

ECM also plays a role in tumor-associated inflammation by functioning as a chemoattractant to immune cells. However, to reach the tumor site, immune cells must encounter the basement membrane. Once passed, they travel through the interstitial matrix [70].

1.3.10. Cytokines and chemokines within the tumor microenvironment

A variety of cytokines, chemokines, and growth factors are produced by cells of TME, as well as tumor cells. Their interactions form a complex and unique network, which regulates tumor growth and response to treatment.

Host-derived cytokines can suppress tumor formation by controlling inflammation and immune response. However, tumor cells can exploit these cytokines to promote growth and dissemination. **IL-2** promotes the activation and proliferation of T and NK cells. Nevertheless, competition for IL-2 is one of the main immunosuppressive mechanisms of Tregs. **TNFα** signaling is necessary for APC migration and activation, as well as for further induction of **IL-6**, which, in turn, is involved in T cell migration and proliferation. **IL-12** is an essential proinflammatory cytokine stimulating the Th1 response. Importantly, IL-12 can induce the proliferation of large amounts of IFNγ. One of the main anti-tumoral cytokine, **IFNγ,** produced by CTL, NK cells, DCs and M1 macrophages, stimulates the antitumor immune response and inhibits tumor growth. IFNγ inhibits the production of immunosuppressive **TGFβ,** which is necessary for Treg differentiation. **IL-10** is another immunosuppressive cytokine, produced by Th2 and Tregs, which inhibits the DC antigen-presenting function**. IL-4** and **IL-13** are necessary for Th2 T cells and M2 cells polarization. **IL-5**, produced by Th2 T cells, promotes B cell influx and tumor growth [72–74].

Immune cells are attracted into the tumors via interactions between chemokines and their receptors. Tumor-suppressing cells, such as CD8+ CTLs, Th1 T cells, and NK cells express CXCR3, which is a receptor for cytokines **CXCL9** and **CXCL10**. Th17 cells are recruited by tumor-derived **CCL20**

chemokine via its interaction with the CCR6 receptor, similarly as immature DCs. **CCL4** is also essential for DC migration and subsequent T cell activation. Another type of APCs, monocytes, which later differentiate into M1 or M2 macrophages, are attracted by tumor-produced **CCL2** and **CCL5** chemokines, that are the ligands for CCR2 and CCR5, respectively. Tumor growth promoting immune cells, MDSCs, are attracted by **CXCL5**-CXCR2 axis. Additionally, monocytic MDSCs can be recruited by **CCL2** and **CXCL12**. Tumor and myeloid cells express **CXCL1** and **CXCL8** that regulate granulocytic MDSCs migration and degranulation. Lymphoid immunosuppressive cells Tregs express CCR4 and are recruited into the TME in response to **CCL22**, which is mainly produced by tumor cells [75,76].

Direct and indirect manipulation of cytokine and chemokine pathways may reshape the immune and biological phenotype of the tumor and modulate its susceptibility to treatment.

Collectively, tumor cells recruit and instruct various cell types: fibroblasts, endothelial cells, and protumoral immune cells (Th2 and Treg lymphocytes, M2 macrophages, MDSCs, B cells) that suppress antitumor immune cells (CTL an Th1 lymphocytes, M1 macrophages, DCs, NK cells) while maintaining inflammation and angiogenesis in tumor. Immune cells of the TME interact via synergistic and mutually augmenting cytokine signaling networks (Figure 5).

1.4. Tumor immunology

1.4.1. Innate and adaptive immune responses in cancer

Although the link between cancer and inflammation was established more than a century ago, the dual role of immune system in enhancing or eradicating the growing tumor mass remains a matter of controversial debate.

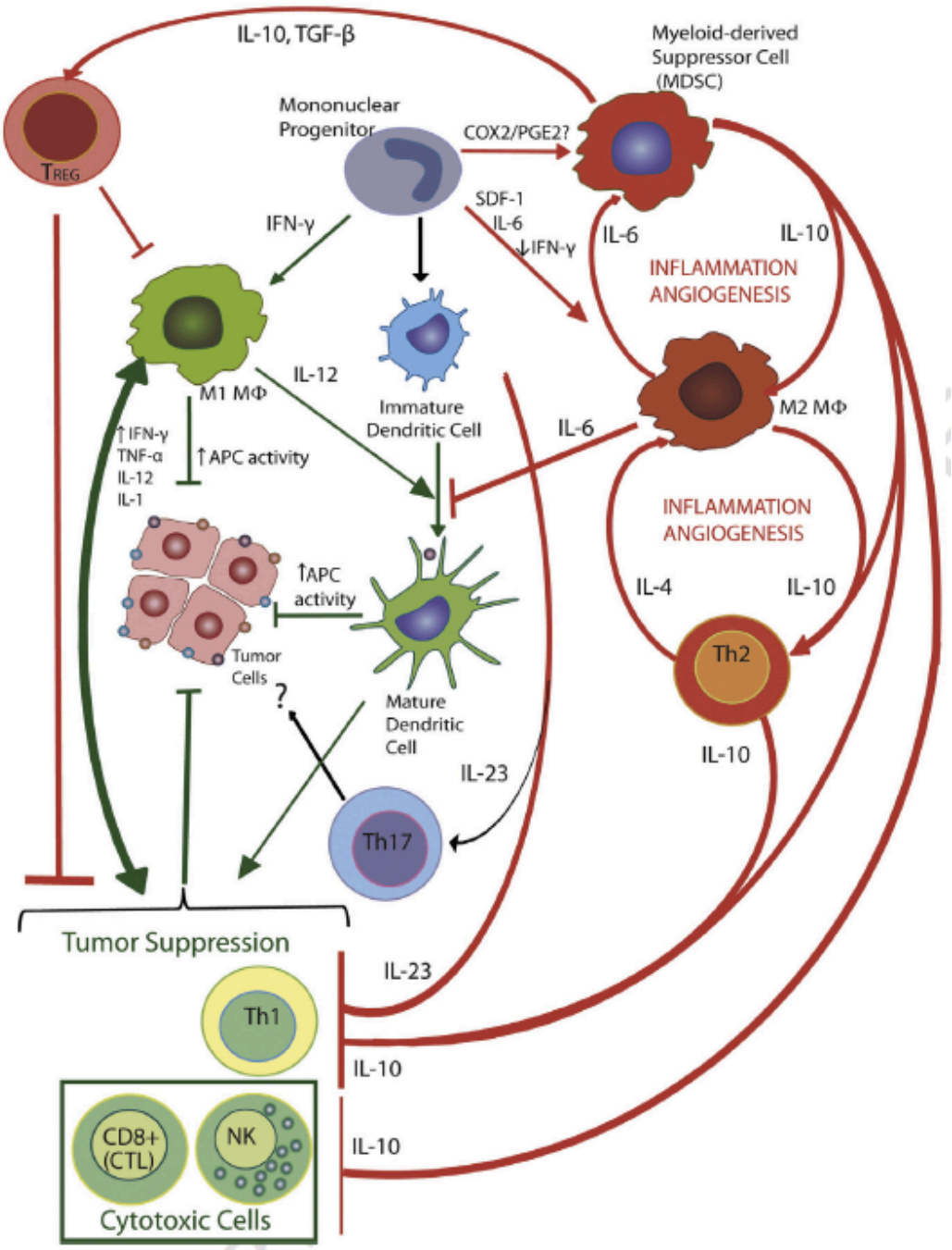

Figure 5. Tumor-supporting immune cell interactions. Th2 lymphocytes, M2 macrophages, and MDSCs mutually reinforce the proliferation and phenotypes of one another, as well as maintain tumor-promoting inflammation and angiogenesis. Along with Tregs, they suppress the activity and proliferation of antitumor cells, including Th1, M1 macrophages, cytotoxic T cells and NK cells. Some pairs of cells types tend to reinforce their own activation profile and inhibit the other. Adapted from [56].

Evidence for the link between cancer and inflammation comes from epidemiology studies, showing that chronic infections or autoimmune diseases predispose for a variety of cancers. The TME of most tumors contains a unique

inflammatory component, varying in size, composition, and topography, that affects the tumor growth. Inflammation is a mechanism of innate immunity and represents the first line of defense that is activated to restore the tissue homeostasis [77]. Normal inflammation is well regulated by inducing the anti-inflammatory cytokines after the pro-inflammatory cytokines. In contrast, chronic inflammation is characterized by the prolonged persistence of pro-inflammatory factors or the failure of control mechanisms [78]. Several inflammatory mediators, such as TNFα, IL-6, TGFβ, IL-10, have been shown to mediate both the initiation and progression of cancer [79]. More, the innate cells of the tumor immune infiltrate can also contribute to cancer-related inflammation by the production of cytotoxic mediators and matrix remodeling proteases.

Nevertheless, the immune surveillance theory involves the adaptive immunity components. High mutation rates drive the expression of immunogenic tumor-specific antigens, towards which the antitumor immune response can be initiated [8]. However, tumors can effectively escape the immune destruction through immunoediting and immune subversion via cell-cell contacts or immunosuppressive cytokine production, resulting in immune tolerance [10]. Therefore, evading immune destruction is an internal hallmark of tumors [1].

1.4.2. The cancer-immunity cycle

Although random oncogenic events are essential for tumor initiation and progression, mutations can lead to the aberrant expression of tumor antigens, including neoantigens, differentiation antigens, or cancer-testis antigens, which can be then recognized by immune cells [6,7]. Initiation, maintenance, and successful completion of an effective antitumor immune response are summarized in a stepwise process, called the cancer-immunity cycle (Figure 6).

First, tumor-associated antigens are released by dying cancer cells and are captured by dendritic cells. Dendritic migrate to draining lymph nodes and present the processed antigens on the MHC class I and II molecules to the naïve

T cells repertoire. Recognition of a cognate antigen is followed by T cell priming and activation. Effector T cells egress into the circulation to home and extravasate into tumor tissue. There, the interaction between the T cell receptor and its cognate antigen presented by MHC class I on the cancer cell leads to the release of mediators such as IFNγ and perforins that induce tumor cell death. The antitumor immune response leads to tumor regression [7,80].

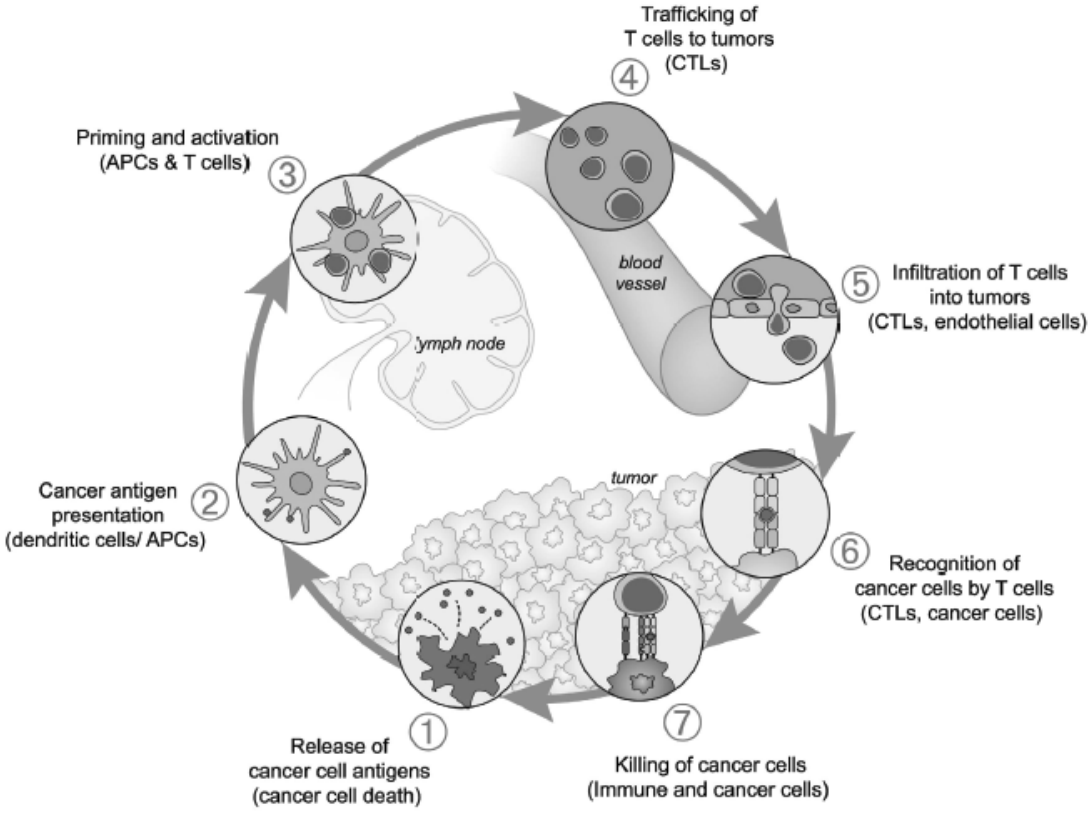

Figure 6. The cancer-immunity cycle. The generation of antitumor immunity is a cyclic process that can be self-sustainable. The cycle represents seven major steps involved in the generation of the antitumor immune response. Primary cell types involved in the cycle, as well as anatomic locations, are listed. Adapted from [7].

However, in order to escape the immune-mediated destruction, tumors evolve mechanisms to inhibit one or more steps of the cancer-immunity cycle. Tumor cells recruit the immunosuppressive stroma that induces DCs to become tolerogenic. MDSCs secrete arginase and inducible nitric oxide synthase, which block the TCR expression and nitrate the preexisting TCRs, making them non-functional. Stromal cells induce the expression of checkpoints that prevent the

T cells from receiving proper co-stimulation, leading them to anergic state. Finally, tumor cells downregulate both antigen processing machinery and MHC molecule expression, making them invisible to activated CTLs [81].

1.4.3. Immune phenotypes

Depending on the immune evasion mechanism, tumors can be divided into three immune phenotypes: immune desert, immune-excluded, and inflamed tumors (Figure 7). Each of them encompasses a part of cancer-immunity cycle and is associated with specific mechanisms that prevent the antitumor immune response [11].

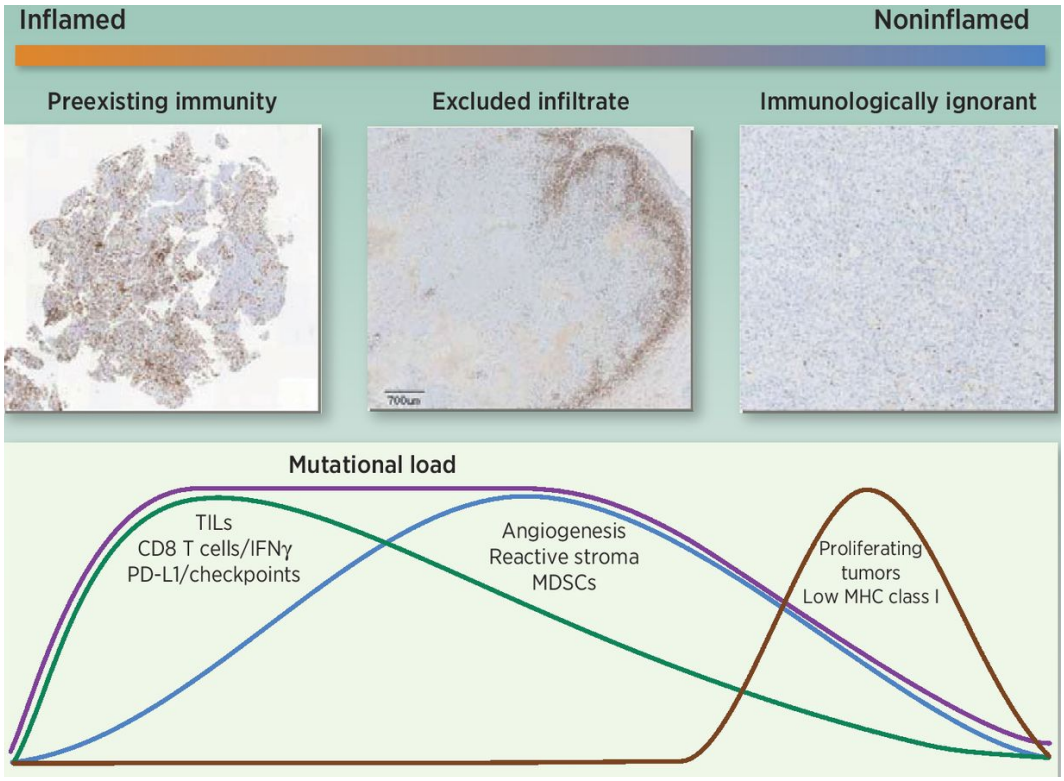

Figure 7. The tumor-immunity continuum. Three patterns of T cell infiltration in tumors exist, as seen in the representative immunohistochemistry staining. Tumors with pre-existing immunity (inflamed phenotype) are densely infiltrated with T lymphocytes that express checkpoint molecules. Immune-excluded tumors are infiltrated with immunosuppressive reactive stroma which, together with increased angiogenesis, prevents T cells from entering the tumor nest. Immunologically ignorant tumors (immune desert phenotype) are rather genetically stable tumors with low T cell infiltration. Adapted from [82].

Immune desert tumors are characterized by the immunologic ignorance, the induction of tolerance, or lack of T cell priming and activation (disruptions in 1-3 steps of the cancer-immunity cycle). Immunologic ignorance may arise from the lack of tumor-specific antigens or MHC I molecules. The immunosuppressive milieu of TME (Tregs, cytokines) may suppress the inflammatory conditions. Lack of co-stimulation impairs T cell priming. Such tumors are usually poorly immune-infiltrated with no intraepithelial T cell lymphocytes, although the myeloid cells can be present. This phenotype reflects the absence of pre-existing antitumor immunity and could be managed by the generation of tumor-specific T cells [11,82,83].

The immune-excluded phenotype is characterized by the abundant presence of immune cells that do not penetrate the tumor parenchyma and accumulate around the tumor nests (disruptions in 4-5 steps of cancer-immunity cycle). The exclusion persists due to a specific chemokine state, vascular barrier and stromal inhibition. Excluded tumors usually recruit CAFs and therefore surround themselves with a dense extracellular matrix of collagen and fibronectin, limiting the access for immune cells. Although stromal cells can create a chemotaxis for immune cell attraction, tumor cells express chemokine peptidases and thus inhibit the T cell migration. These features suggest that pre-existing antitumor response might be present, but is rendered ineffective by retention of immune cells in the stroma. Immune-excluded phenotype reflects the ineffective T-cell migration into the tumor stroma, and therefore could be addressed by inhibiting stromal barrier, and engaging the infiltration of T cells [11,82,83].

Inflamed phenotype in characterized with considerable infiltration of T cells that are not functioning properly (disruptions in 6-7 steps of the cancer-immunity cycle). Such tumors usually have the higher mutational load, resulting in the emergence of neoantigens and their recognition by T cells. However, due to the chronic TCR stimulation, T cells are often exhausted. Although the proinflammatory and effector cytokines are often present, the abundance of immunosuppressive cell subtypes (including Tregs, MDSC, M2 macrophages,

Bregs) creates tumor-promoting microenvironment. This phenotype represents the arrest of pre-existing immunity which could be re-invigorated by blocking the inhibitory pathways and redirecting T cells [11,82,83].

1.5. Cancer immunotherapy

Cancer is no longer perceived as a disease solely caused by the uncontrolled proliferation of cells, but also due to the failure of immune system surveillance to effectively control the neoplastic processes in the body. Cancer immunotherapy intends to establish an efficient antitumor immune response by launching and reinforcing the cancer immunity cycle. As there are several immune evasion strategies (recruitment of immunosuppressive stroma, upregulation of regulatory checkpoint molecules, downregulation of MHC molecules, etc.), numerous immunotherapy strategies exist [84].

The approach aiming to use the immune system to fight cancer has been attempted for decades with modest success. The roots of immunotherapy date back to the end of 19th century, when William Coley started treating the cancer patient with intratumoral injections with 'Coley toxins', a mix of inactivated streptococci. Although initially effective, they were discontinued due to high treatment risks [85]. Later, documented observations, including the occurrence of spontaneous remission or higher incidence of cancer in immunosuppressed patients had shed the light on cancer immunotherapy research. In 1976, Bacillus Calmette Guerin vaccine, first developed as a vaccine against tuberculosis, was reported as a promising new treatment for bladder cancer [86]. In 1986 and 1992, IFNα and IL-2 received FDA approval for treatment of leukemia and renal carcinoma, respectively [72]. In the late 20th century, it was identified that Tregs are particularly enriched in tumors. Simultaneously, the discovery of CTLA-4 and PD-1 as targetable immune checkpoints accelerated the development of immunotherapy. The beginning of 21st century became a dawn of cellular immunotherapy, after demonstrating the effectiveness of *ex vivo* expanded and reinfused TILs [87] or engineered T cells expressing a chimeric antigen receptor

(CAR) [88]. Numerous clinical trials including novel immunotherapeutic agents, as well as combination immunotherapy strategies, are currently ongoing. Current immunotherapeutic strategies aim at targeting various steps of cancer-immunity cycle (Figure 8).

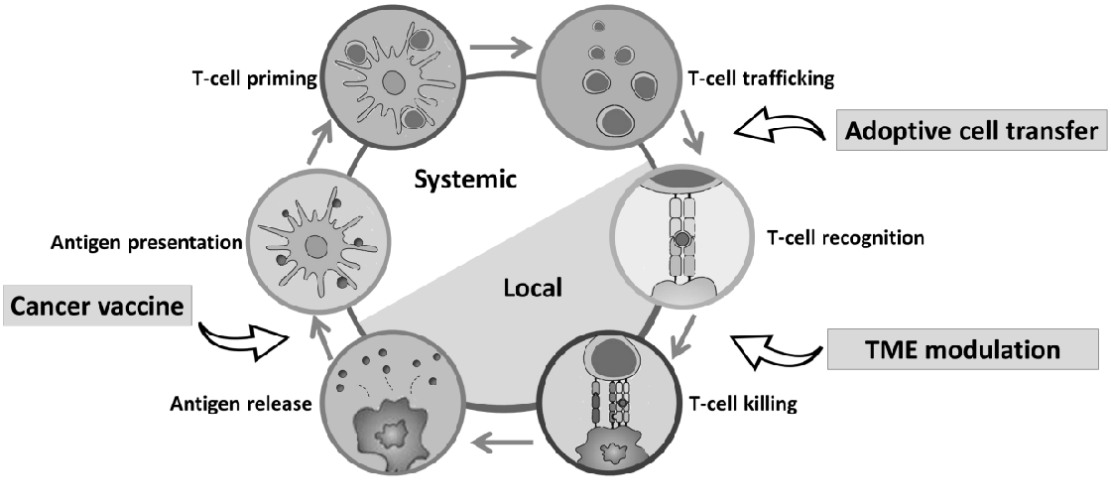

Figure 8. Cancer immunotherapy aims to initiate or re-activate the self-sustaining cancer-immunity cycle. Different cancer immunotherapy types target different steps of the cycle. Cancer vaccines are designed to promote antigen presentation on DCs and facilitate the T cell production. In adoptive cell transfer, *ex vivo* expanded antigen-specific CTLs infiltrate the tumor and promote more efficient tumor cell killing. Tumor microenvironment (TME) modulation, including checkpoint inhibitors, aims to release the brake for CTLs in the immunosuppressive environment. Adapted from [89].

Cancer immunotherapies can be classified as tumor-associated antigen-specific or -unspecific, as well as passive or active [90].

1.5.1. Cancer vaccines

Cancer vaccines are an example of antigen-specific active immunotherapy. Prophylactic cancer vaccines proved successful for prevention of virus-induced cancers, such as HPV-caused cervical cancer or head and neck squamous carcinoma, as well as hepatitis B virus-caused hepatic carcinoma [91]. The success of therapeutic cancer vaccines is so far limited. The goal of therapeutic cancer vaccination is to either *de novo* trigger the CD4 or CD8 T cell response or boost the preexisting latent antitumor immune response. Examples

of therapeutic cancer vaccines include tumor cell vaccines, antigen vaccines, dendritic cell vaccines, DNA vaccines, vector-based vaccines. They can be combined with an adjuvant that can further boost the immune response. The first FDA-approved cancer vaccine was Provenge in 2010, a dendritic cell-based vaccine for metastatic castration-resistant prostate cancer [92]. Recent findings highlight the potential of personalized vaccines, designed with the help of high throughput approaches [93]. Mass spectrometry and exome sequencing, combined with prediction algorithm, allow to identify potential epitopes, which are then used in peptides- or RNA-based vaccines and are shown to elicit strong antitumoral T cell response [94].

1.5.2. Adoptive cell therapy

Adoptive cell therapy (ACT) is a type of passive tumor antigen-specific immunotherapy, which relies on the immunization with *ex vivo* activated and expanded tumor-specific cells. Although TILs are present in immune suppressed tumors, they sometimes fail to eliminate the cancer cells. However, when isolated and cultured in appropriate conditions, they can proliferate and become less susceptible to immunosuppressive cues [84]. This is a relatively novel approach, which was shown to mediate durable complete response in patients with metastatic melanoma [87,95]. *Ex vivo*, T cells can be selected by their specificity to tumor antigens. More, antigen specificity can be improved by engineering the T cell receptors via *in vitro* reactivity screening, cloning, and transforming into lymphocytes. Until now, TIL ACT was shown to perform best in cancers with the broad mutational landscape, such as melanoma. ACT with TIL is still an experimental therapy and is not approved by FDA.

Another promising type of ACT is the therapy with CAR T cells. Alternatively to using autologous T cells, host cells can be genetically engineered to carry chimeric antigen receptor – CAR. CARs encode for transmembrane chimeric molecules with dual immune recognition of tumor antigens as well as active promotion of cell lysis machinery. Enabling T cell activation and tumor cell killing in a TCR and co-stimulation independent

manner allows bypassing MHC-mediated antigen recognition and tolerance acquired by tumor cells [96]. CAR T cells targeting CD19 have been especially successful in the treatment of hematological malignancies, with complete response rates of up to 60%, and recently earned the FDA approval [97,98]. T cells have difficulties accessing the solid tumors. The TME may not express the required chemokines, the vasculature is aberrant, and the endothelial cells may not support the trans-endothelial migration. If T cells manage to enter, they encounter a largely immunosuppressive stroma, which can render them anergic. with CAF, MDSC, M2 macrophages, tolerogenic DCs, Tregs. In addition, activated T cells must survive and proliferate in a largely hypoxic and nutrient-depleted environment. Therefore, localizing sufficient numbers of T cells to eliminate the tumor bulk remains a challenge [99]. Focusing CAR T on a minor but crucial population of CSCs may eliminate the need to recruit high numbers of T cells to the tumor [100].

Despite the promising clinical performance of adoptive cell therapies, broad implementation of these treatments remains a challenge, as it is expensive, resource-consuming, and requires specialized GMP facilities.

1.5.3. Checkpoint blockade

Checkpoint inhibition therapy is a type of active, yet tumor antigen-unspecific immunotherapy. Immune checkpoints are cell surface receptors that regulate the immune activation of T cells. First one, CTLA-4, discovered in 1995, is a key regulator functioning in a negative feedback loop upon T cell activation. It competes with CD28 for the B7 costimulatory molecules expressed on DCs and other APCs. CTLA-4 and B7 interaction dampens the T cell activation and expansion [101]. CTLA-4 is largely overexpressed in intratumoral T cells and is an important immune suppressive mechanism found in Tregs [102]. A monoclonal antibody targeting CTLA-4, ipilimumab, was approved by FDA in 2011, after showing the improved survival in patients with metastatic melanoma [103].

Another important checkpoint pathway is PD-1/PD-L1(2) axis. Even when the T cell activation is achieved in tumor-draining lymph nodes, tumors still have the capacity to inhibit the effector T cells once they enter the tumor. PD-1, expressed on T cells, binds to the ligands PD-L1 or PD-L2, expressed on target cells. Ligand interaction induces T cell exhaustion. Exhausted T cells lose their cytotoxic capacity and ultimately die out [102]. Although this regulatory mechanism normally serves as a brake of T cell response to chronic virus infection, however, it is hijacked by tumors to quench the antitumor immune response [104]. Several anti-PD-1 antibodies, nivolumab, and pembrolizumab, are now clinically validated for the treatment of melanoma or gastric cancer, respectively [105,106]

Blocking of pathways essential to T cell suppression with the combination of anti-CTLA-4 or anti-PD-1 monoclonal antibodies has resulted in complete response rates of up to 22% in human clinical trials [107,108].

New potentially targetable immunoregulatory checkpoint molecules are now emerging, among them both activating (OX40, GITR, CD27, CD28) and inhibitory (TIM-3, VISTA, LAG-3) T cell receptors [91].

1.5.4. Biomarkers in cancer immunotherapy

Despite the encouraging results from clinical trials employing immunotherapy, there are currently no validated biomarkers for patient stratification that could improve the efficacy of immune-based treatment [109]. Ostensively, the expression of PD-1 ligands PD-L1 or PD-L2 on tumor cells could seem a prognostic marker for checkpoint inhibition using antibodies blocking the PD-1 pathway. However, the findings on this topic are contradictory – some studies have found the correlation between the tumor PD-L1 expression and patient outcome [110], while others did not [111].

The diversity of cells and their dynamic interactions within the TME implies that a single parameter could not reliably serve as a predictive biomarker for cancer immunotherapy. For example, the secretion of the principal effector cytokine IFNγ by the CD8 TILs, in parallel induces the adaptive resistance of

the TME, including the upregulation of IDO, PD-L1, and the influx of Tregs. However, recent research agrees that preexisting inflammation within the TME has been shown to correlate with good response to immunotherapy [11,112]. It has been suggested that inducing immune infiltration in immune-cold tumors might improve the immunotherapy outcome [113]. Also, it has been shown that the mutational load of the tumor and the number of generated neoantigens correlated with immunotherapy outcome [6,114]. Interestingly, the density of immunogenic antigens does not determine the presence or absence of the T cell infiltration in the TME [115].

Taken together, even though cancer immunotherapy created a paradigm shift in cancer patient treatment, there is still the need of better understanding of the molecular mechanisms dictating the clinical response to immunotherapy, as well as stratification biomarkers for improved treatment benefit. As different tumors rely on different immunosuppressive mechanisms to interfere with the cancer-immunity cycle, personalized immunotherapies combining multiple approaches are believed to lead to even better responses in future.

MATERIALS AND METHODS

2.1. Cell lines

Human melanoma cell line SK-MEL-28, human renal cell carcinoma cell line 786-O, human glioblastoma cell line U-87, human colon cancer cell lines HCT116, HT29, human ovarian cancer cell line A2780 and human leukemic monocyte cell line THP-1 were obtained from American Type Culture Collection (USA). Human colon cancer cell lines COLO320, SW620, and NCI-H508 were a kind gift from Courtney Thomas from Swiss Federal Institute of Technology in Lausanne. SK-MEL-28, U-87, HCT116, COLO320, SW620, NCI-H508, A2780, and THP-1 were maintained in RPMI-1640 (Lonza), supplemented with 10% FBS (Thermo Fisher Scientific) and antibiotics (100 U/ml penicillin and 100 μg/ml streptomycin) (Lonza). 786-O and HT29 were maintained in DMEM (Lonza) and supplemented as above. All cells were regularly passaged after reaching confluence. During all experiments, cells were maintained at 37 ºC in a humidified atmosphere at 5% CO_2.

2.2. Cell lysate preparation

For protein extraction, cells were detached and centrifuged for 5 min at 250 g. Supernatant was discarded and cell pellet was lysed with T-PER Tissue Protein Extraction Reagent (Thermo Fisher Scientific), supplemented with protease/phosphatase inhibitor cocktail (Thermo Fisher Scientific), followed by 15 min centrifugation at 10 000 g and debris removal.

2.3. Preparation of conditioned media

Colon cancer cell lines were plated at 1×10^5 cells/ml in 100 mm Petri dishes in 10 ml of supplemented respective growth medium. At 80% confluence, old growth medium was removed, cells were washed with PBS (Lonza) and supplied with 10 ml of serum-free medium. After 24 hours, the growth medium was collected and centrifuged for 10 min at 1000 g to precipitate any floating or

dead cells. A cleared fraction was aspired and used for macrophage conditioning.

2.4. Isolation and development of PBMC-derived dendritic cells and macrophages

Peripheral blood mononuclear cells from fifteen healthy donors (approved by Lithuanian Bioethics Committee) were freshly isolated from blood packs by density centrifugation with Ficoll (Sigma Aldrich) at room temperature for 30 min at 900 g without braking. PBMCs were aspired, washed 5 times with ice-cold PBS by spinning at 4 ºC for 7 min at 250 g with half-brake, and counted.

Dendritic cell generation: Counted cells were plated at the density of 5×10^6 cells/ml in 75 cm^2 flasks in 20 ml of X-VIVO medium (Lonza). After two hours incubation at 37 ºC in a humidified atmosphere at 5% CO_2, the unattached lymphocytes were removed and stored for further experiments. Adherent monocytes were resuspended in X-VIVO medium with 2% FBS, supplemented with GM-CSF (1000 U/ml) (Miltenyi Biotec) and IL-4 (3000 U/ml) (Miltenyi Biotec), and incubated for 6 days at 37 ºC in a humidified atmosphere at 5% CO_2 with half-medium change every second day.

Macrophage generation: Counted cells were plated at the density of 3×10^6 cells/ml in 100 mm low-attachment Petri dishes in 10 ml serum-free RPMI medium. After two hours incubation at 37 ºC in a humidified atmosphere at 5% CO_2, the unattached lymphocytes were removed. RPMI medium, supplemented with 10% FBS and 20 ng/ml M-CSF (Thermo Fisher) was added and cells were left overnight. On the next day, attached monocytes were detached with Accutase (Stemcell Technologies) and plated at 2.5×10^5 cells/ml in 6 well plates in 2 ml of RPMI medium, supplemented with 10% FBS and 100 ng/ml M-CSF. Monocytes were differentiated into macrophages for 6 days with half-medium change every second day.

2.5. DC maturation with cancer cell lysate

The medium was gently aspired from immature DCs, the cells were resuspended in fresh X-VIVO medium in presence of LPS (200 ng/ml) (eBioscience) and IFNγ (50 ng/ml) (eBioscience) and, optionally, 30 μg/ml of cancer cell lysate mix. DCs were matured for 24 h at 37 ºC in a humidified atmosphere at 5% CO_2

2.6. Isolation of CD3+ T cells and their subsets

CD3+ T lymphocytes were isolated from healthy donors' PBMCs by negative magnetic separation using Pan T Cell Isolation Kit (Miletnyi Biotec), according to manufacturer's recommendations. T cells were next magnetically sorted into CD4+ and CD8+ subsets using CD8+ T cell Isolation Kit (Miletnyi Biotec), according to manufacturer's recommendations.

2.7. T cell proliferation assay

CD3+ T lymphocytes were incubated with 1 μM carboxyfluorescein succinimidyl ester (CFSE) (Thermo Fisher Scientific) in the dark for 20 min. Mature DCs and T lymphocytes were co-cultured at a ratio of 1:10 (1×10^4 DCs and 1×10^5 T cells per well) in U bottom 96-well plates for 7 days in a serum-free X-VIVO medium at 37 ºC in a humified 5% CO_2 atmosphere. Stimulated cells were stained with anti-CD3 antibody and acquired on an LSR II flow cytometer. The data were analyzed with FlowJo software. Autologous CD3+ T cells incubated with 5 μg/mL phytohemagglutinin (Sigma Aldrich) served as a positive control, whereas CD3+ T cells incubated alone (spontaneous T cell proliferation) served as a negative control.

2.8. Co-culture of mature DCs with autologous T cells

Autologous CD4+ T cells were stimulated with mature DCs at a ratio of 10:1 10 (1×10^5 T cells and 1×10^4 DCs per well) in U-shaped 96-well plates. CD4+ cells were stimulated in two 7-day cycles. On day 2 of each cycle, IL-2

(25 U/ml) (BD Biosciences) was added to the cell culture medium. Half of cell culture medium was replaced with fresh IL-2- supplemented medium on days 4 and 6 of each stimulation cycle. On day 7 of the second cycle, the stimulated CD4+ T cells were extensively washed, re-stimulated with 1×10^4 mature DCs without IL-2 for 24 h and subjected to phenotypic flow cytometry analysis.

2.9. Macrophage polarization and conditioning

On the 6th day of macrophage differentiation, medium with M-CSF was removed. To retain the M0 phenotype, 5% FBS-supplemented RPMI medium was added. To polarize macrophages into M1 type, RPMI medium supplemented with 5% RPMI, 15 ng/ml LPS and 25 ng/ml IFNγ was added. To polarize macrophages into M2 type, RPMI medium supplemented with 5% RPMI, 25 ng/ml IL-4 and 25 ng/ml IL-13 (Miltenyi Biotec) was added. For preparing tumor-conditioned macrophages from differentiated M0 macrophages, 1:1 ratio of 10% FBS-supplemented RPMI medium and cancer cell conditioned medium was added. All treatments were carried out for 48 hours.

2.10. Drugs

Cisplatin (1 mg/ml) was from Teva Pharmaceuticals (Israel). Drug stocks were stored in accordance with the manufacturer's recommendations. Drug solutions in the medium were prepared fresh on the experiment day.

2.11. Development of chemotherapy-resistant cell lines

To develop the resistant cell lines, we applied a low-dosage cisplatin pulsed incremental inducement strategy [116,117]. As a result, we generated a cisplatin-resistant cell line A2780Cis. Drug-resistant clones were intermittently selected by incubating semi-confluent monolayer with the drug-containing medium for 24 hours and then switching to drug-free medium. After treated cells reached confluency, they were passaged and repeatedly subjected to treatment.

A2780Cis subline was generated by pulsed treatment with incremental doses of cisplatin, reaching up to 60 μM and was established over a period of 12 months. At the end of the treatment, resistant cell line displayed distinct morphological profile (phase contrast microscopy, Leica), which was stable during freeze-thawing and passaging cells in drug-free medium for the next 2 months, over subsequent experiments. Maintenance conditions of resistant cell line A2780Cis were the same as of parental A2780 cell line, which was cultured in parallel throughout the whole experiment.

2.12. Drug toxicity assay

Chemotherapy-sensitive and -resistant ovarian cancer cells were plated in a white-walled 96-well microtiter plate at the density of 1×10^4 cells per 100 μl of supplemented drug-free medium per one well and allowed to attach for 24 hours. On the following day, the drug-free medium was replaced with medium containing 1.67-333 μM of cisplatin. After 24 h incubation, drug was removed and cells were allowed to rest in a drug-free medium for another 24 hours. Finally, cell viability was analyzed by the Cell Titer Glo luminescence assay (Promega), using Centro LB 960 luminescence microplate reader (Berthold Technologies). Control wells for luminescence contained the cell-free medium. The experiment was repeated three times. Inhibitory concentration 50% (IC_{50}) values were derived from dose-response curves.

2.13. Wound healing assay

1×10^6 cells were plated in 35 mm Petri dish. After cells reached 70-80% confluence, 200 μl pipette tip was used to gently introduce two perpendicular scratches in the monolayer. Later on, wound healing was regularly monitored for the next 24 hours and pictures of the scratch intersection were taken with computer-aided phase contrast microscope. The area of the wound was measured using ImageJ software (NIH). The percentage of wound closure was normalized to the total wound area at the starting point of the assay. Results were

obtained from three independent experiments, each with four measurement points per cell line.

2.14. Clonogenic assay

Ovarian cancer cell lines were plated in six-well plates at a density of 100 cells per well (six wells per one cell line, two repetitions) and allowed to grow for one week in complete RPMI medium. Afterward, colonies were fixed (15 min in 70% ethanol, 15 min in 96% ethanol), stained with crystal violet and counted manually.

2.15. Indirect co-culture of macrophages and ovarian cancer cells

The co-culture was performed as described in [118] with adjustments in cell density. Briefly, 5×10^5 THP-1 cells were plated in a six-well plate with 0.4 μm pore transwell insert in RPMI medium containing 10 ng/mL of phorbol 12-myristate 13-acetate (Sigma Aldrich). M0 macrophages obtained after 24 hours of differentiation were then polarized for the next 48 hours in fresh RPMI medium containing 15 ng/mL of LPS and 25 ng/mL of IFNγ for M1 macrophages or 25 ng/mL of IL-4 and 25 ng/mL of IL-13 for M2 macrophages. Simultaneously, ovarian cancer cell lines (A2780 and A2780Cis) were plated in six-well plates in RPMI medium at a density of 2×10^5 cells per well. On the day of co-culture, differentiated THP-1 cells were transferred onto the top of ovarian cancer cell culture. All media were replaced with fresh RPMI and co-cultured for 24 hours. Later, co-culture medium was selectively supplemented with 2 μM of cisplatin and incubated for the next 24 hours. Cells were co-cultured in two independent repeats before testing for gene expression.

2.16. Mice

IBIP2 mice (FVB/N background) were generated by crossing the previously published iBIP mice [119] into an FVB/N line with floxed Cdnk2a alleles. iBIP2 mice have a Tet-inducible human BRAF V600E transgene, floxed alleles of

Cdkn2a and Pten, and inducible Cre expression under melanocyte specific-control. Mice were bred in-house. All experiments were performed with approval from the Veterinary Authority of the Canton de Vaud, Switzerland.

2.17. Tumor induction and measurements

To induce iBIP2 tumors, mice received one microliter of 5 mM 4-hydroxytamoxifen (70% Z-isomer, 30% E-isomer, Sigma Aldrich) dissolved in 70% EtOH topically applied on the ventral side of the ear. Upon topical application of tamoxifen, Cdkn2a and Pten were specifically deleted only in the treated melanocytes, and rtTA was activated. Subsequent continuous administration of doxycycline in the drinking water (1 mg/ml, Research Products International) activated the BRAF V600E transgene only in the cells in which the LSL-Stop-rtTA cassette, as well as Cdkn2a and Pten, were co-deleted. iBIP2 tumors were measured with a caliper, and volumes were calculated as ellipsoids ($V=4/3\times\pi\times length\times width\times height/8$). Mice were sacrificed when mice when tumor volumes were between 500 mm^3 and 1 cm^3.

2.18. Antibody injections

For checkpoint blockade therapy, mice were treated with 250 ug anti-CTLA-4 antibody (BE0164, BioXCell) every 3 days and 100 ug anti-PD-1 (BE0146, BioXCell) every 3 days. Both antibodies were rat anti-mouse. Control mice received the respective quantities of rat IgG isotype control antibodies (BioXCell).

2.19. Tumor cell isolation

Removed tumors were placed in the conical tubes in digestion buffer containing 5 mg/ml collagenase II, 5 mg/ml collagenase IV and 1 mg/ml DNase in HBSS buffer. Tumors were shredded with scissors and incubated for 30 min in 37 °C water bath. The supernatant was collected, passed through a 70 μm cell strainer and kept on ice in a separate tube. The undigested pieces of tumor were

subjected to the second round of digestion in the fresh digestion buffer for 30 min in 37 °C water bath. The suspension was pipetted every 10 minutes. Again, the supernatant was passed through a 70 μm cell strainer into the first-round digestion suspension. The suspension was 10 times diluted with FACS buffer (PBS with 2% of FBS) and centrifuged for 6 minutes at 500 g. Red blood cell lysis was performed with BD Lysing Solution (BD Biosciences) according to the manufacturer's recommendations. The suspension was filtered through a 45 μm cell strainer and centrifuged with FACS buffer for 6 min at 500 g.

2.20. Mass cytometry

The prepared single cell suspension was purified by layering on Percoll 40%/60% (Sigma Aldrich) and density centrifugation for 30 min at 450 g with no brake. The layer of viable cells between 40% and 60% fractions of Percoll was carefully aspired and washed with FACS buffer several times. Cells were incubated for 5 min with 1.5 μg/ml of cisplatin for dead cell exclusion. After 5 min centrifugation at 500 g, the cell pellet was labeled with antibodies of MAxpar Mouse Sp/LN Phenotyping Panel Kit (Fluidigm) according to the manufacturer's guidelines. Cells were then fixed with 2% paraformaldehyde for 20 min at RT. After centrifugation for 5 min at 700 g, the pellet was resuspended in 0.5 ml of DNA intercalator (Fluidigm) and incubated for 15 min at RT. The cells were then washed with ddH2O (Mili-Q water) twice. Samples were run on a CyTOF mass cytometer (Fluidigm) by the mass cytometry technician. Files were analyzed with Cytobank online software (Cytobank).

2.21. Patient cohort

A total of 40 patients with confirmed diagnosis of OC of III-IV FIGO stage with no prior cancer history or immune disorders were involved in this study. All patients underwent primary cytoreductive surgery and completed 6 cycles of adjuvant carboplatin-based chemotherapy between April 2013 and April 2015. For each patient, a pre-operative serum and surgically removed

tumor samples were collected. Clinical data were obtained from the patients' medical records. Patients were followed up until April 2018 for determining platinum status and recurrence. This study was approved by the Lithuanian Bioethics Committee. All patients signed the informed consent form.

2.22. Patient sample preparation

Serum was centrifuged at 2000 g for 10 min, aliquoted, and stored at -80 C until analysis.

Tumor tissue was collected during surgery. Fresh tissue was immediately divided into four parts for enzymatic dissociation, protein extraction, RNA extraction, and fresh-frozen backup. All samples were processed on the same day.

For preparing single cell suspension, tumor tissue was incubated in digestion solution, containing 5 mg/ml collagenase II (Sigma Aldrich), 5 mg/ml collagenase IV (Sigma Aldrich) and 1 mg/ml DNase (Worthington) in HBSS buffer for 30 min in 37 °C. After gentle pipetting, the solution was filtered, washed with PBS and treated with BD FACS Lysing solution (BD Biosciences) for red blood cell lysis.

For protein extraction, tumor tissue was homogenized and lysed with T-PER Tissue Protein Extraction Reagent (Thermo Fisher Scientific, Waltham, MA, USA), supplemented with protease/phosphatase inhibitor cocktail (Thermo Fisher Scientific), followed by 15 min centrifugation at 10 000 g and debris removal.

For RNA extraction, tumor tissue was homogenized with TRIzol Reagent from TRIzol Plus RNA Purification Kit (Thermo Fisher Scientific) and RNA was purified according to the manufacturer's protocol.

2.23. The Cancer Genome Atlas dataset

We used level 3 mRNA expression data of primary ovarian tumor specimens measured by Affymetrix U133A microarray, extracted from The Cancer Genome Atlas (TCGA) database. A total of 489 samples, containing

information about platinum resistance status and disease outcome, were selected. Data was public per TCGA policy.

2.24. Histological assessment of tumor tissue

Tissue sections from FFPE blocks were stained with hematoxylin and eosin (H&E) (Sigma Aldrich). Tumor type and grade were assessed. Qualitative evaluations for the presence of either intraepithelial or stromal T lymphocytes within tumor tissue were conducted by the pathologist.

2.25. Cytokine and chemokine measurement

Secretion of DC cytokine production (IL-12, TNFα, IL-6, IL-10, TGFβ) was measured with cytometric bead array kits, BD CBA Flex Set and BD CBA Human Soluble protein Master Buffer Kit (BD Biosciences), according to manufacturer's guidelines. Samples were collected with BD LSR II flow cytometer (Becton Dickinson) and analyzed using BD Cell Quest software (Becton Dickinson).

For cancer cell cultures, a panel of 8 cytokines (IFNγ, TNFα, IL-2, -4, -5, -6, -10, -13) was measured using LEGENDplex Human Th1/Th2 Cytokine Panel (BioLegend), according to manufacturer's guidelines. For OC patient serum and lysate samples, a panel of 13 chemokines (CCL2, -3, -4, -5, -11, -17, -20, CXCL1, -5, -8, -9, -10, -11) was measured using LEGENDplex Human Proinflammatory Chemokine Panel (BioLegend) according to the manufacturer's guidelines. Samples were assayed in duplicates in 96-well plates, collected with BD LSR II flow cytometer (Becton Dickinson) and analyzed with LEGENDplex data analysis software (BioLegend).

2.26. Flow cytometry

Single cell suspension was stained for 20 min at 4 °C with pre-titrated amounts of monoclonal antibodies (Appendix 2). Cells were collected with BD

LSR II flow cytometer (Becton Dickinson) and analyzed using BD FACSDIVA software (Becton Dickinson).

2.27. Evaluation of gene expression by real-time quantitative polymerase chain reaction

Total RNA from samples was extracted by TRIzol Reagent (Thermo Fisher Scientific) according to the manufacturer's protocol. To obtain cDNA, 500 ng of RNA from each sample was subjected to reverse transcription using Maxima First Strand cDNA Synthesis Kit (Thermo Fisher Scientific) as described in accompanying instructions. qPCR was performed in triplicate in Eco Real-Time thermocycler (Illumina, USA). The reaction volume of 10 μL contained 5 μL of Maxima SYBR Green qPCR Master Mix 2X (Thermo Fisher Scientific), 2,5 μL of 0,8 μmol/L sequence-specific forward and reverse primers mix, 1 μL of cDNA reaction product, and 1,5 μL of water. The reaction was started by 5 min at 95 °C and continued with 40 cycles of 10 s denaturing at 95 °C and 30 s of annealing/extension at 60 °C. Primer sequences are given in Appendix 1. The expression level of selected genes was evaluated, using glyceraldehyde-3-phosphate dehydrogenase (*GAPDH*) and ribosomal protein L13 (*RPL13*) as the reference genes. The analysis was performed with EcoStudy software (Illumina, USA) using ΔΔCq relative quantitation method with Pfaffl correction for PCR efficiency [120].

2.28. Statistical analysis and data visualization

Data were analyzed using GraphPad Prism 7 (GraphPad Software, USA) statistical software. All charts, except for heat maps, were plotted using GraphPad Prism 7. Where applicable, quantitative data were presented as a mean ± standard deviation. Heat maps for gene and expression profile were generated using Morpheus software (Broad Institute, USA). In cell lines experiment, log2 transformed mean relative expression levels are depicted in heat maps as color intensity and circle size variation. For ovarian patients and TCGA datasets, z-

scores of gene expression levels are depicted in heat maps as color intensity variation.

Dose-response curves were generated by curve fitting using the nonlinear regression. To combine cytokines, logistic regression was applied. Receiver operator characteristic (ROC) curves were created to determine the predictive performance of the cytokines and their combinations. The area under the curve (AUC), sensitivity, and specificity were calculated from ROC curves. Performance metrics and clinical utility were calculated and converted into qualitative grades: excellent utility >=0.81, good >=0.64, fair >=0.49, and poor <0.49, as suggested in [121].

For data with normal distribution, significance was determined using a two-tailed unpaired Student's t-test was used, and Welch correction applied where necessary. In other cases, significance was determined using the Mann-Whitney U test. In *in vitro* experiments, false discovery rate (FDR) for multiple comparisons was controlled with a two-stage step-up method of Benjamini, Krieger, and Yekutieli. In experiments with OC patients and mice, p-values were not adjusted for multiple testing, given the exploratory nature of this study. Dose-response curves were compared with extra sum-of-squares F test. The slopes for cell migration speed were analyzed using the linear regression comparison. Patient cohort clinicopathological features were compared with the chi-square test. The Kaplan-Meier survival curves and hazard ratios were analyzed with a Log-rank test. Statistically significant results in some charts are encoded as *p<0.05, **p<0.01, ***p<0.0001 or as circle borders in heat maps.

RESULTS

4.1. Effect of cancer cell lysate on dendritic cell maturation and immunostimulatory properties

4.1.1. Rationale

Tumor development is a subtle process, accompanied by the changes in the surrounding microenvironment. The tumor tissue comprises a large and diverse set of myeloid lineages. Monocytes, a part of the myeloid family, are precursors of macrophages, monocytic DCs and monocytic MDSCs [122]. The origin of DCs in the tumor remains obscure. However, it is accepted that monocytic DCs, although not derived from common DC progenitor, support the innate and adaptive immune responses, and are capable to transport the tumor antigen to lymph nodes and activate naïve T cells [49]. Their recruitment into the tumor is enhanced by inflammatory conditions and the presence of TLR ligands, which promote the expression of TNFα and iNOS by monocytic DCs. Functions of DCs depends on their maturation level. Immature DCs have strong migratory and antigen uptake capacity. Upon antigen processing, immature monocytic DCs experience a dramatic change in morphology and start exhibiting strong costimulatory and T cell activating capacity, resulting in the production of large amounts of IL-12 and preferentially inducing Th1 type response. Maturation is a terminal differentiation process that transforms DCs from cells specialized in antigen capture into cells specialized in T-cell stimulation [123]. This feature is widely exploited in designing DC-based cancer vaccines, where immunogenic and immune response-initiating properties of DCs are employed. For vaccine preparation, DCs are generated *in vitro* from monocytes, and then primed with tumor antigens. Using tumor lysate as a source of an entire repertoire of antigens is particularly useful [124].

However, the local milieu and inflammatory stimuli may skew the differentiation of immature DCs from immunogenic into tolerogenic phenotype, and thus further polarize the T cell-mediated immune response [125]. DCs may

be rendered tolerogenic by several mechanisms, including exposure to modulating substances (such as immunosuppressive cytokines IL-10 or TGFβ), inhibition of costimulatory receptor CD40, or exposure to Tregs [126]. The first step of cancer-immunity cycle, an effective exposure of DCs to neo-antigens, occurs upon immunogenic or necrotic cancer cell death, however it may be affected by the accompanied release of immunosuppressive factors. Modulation of DC maturation profile is a challenge in designing DC-based cancer vaccines, as well as overcoming the TME-exerted immunosuppression.

Despite successful maturation, the balance of immunogenic and tolerogenic properties of DC, although often omitted in DC-based vaccine studies, is critical for the proper initiation of antitumor immune response. Here, we aimed to **evaluate the effect of cancer cell lysate on dendritic cell maturation and immunostimulatory capacity** with an emphasis on the immunogenic and tolerogenic DC properties. We differentiated dendritic cells from healthy donor-derived PBMC (2.4.). Next, we measured their surface markers (2.26.) and cytokine secretion profile (2.25.) after maturation (2.5.) with or without cancer cell lysate (2.2.), composed from melanoma, renal cell carcinoma, and glioblastoma cell lines (2.1.). To evaluate the DC-induced T cell proliferation (2.7.), we co-cultured mature DCs with magnetically sorted (2.6.) and CFSE-labeled CD3+ T cells. To assess the induction of Tregs, we co-cultured (2.8.) mature DCs with magnetically sorted (2.6.) CD4+ T cells and then measured the expression of specific Treg markers by flow cytometry (2.26.).

4.1.2. Dendritic cell maturation

Although cancer cells are able to express mutated neoantigens that are detectable by antigen presenting cells, they can also orchestrate the immunosuppressive cues in the TME. We first aimed to evaluate the immunomodulatory effect of the inactivated cancer cells. We set up a model of the first and second steps of the cancer-immunity cycle by exposing *in vitro* generated immature DCs to the mix of tumor antigens in form of cancer cell

lysate. We used lysates of three human cancer cell lines characterized by high frequency of mutations – melanoma (SK-MEL-28), renal cell carcinoma (786-O), and glioblastoma (U-87). After 6 days culture of PBMC-derived monocyte with GM-CSF and IL-4, we exposed the generated immature DCs to standard maturation procedure - 24 hours incubation with LPS and IFNγ in the absence (control group) or presence of cancer cell (CC) lysate. Upon maturation, DCs receive the activation signal by LPS and uptake the antigens in the medium. In parallel, they upregulate the expression of MHC and co-stimulatory molecules, and start secreting cytokines. We compared the expression of markers representing DCs maturation state as well as cytokine secretion profile in DCs incubated with LPS only versus LPS + cancer cell lysate. IFNγ was used in both groups as an autocrine mediator of DC maturation.

Both maturation types induced typical maturation-associated morphological changes of DCs: immature DCs showed typical spindle-shaped morphology with prominent dendrites, whereas after maturation they lost their dendrites and acquired rounded shape, typical to mature DCs. The impact of CC lysates on the expression of various DC surface markers is presented in Table 1.

Table 1. Effect of different CC lysates on DC surface marker expression. Results are presented as mean percentage ± SD of marker-positive DCs in total cell population. Pooled data from 15 healthy donors is presented, unpaired two-tailed Student's t-test was used for comparison, *p<0.05, **p<0.01.

DC markers	LPS+IFN-γ	LPS+IFN-γ + SK-MEL-28	LPS+IFN-γ + 786-O	LPS+IFN-γ + U-87	LPS+IFN-γ + lysate mix
Identity					
CD14	12.2 ±1.9	12.2 ± 1.3	12.6 ± 1.7	12.2 ±1.4	12.3 ± 2.0
CD11c	96.1 ± 3.2	95.9 ± 3.3	96.5 ± 3.9	96.3 ± 4.0	96.7 ± 2.9
Maturation					
CD83	84.2 ± 6.6	79.5 ± 5.2	82.3 ± 3.5	81.3 ± 2.3	82.8 ± 1.8
Immunogenicity					
CD80	92.4 ± 7.7	89.8 ± 4.9	90.3 ± 5.2	88.6 ± 4.5	91.2 ± 3.7
HLA-DR	98.7 ± 4.6	98.1 ± 4.1	97.5 ± 4.1	97.8 ± 2.9	98.8 ± 4.2
Migration					
CD197 (CCR7)	29.6 ± 4.0	28.8 ± 4.4	27.7 ± 3.1	28.3 ± 3.6	27.9 ± 3.6
Tolerogenicity					
CD274 (PD-L1)	81.0 ± 4.4	82.2 ± 6.6	81.9 ± 5.9	83.3 ± 6.7	82.6 ± 6.7
CD85k (ILT3)	31.0 ± 4.3	61.8 ± 9.1*	60.0 ± 8.5**	59.5 ± 9.8**	61.1 ± 7.2**

The expression of markers representing DCs identity, maturation state, immunogenicity and migratory potential was identical irrespective of the presence or absence of cancer cell lysate during maturation. However, a significantly higher proportion of tolerogenic marker CD85k (ILT3), but not CD274 (PD-L1), was induced by maturation in the presence of CC lysate in comparison to the maturation in the absence of CC lysate, suggesting that various immunosuppressive components in the lysate could be responsible for such pro-tolerogenic activity. Interestingly, this effect did not depend on the histological origin of tumor cell line used for CC lysate preparation, suggesting that all three cancer cell lines may contain immunosuppressive components as part of their immune escape mechanisms. Therefore, for further experiments we only used the CC lysate mix, representing the lysates of three different cell lines, pooled in equal proportions.

We next measured the concentration of immunogenic cytokines (IL-12, TNFα, IL-6) and immunosuppressive cytokines (IL-10, TGFβ) in the DCs culture medium after 24 maturation with or without cancer cell lysate (Figure 9).

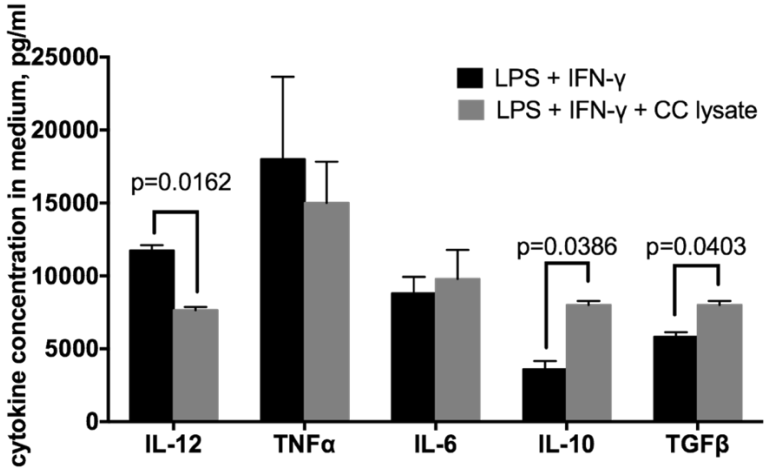

Figure 9. Dendritic cell secretory profile after maturation with or without cancer cell lysate. Cytokine concentration was measured in DC medium after 24 hours of incubation with LPS and IFNγ, in presence or absence of CC lysate mix. Results are presented as mean ± SD. Pooled data from 15 healthy donors are presented. CC lysate represents pooled lysates of SK-MEL-28, 786-O and U-87 cell lines in equal proportions. Two-tailed unpaired Student's t-test with Welch correction was used for comparisons. CC – cancer cell, LPS – lipopolysaccharide.

In the presence of cancer cell lysate, the secretion of Th1-type immune response polarizing cytokine IL-12, but not TNFα and IL-6, was significantly lower in comparison to the LPS-only group. More, the secretion of immunosuppressive tumor-promoting cytokines IL-10 and TGFβ was significantly higher in LPS+IFNγ+CC lysate group in comparison to LPS+IFNγ. Hence, DCs matured in presence of CC lysate were likely to induce the mixed Th1/Th2 type antitumor immune response. Although the maturation with CC lysate results in fully mature DCs that secrete the considerable amounts of IL-12, the upregulation of CD85k and increased production of Th2 type cytokines suggests that cancer cell lysate may have an immunosuppressive effect on antigen presenting cells.

4.1.3. Immunostimulatory capacity of mature dendritic cells

Next, we aimed at investigating the indirect effect of cancer cell lysate on the third step of cancer-immunity cycle: T cell priming and activation by DCs. We evaluated the ability of *ex vivo* generated mature DCs to stimulate T cell proliferation by one-way autologous mixed lymphocyte reaction, using CFSE-labeled CD3+ T cells as responder cells. As shown in Figure 10 A, DCs matured with LPS+IFNγ+CC lysate induced significantly higher proliferation of autologous CD3+ T cells compared to DCs matured with LPS+IFNγ, presumably due to the presence of tumor antigens that could be presented to T cells.

We next measured the induction of CD4+/CD25+/FoxP3+/CD127- Treg cells in CD4+ T cells stimulated with differentially matured DCs. We found that stimulation of CD4+ cells with DCs in the absence of cancer cell lysate resulted in a negligible increase in Treg level in comparison to baseline (isolated CD4+ T cells with no stimulation, not shown). This increase may be attributed to the stimulatory effect of IL-2 which was used during co-culture of CD4+ T cells and DCs. However, DCs matured with CC lysate induced significantly higher levels of Treg cells, potentially due to the increased secretion of IL-10 and TGFβ, that

are known as Treg inducers (Figure 10 B). Although the direct antigen-presenting activity of DCs matured with CC lysate is obvious, the CC lysate may exert an indirect immunosuppressive effect, leading towards induced stimulation of Tregs.

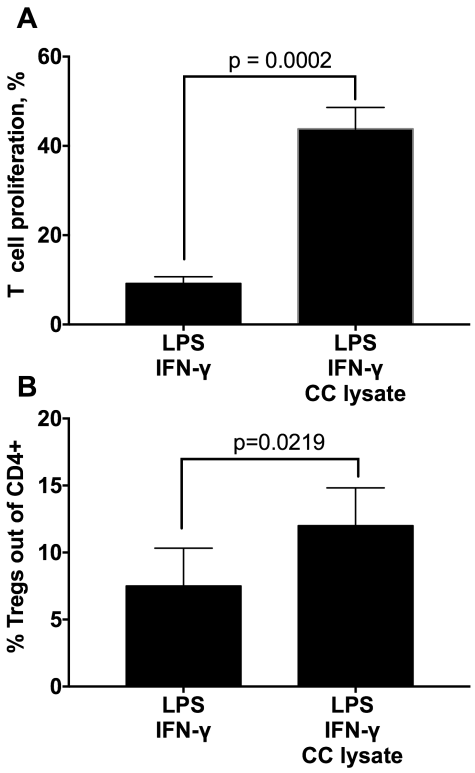

Figure 10. The immunostimulatory capacity of DCs matured in the presence or absence of cancer cell lysate. A. The proliferation of autologous CD3+ T cells was measured after 7 days of their co-culture with mature DCs. T cell proliferation was evaluated by the percentage of CD3-positive cells with flow cytometry. B. Induction of Tregs was measured after 14 days co-culture of mature DCs with magnetically-sorted CD4+ T cells in presence of IL-2. The percentage of Tregs was evaluated as the percentage of CD4+CD25+FoxP3+CD127- cells. Results are presented as mean ± SD. Pooled data from 15 healthy donors are presented. CC lysate represents pooled lysates of SK-MEL-28, 786-O and U-87 cell lines in equal proportions Two-tailed unpaired Student's t-test with Welch correction was used for comparisons. CC – cancer cell, LPS – lipopolysaccharide.

4.1.4. Discussion

Although the role of host stromal cells in tumor development is indisputable, the full picture and magnitude of microenvironmental regulation of cancer-related processes is not yet fully understood. Here, we addressed first, second, and third steps of cancer-immunity cycle by investigating the monocyte-derived DCs upon classical maturation with LPS versus maturation with the addition of cancer cell lysate, a mix of specific tumor antigens from melanoma, glioblastoma, and renal cancer cell lines. We also emphasized a frequently disregarded feature - the tolerogenic properties of mature DCs.

In vitro DC maturation with different molecular or cellular stimuli is an approach relevant to both understanding the mechanistic relationship between these two components, as well as to the design of DC-based cancer vaccines. The limited clinical success of this kind of immunotherapy partially depends on the lack of successful maturation strategies, that would result in highly immunogenic DCs capable to initiate the antitumor immune response. The combination of LPS and IFNγ has eventually become one of the most widely used maturation choice for generating mature DCs, as LPS is a prototypical pathogen-associated molecular pattern and TLR4 agonist [127]. Cancer cell lysate, as a source of tumor antigens, is a potent DC maturation agent, except for the cases of immune escape that results in the loss of antigens during immunoediting process [10]. To minimize this effect, we used the mix of lysates from three different cell lines. However, tumor lysates may possess various immunosuppressive components that interfere with the immunogenic maturation and even promote tolerogenic maturation of human or murine DCs [128,129]. In our study, we observed the similar trend. Although cancer cell lysate did not affect the level of immunogenic markers, the expression of tolerogenic marker CD85k was significantly higher upon maturation in presence of the tumor antigen source, independent on histological origin of cancer cell line. CD85k-expressing DCs were shown to anergize CD4+ T cells and elicit their differentiation to Tregs [130], similarly as in our study. Considering this data, we anticipated that increased level of CD85k on lysate-matured DCs may be associated with lower immunostimulatory potential, as seen from the cytokine expression profile, where we noticed the increased production of IL-10 and TGFβ, but not IL-12, oppositely to DCs matured in the absence of lysate, similarly as shown in previous studies [131].

In conclusion, our findings demonstrate that maturation with CC lysate induces a typical mature DC surface phenotype, as well as considerable production of IL-12 and overall T cell stimulation, however, it may also promote a mixed Th1/Th2 type antitumor response and thus render DCs more tolerogenic. Although this effect did not depend on the histological origin of

cancer cells, our results provide a background for further investigation of potential immunomodulatory cancer cell properties, such as level of differentiation or stemness potential.

4.2. Influence of cancer cell stemness capacity on macrophage polarization

4.2.1. Rationale

In the previous chapter, we investigated the influence of cancer cells of different histological origins on the maturation and polarization of monocyte-derived DCs. Quantitative analyses of tumor tissue composition revealed the heavy infiltration of yet another monocyte-derived cell type, macrophages, in cancers of different origins [132,133]. Macrophages are essential immune cells, playing a critical role in carcinogenesis and tumor progression [134]. They are highly plastic cells that undergo different functional reprogramming in response to various stimuli, M1-type (classically activated) and M2-type (alternatively activated) being the polarized extremes of the spectrum. The contexture of immune infiltrate in the tumor tissue is associated with cancer prognosis and response to treatment. In cancer, M1-type and M2-type macrophages are considered as anti-tumoral and tumor-promoting, respectively, based on their cytokine secretion profile [135]. Studies indicate that cancer cells are capable of recruiting circulating monocytes into tumors [136,137]. Macrophages, in turn, secrete a wide array of angiogenesis-promoting and other growth factors, shaping a complex interplay between the cancer cells and TME [138].

Recently, macrophages were reported to participate in the regulation of EMT in the breast, pancreatic and hepatocellular carcinomas [139–141]. EMT is a process that allows the functional plasticity of an epithelial cell, characterized by a gradual decrease of epithelial markers, cytoskeleton remodeling and gain of invasive mesenchymal morphology and phenotype. Activation of EMT requires reprogramming of gene expression. Loss of a critical epithelial adhesion molecule, E-cadherin, is orchestrated by the series of TFs, including Snail, Slug, ZEB1, Twist and FOXC2 [142]. In many cancer types, EMT is associated with

increased plasticity, motility, invasion and resistance to therapy [143]. EMT was also shown to be linked to CSC formation, as cancer cells may acquire stemness properties through the activation of the EMT [34]. The emergence of CSCs, a subpopulation of cancer cells able to self-renew and promote tumor evolution, promotes the tumor heterogeneity and expands the pool of potential therapeutic targets.

Despite recognition of CSCs as a major contributor to the diversity of neoplastic cells, it is to a great extent unknown how they participate in shaping of the immune TME. Here, we aimed to **determine the macrophage polarization ability in colon cancer cell lines with varying levels of stemness traits**. We evaluated the CSC- and EMT-related transcription profile of five colon cancer cells lines (2.1.) by qPCR (2.27.). For each cell line, we prepared the conditioned medium (2.3.). We measured the Th1/Th2 cytokine level (2.25.) in both cell lysate (2.2.) and conditioned medium. Next, we differentiated the macrophages from healthy donor-derived PBMCs (2.4.), cultured them with either classical M1 or M2 phenotype inductors or cancer cell-conditioned medium (2.9.), and evaluated the expression of M1/M2 macrophage markers by flow cytometry (2.26.).

4.2.2. Characterization of the stemness-related expression profile in colon cancer cell lines

Studies of cancer cell lysate influence on DCs proved that, despite being the source of tumor antigens and inducing T cell proliferation through DCs, cancer cells are also able to induce the tolerogenicity and immunosuppressive features of DCs. We next aimed at investigating if cancer cells alone can modulate the differentiation of another monocyte-derived cell type, macrophages. In cancer cell lysate experiments, we used pool cancer cell lysates from cell lines representing several different localizations. Here, we chose a single localization – colon cancer – as it represents one of the most heterogeneous tumor types.

To test the interaction of cancer and immune cells, we selected five colorectal adenocarcinoma cell lines of different reported molecular subtypes: HT29, SW620, NCI-H508, COLO320, and HCT116 (Table 2). Several independent groups tried to classify colorectal tumors and cell lines based on their gene expression profile. One of the most prominent, Sadanandam et al. classification, distinguished five clinically relevant molecular subtypes, associated with the distinctive anatomical regions of the colon crypt and the degree of stemness [144]. According to this classification, COLO320 and HCT116 represent the least differentiated stem-like subtype with upregulated Wnt pathway and high expression of stem cell and mesenchymal markers. HT29 represents a well-differentiated epithelial goblet-like subtype with low expression of stem cell markers. NCI-H508 and SW620 represent a moderately differentiated heterogeneous transit-amplifying subtype with variable expression of stem cell and Wnt-target genes. Other authors fully or partially confirmed these findings, agreeing that COLO320 and HCT116 cell lines represent stem-like or mesenchymal subtype. Budinska et al. and Roepman et al. also attribute the SW620 cell line to this group [145,146]. Marisa et al. reported upregulated Wnt pathway in SW620 cell line [147]. HT29 and NCI-H508 were characterized as differentiated epithelial-like subtypes with downregulated immune-related genes.

Table 2. Molecular subtypes of selected colon cancer cell lines. The table summarizes the original molecular subtypes, proposed by several independent classifications.

	HT29	**SW620**	**NCI-H508**	**COLO320**	**HCT116**
Sadanandam subtypes [144]	Goblet-like	Transit-amplifying	Transit-amplifying	Stem-like	Stem-like
Marisa subtypes [147]	CIN ImmuneDown	CIN WntUp	CIN ImmuneDown	Stem-like	Stem-like
Budinska subtypes [145]	Hyper methylated	Mesenchymal	Surface crypt-like	Mesenchymal	Mesenchymal
Roepman subtypes [146]	MMR-deficient epithelial	Mesenchymal	Proliferative epithelial	Mesenchymal	Mesenchymal

CIN – chromosome instability, MMR – mismatch repair system.

In our study, we followed the Sadanandam et al. molecular subtyping, which classifies HT29 as non-stem-like well-differentiated subtype; COLO320 and HCT116 as stem-like poorly differentiated subtype; and SW620 and NCI-H508 as cells with intermediate differentiation potential and variable stemness properties. To confirm this categorization, we performed the qPCR analysis of mRNA expression of selected stemness- and EMT-associated TFs and markers (Figure 11). Indeed, HT29 cell line was characterized by low level of stemness and mesenchymal markers, with high mRNA expression of epithelial protein E-cadherin (*CDH1*). Intermediate SW620 cell line had low expression of all genes, whereas NCI-H508 had higher expression of stemness TF *SOX2*, several EMT TFs – *SNAI1* and *SNAI2*, and the gene coding for mesenchymal-associated protein *VIM*. Poorly differentiated COLO320 had high expression of CSC TFs and some EMT proteins, whereas HCT116 had high expression of several EMT TFs, as well as *NOTCH1*. Both cell lines had low *CDH1*, which is one of the hallmarks of EMT.

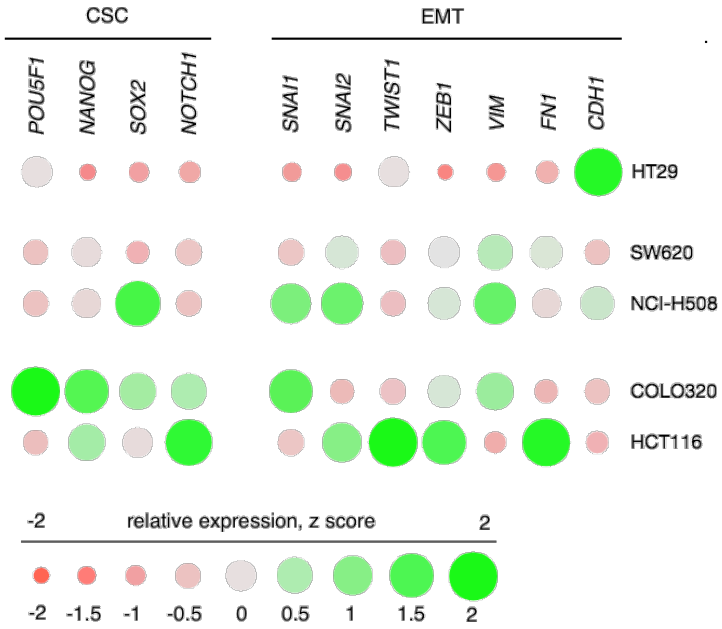

Figure 11. Expression profile of colon cancer cell lines. We measured the relative expression of selected genes in colon cancer cell lines with qPCR. The relative expression levels, transformed to z-scores, are depicted as color intensity and circle size variation. Each circle represents the mean relative expression value from two independent measurements with three technical repeats, normalized to the expression level of *GAPDH* and *RLP13A* housekeeping genes. CSC – cancer stem cells, EMT – epithelial-mesenchymal transition.

Our results support the Sadanandam et al. grouping and allow to classify these cell lines as models of cancer cells of different stemness potential, and address them as stem-like poorly differentiated cells (COLO320, HCT116), epithelial-like well differentiated cells (HT29), or cells with intermediate differentiation and stemness potential (NCI-H508, SW620).

4.2.3. Polarization of colon cancer cells-conditioned macrophages

To test the potential of cell lines with different differentiation and stemness capacity to polarize macrophages, we set up a culture of PBMC-derived and differentiated macrophages in medium with 1:1 ratio of FBS-supplemented RPMI and serum-free colon-cancer cell line-derived conditioned medium representing the secretome of these lines. This indirect culture model system was chosen to minimize the effect of macrophages on cancer cell secretome. We performed the conditioning for 48 hours. As controls, we treated M0 macrophages with IFNγ and LPS for classical M1 polarization, or with IL-4 and IL-13 for alternative M2 polarization. Afterward, we measured the expression of representative M1 and M2 markers by flow cytometry. To evaluate the polarization of conditioned macrophages, we compared the surface marker expression with the expression of control M1 or M2 macrophages. The cytometry spectra are presented in Figure 12 and median fluorescence intensities in Table 3.

Culturing M0 macrophages with colon cancer cell medium could not induce classical M1 markers, such as co-stimulatory molecules CD80 or CD86, or activation marker CD69. However, the increase of CD274 was noted in almost all tumor-conditioned macrophages, although the level of this marker did not reach the M1 level and stayed rather the same as in M2 polarized macrophages. In NCI-H508-conditioned macrophages, the level of CD274 remained similar as in M0 macrophages. The level of CD206 marker in tumor-conditioned macrophages was increased, in comparison with M0. HCT116 and COLO320 cell line secretomes induced the highest CD206 expression in

macrophages, similarly as in control M2 macrophages. Another feature of M2 macrophages is the loss of HLA-DR, CD197, CD11c and CD195 markers.

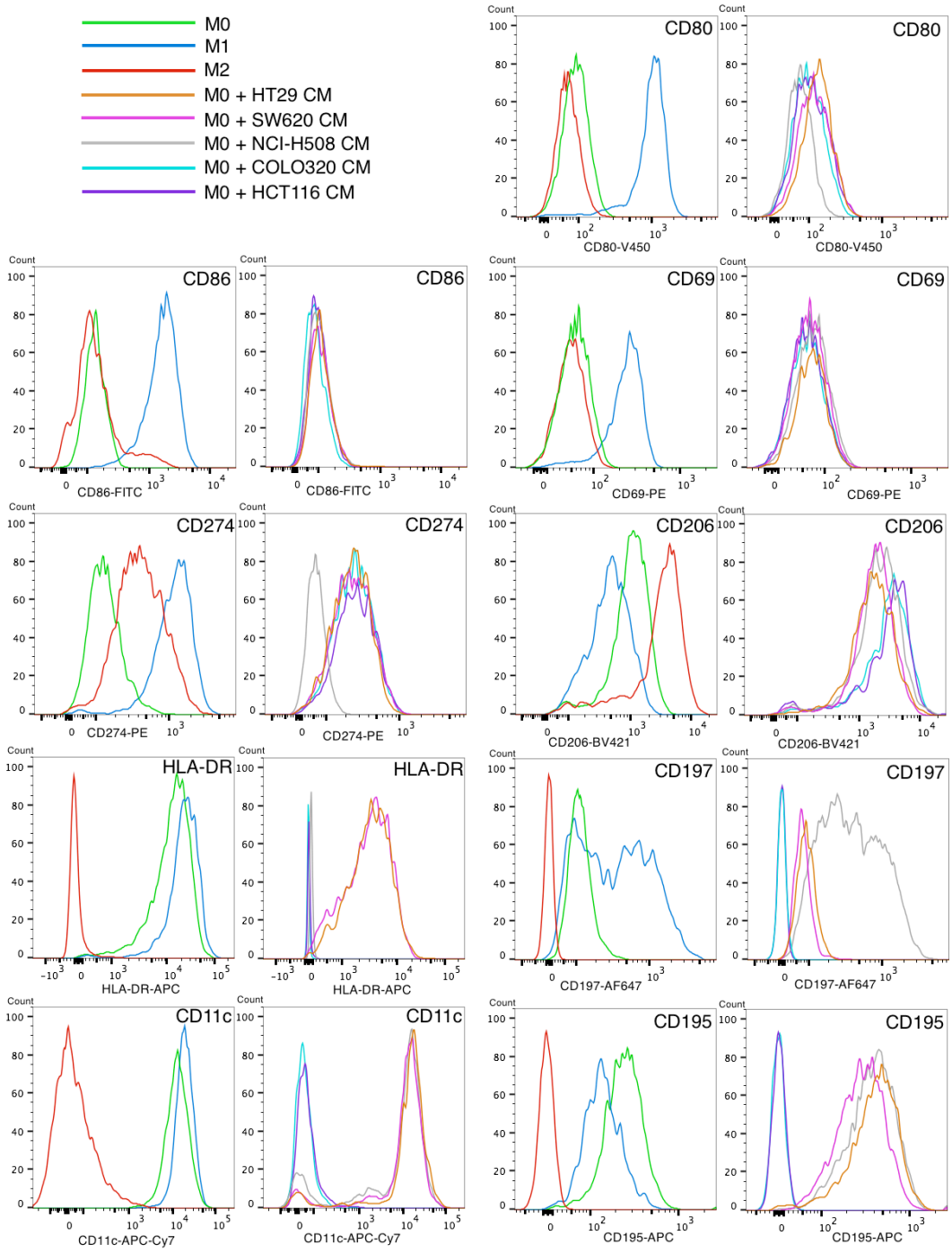

Figure 12. The polarization of tumor-conditioned macrophages. We measured the expression of selected macrophage markers by flow cytometry in PBMC-derived and polarized M0, M1 and M2 macrophages (left panel for each marker), as well as in M0 macrophages, co-cultured with colon cancer cell conditioned medium (CM) (right panel for each marker). The experiment was repeated twice with two technical repeats. Representative spectra are depicted, varying in color for each condition.

Only COLO320- and HCT116-conditioned macrophages had no expression of all four of these markers. HT29- and SW620-conditioned macrophages retained the initial level of these markers. NCI-H508-conditioned macrophages lost the HLA-DR expression (M2-like feature) but had the CD197 expression increased (M1-like feature).

Table 3. Median fluorescence intensities of control M0, M1, M2 or tumor-conditioned macrophages, labeled with antibodies against macrophage surface markers. The experiment was repeated twice with two technical repeats. Color legend is given below for better visual perception.

	M0	M1	M2	M0 with HT29 CM	M0 with SW620 CM	M0 with NCI-H508 CM	M0 with COLO320 CM	M0 with HCT116 CM
CD80	99	1186	66	145	97	71	101	114
CD86	149	1686	143	113	42	112	87	108
CD69	59	302	50	75	33	73	59	57
CD274	152	1396	442	258	204,5	61	266	284
CD206	1077	496	3474	1772	1549	1665	3132	3325
HLA-DR	15721	27728	-77	3378	2422	72	-1	14
CD197	123	927	0	93	77	823	-2	0
CD11c	18499	12826	35	16639	12000	15574	37	48
CD195	254	183	-2	432	218	400	-1	0

Color legend: M0 | M1 | M2 | M0 and/or M2 | M0 and/or M1

CM – conditioned medium.

On the whole, only stem-like poorly-differentiated cell lines COLO320 and HCT116 seemed to clearly induce the M2 polarization of M0 macrophages. HT29, SW620, and NCI-H508 cells did not sharply induce neither M1 nor M2 properties. To test if stem-like cells were secreting specific polarizing factors into the medium, we measured the concentration of several Th1/Th2 cytokines, that are known to be able to induce the M1- or M2-type macrophage polarization, respectively. We evaluated the concentration of selected cytokines in the conditioned medium (prior to macrophage culture) (Figure 13). We detected the significantly higher level of Th2 cytokines IL-10 and IL-13 in the growth medium of COLO320 and HCT116 in comparison to non-stem-like cell lines. More, the Th2 cytokine IL-5 was present in the growth medium of COLO320 and HCT116 as well as in, but not in HT29 or NCI-H508. The Th1 cytokine, TNFα, was high in COLO320, but low or absent in other cell lines

growth media. However, the differences in IL-5 and TNFα expression were not statistically significant.

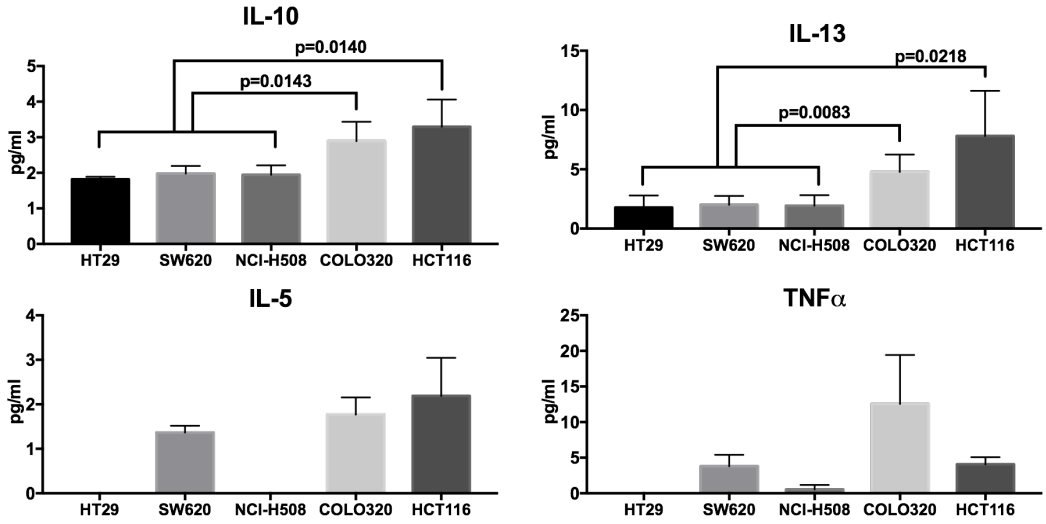

Figure 13. Expression of selected Th1/Th2 cytokines in colon cancer cell line-conditioned media. Cytokine concentrations were measured with multiplex flow cytometric bead assay. Bars represent the mean concentration of cytokine ± SD, N=3. Two-tailed unpaired Student's t-test was used for comparisons.

As shown above, none of the cell lines were able to induce M1-like macrophage polarization, except for the culture of macrophages with COLO320 or HCT116 growth media induced the M2-like polarization, based on the surface marker expression profile. Also, these two cancer cell lines produce and secrete significantly higher quantities of Th2 cytokines, IL-10 and IL-13. These findings support the hypothesis that stem-like poorly-differentiated cancer cells have a higher potential of polarizing macrophages into the tumor-promoting M2 subtype.

4.2.4. Discussion

We assessed how stemness and EMT properties influence the ability of cancer cells to affect the formation of the TME, in terms of secreted cytokine profile and interactions with macrophages. For this purpose, we determined how stemness properties influence the ability of colon cancer cell lines to induce phenotypical polarization of macrophages. We classified the colon cancer cell

lines based on Sadanandam et al. subtyping [144]: poorly differentiated stem-like HCT116 and COLO320, well-differentiated epithelial goblet-like HT29, and intermediate stemness potential SW620 and NCI-H508. We assessed their production and secretion of Th1 and Th2 cytokines and studied the phenotype of PBMC-derived macrophages, conditioned with cancer cell medium.

Macrophages play a contradictory role in colon cancer: the general macrophage infiltration was found to be associated with both better [148–150] and worse prognosis [151,152]. Nevertheless, these studies agree that macrophages have both pro-tumorigenic as well as antitumorigenic properties in colon cancer. Their prognostic value highly depends on the M1/M2 phenotype and is influenced by the TME [153]. In our study, we extend this hypothesis by showing that stem-like colon cancer cell lines HCT116 and COLO320 have better potential to induce PBMC-derived macrophage polarization than the non-stem-like cell lines SW620, NCI-H508 or HT29. *In vitro* studies have shown the ability of colon cancer cells to induce macrophage polarization, which is one of the reasons behind the formation of immunosuppressive microenvironment and tumor promotion. Some mechanisms behind this process were proposed, such as active EGFR or IL-6 signaling being necessary to promote M2-like polarization in HCT116-conditioned macrophages [154,155]. The role of colorectal cancer-derived extracellular vesicles as signaling units able to affect macrophages is also highlighted: SW620-derived extracellular vesicles were shown to induce IL-10 secretion in monocytes or macrophages [156], and prolonged contacts with EVs enabled the development of regulatory IL-12-secreting macrophage subset [157].

During the EMT process, cancer cells acquire mesenchymal characteristics, such as the expression of specific cell-surface proteins, activation of TFs, ability to migrate and invade other tissues [38]. The classical mesenchymal stem cells (MSC) are known to modulate the M1/M2 balance of macrophages by mechanisms such as cell-to-cell contact, secretion of regulatory cytokines, expression of inhibitory membrane molecules, and induction of cell anergy and apoptosis [158]. Adipose-derived MSCs secrete EVs, internalized by

responding bone marrow-derived macrophages, eliciting their switch from M1 to M2 phenotype [159]. Bone marrow-derived MSCs were also able to reprogram M1 macrophages into M2 by altering their metabolic status [160] or cell-to-cell contact [161]. Our findings also support the implication that mesenchymal-like cancer cells are prone to induce M2 polarization *in vitro*. However, there are little studies that compare the macrophage polarizing potential of cells with different level of stemness or mesenchymal properties. One of the few examples is the ability of ovarian cancer stem cells to induce the M2 polarization, unattainable to non-cancer stem cells [162], or the feature of more aggressive mesenchymal-like breast cancer cell line MDA-MB231, secreting high levels of M-CSF, to skew macrophages toward the M2 subtype, oppositely to less aggressive cell lines T47D or MCF-7 [163,164]. Our study not only compared the polarization of macrophages, conditioned with colon cancer cell lines of different molecular subtypes and differentiation level but also highlighted the production and secretion of IL-10 and IL-13 in cancer cells as the possible mechanism of M2-phenotype induction. The M2 phenotype can be further subdivided into M2a, M2b, M2c, M2d, and tissue-resident subtypes [59,165]. According to the upstream signaling determining the functional M2 subtype, IL-10 alone can induce M2c type macrophages, IL-13 alone – M2a type macrophages, whereas the combination of IL-10 and IL-13 can induce the tissue-resident macrophage subtype, which is likely the case in conditioning the macrophages with cancer cells growth medium.

In conclusion, we suggest that stem-like colon cancer cells produce and secrete elevated levels of IL-10 and IL-13 and are more likely to polarize macrophages towards tumor promoting M2 phenotype in comparison to non-stem-like colon cancer cells. Although we only used the cancer cell secretome and investigated its unidirectional influence, our findings provide background for further studying the bidirectional interplay between macrophages and cancer cells.

4.3. Interplay between ovarian cancer cells and macrophages

4.3.1. Rationale

In the previous chapter we have shown that the factors, secreted by the stem-like cancer cells, are able to *in vitro* induce M2 macrophage polarization and thus promote tumor growth. Upregulated stemness and EMT properties may lead to the emergence of CSC, which, through the ability to self-renew and promote tumor evolution, contribute to the diversity of neoplastic cells. The heterogeneity of cells in the tumor expands the pool of potential therapeutic targets while decreasing the effectiveness of monotherapies. More, CSCs are intrinsically more resistant to chemotherapy, making poorly differentiated tumors harder to treat [34].

Along with multiple chemotherapy-resistance acquisition mechanisms, associated with genetic changes in tumor cells [166,167], the microenvironmental adaptation was recently proposed as another level of complexity to overcome in cancer treatment [168,169]. Immunosuppression was shown to support the chemotherapy resistance in carcinomas of various origin [170–172]. *In vivo* studies have revealed that macrophages can regulate tumor cell survival pathways; both by secreted factors and cell-cell contacts [173]. However, the interactions of cancer cells and macrophages in the context of anticancer therapy and resistance development are to a great extent unknown.

Here, we aimed to **study the bidirectional interplay between macrophages and ovarian cancer cell lines of varying level of chemotherapy resistance.** We generated the drug-resistant ovarian cancer cell line from the parental A2780 line (2.1.) by treating it (2.11.) with cisplatin (2.10.). We evaluated the toxicity profile (2.12.), morphology, motility (2.13.), clonogenicity (2.14.), cytokine production (2.25.) and gene expression profile (2.27.) of both cell lines. Next, we set up the co-culture with THP-1 cell line (2.1.) derived and polarized macrophages alone or in presence with chemotherapeutic agents (2.15.). We evaluated the transcriptome changes in both cancer cells and macrophages (2.27.).

4.3.2. Development of cisplatin-resistant ovarian cancer cell line

After showing the ability of stem-like cancer cells to *in vitro* induce M2 macrophage polarization and thus promote tumor growth, we next aimed to assess how these findings translate into the more clinically-relevant co-culture model of cancer cells and macrophages in presence of a chemotherapeutic drug. Here, we investigated how cisplatin resistance mediates the crosstalk between macrophages and ovarian cancer (OC) cells. For this, we aimed to develop drug resistance in OC cells by exposing them to increasing drug concentrations. We used a cisplatin-sensitive OC cell line A2780, derived from a solid well-differentiated chemotherapy-naïve ovarian tumor [174]. We intermittently treated the cells with cisplatin, a first-line chemotherapy drug used for OC treatment, while escalating the dose over time for nearly a year, until we noticed a growth adaptation and apparent change in cell morphology. The newly developed cell line was called A2780Cis.

To confirm the resistance profile, we performed a luminescence-based drug toxicity screening. After 24 hours of treatment with cisplatin (1.67-333 μM) and 24 hours of rest in drug-free medium, we measured cell viability, generated dose-response curves (Figure 14) and derived IC_{50} value. IC_{50} of parental A2780 was 17.6 μM, whereas IC_{50} of derived cisplatin-resistant A2780Cis was 62.2 μM, making it 3.5 times more resistant than the original cell line.

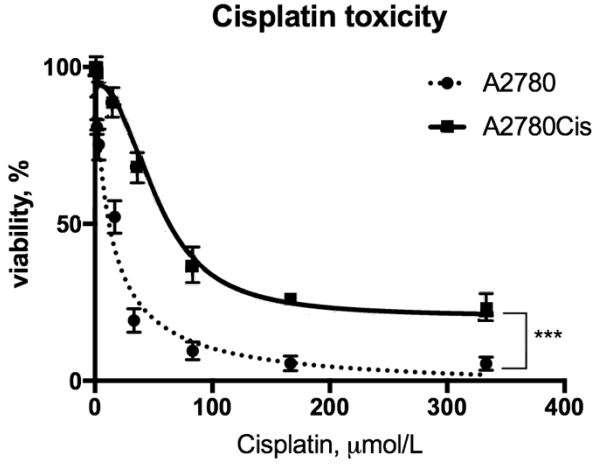

Figure 14. Development of *in vitro* model of drug resistance. We developed a resistant cell line A2780Cis by treating the parental cell line A2780 with cisplatin. We measured cell survival after 24 h treatment with increasing drug concentration using viability assay. Dose-response curves were generated by logistic regression analysis. Inhibitory concentration 50% (IC_{50}) values were deduced from dose-response curves. N=3, mean ± SD, extra sum-of-squares F test. ***p<0.0001, ns – non-significant.

Based on the results of drug toxicity profile, we succeeded in developing a drug-resistant cell line. In further sections we will refer to parental and derivative cell lines as models, representing different levels of cisplatin resistance: sensitive A2780 and resistant A2780Cis.

4.3.3. Molecular and functional characterization of ovarian cancer cell lines

We aimed to characterize a cisplatin-sensitive A2780 and its derivative, cisplatin-resistant A2780Cis, at molecular and functional level. We focused on exploring the stemness-, multidrug resistance (MDR)- and EMT-related features, which are reported to be the possible contributors to anticancer drug resistance [34,38,175]. Also, we evaluated the production of Th1/Th2 cytokines in these cell lines.

Changes in morphology were the first sign of acquisition of drug resistance. At the endpoint, in resistant cell line A2780Cis we observed the acquisition of mesenchymal, spindle-shaped morphology, while parental A2780 cell line remained rounded and epithelial-like (Figure 15 A). These alterations suggested that A2780Cis may undergo EMT-like processes during exposition to chemotherapeutics.

Colony formation is a substantial feature of CSC that represents the ability of cancer cells to restore the population. We determined the fraction of colony-forming units in cell lines by seeding them at the low density. Cisplatin-resistant cell line formed significantly more colonies compared to parental cisplatin-sensitive cell line (Figure 15 B).

Wound healing assay reflects cellular motility. We monitored the wound closure for 24 hours and found that the drug-sensitive cell line A2780 demonstrated significantly lower motility in comparison to drug-resistant cell line (Figure 15 C).

Resistant cells produced significantly more Th1 (IL-2, IL-6, TNFα) and Th2 (IL-10, IL-4, IL-5, IL-13) cytokines than the parental sensitive cell line (Figure 16).

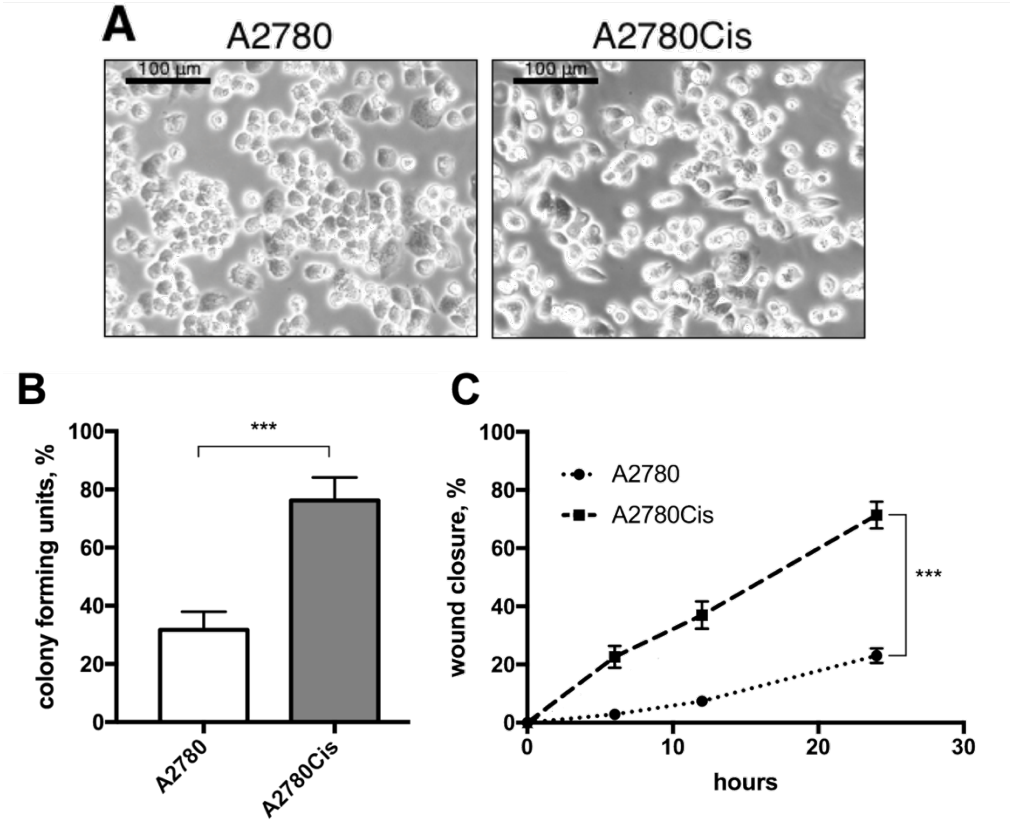

Figure 15. Characterization of cisplatin-sensitive and -resistant cell lines. A. Representative microscopy images of parental and derivative cells, taken at 20× magnification. B. Cells were plated at low density and allowed to grow for 7 days. Colonies were stained with crystal violet and counted. The ratio of colony forming units to the number of cells plated is presented in the bar graph as mean ± SD, N=6, unpaired Student's t-test. C. We monitored the closure of a scratch in a monolayer culture for 24 hours. The speed of wound closure is presented as a line chart. N=4, mean ± SD, linear regression comparison, ***p<0.0001.

Next, we examined a panel of key human CSC, MDR and EMT markers at the mRNA level. We observed a significant increase in *SOX2, POU5F1, NANOG, SNAI1, SNAI2, ZEB1, ABCG2* gene expression level in A2780Cis in comparison to A2780 (Figure 17 A). Also, A2780Cis demonstrated another EMT-characteristic feature, the reduction in *CDH1* mRNA.

Altogether, we observed that cisplatin-resistant OC cell line had mesenchymal morphology, increased migratory and clonogenic potential together with the upregulated mRNA expression of TFs characteristic of CSC and EMT, as well as higher production of cytokines participating in the immune processes. Collectively our data suggest that development of cisplatin resistance

in A2780 cell line is associated with the acquisition of mesenchymal phenotype and potential immune function.

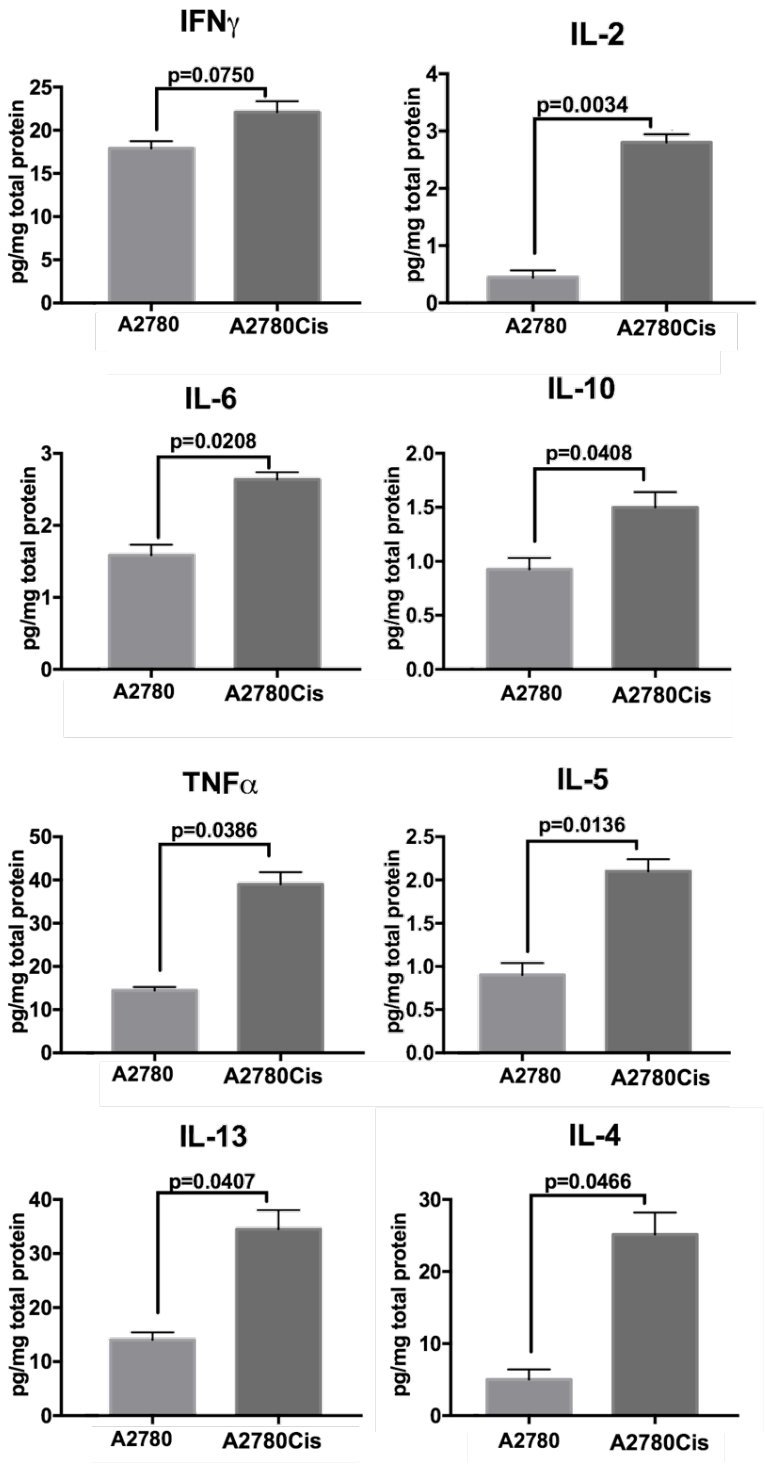

Figure 16. Expression of selected Th1/Th2 cytokines in ovarian cancer cell lysates. Cytokine concentration was measured with multiplex flow cytometric bead assay. Bars represent the quantity of cytokine per mg of total protein in the lysate. Results are presented as mean ± SD, N=2. Two-tailed unpaired Student's t-test was used for comparisons.

4.3.4. Ovarian cancer cells mRNA expression profile upon co-culture with macrophages

Next, we examined how drug-sensitive and -resistant cells react to the presence of a chemotherapeutic agent in medium (2 μM of cisplatin), or indirect co-culture with macrophages, or the combination of both.

M0-, M1- and M2-like macrophages were generated from the THP-1 cell line using standard differentiation and polarization protocols. Inserts containing polarized macrophages were transferred onto the cancer cell culture for 48-hour long indirect co-culture. To investigate the combined effect of macrophages and chemotherapy, we added 2 μM of cisplatin to the medium after the 1st day of co-culture.

We determined the changes in the expression of a panel of CSC-, MDR-, EMT-, and drug response-related genes in OC cells under different conditions (Figure 17 B). In general, we observed that the cisplatin-sensitive A2780 cell line was susceptible to gene expression changes after chemotherapy treatment and co-culture with macrophages. Cisplatin treatment induced considerable changes in CSC, MDR and EMT markers expression. Co-culture with macrophages induced upregulation of CSC TFs and *ABCG2*. When co-cultured with macrophages in the presence of cisplatin, cancer cells upregulated EMT TFss and downregulated *CDH1*, independently on macrophage polarization.

In A2780Cis, addition of cisplatin induced the upregulation of *NANOG* and *TWIST1*. Macrophages promoted the upregulation of *ABCC1, ZEB1* and *VIM*. However, the combination of chemotherapy and macrophages did not act synergistically. Co-culture with M0 in presence of cisplatin resulted in more CSC and EMT promoting changes than with M1 or M2 in the same setting. Co-culture with M1 in the presence of cisplatin reduced the mRNA level of CSC-relateds.

However, short-term co-culture with macrophages does not influence the ovarian cancer cells' cisplatin resistance level (not shown), although it already induces the changes in CSC, MDR and EMT-related gene expression profile of cisplatin-sensitive, but not -resistant cell lines.

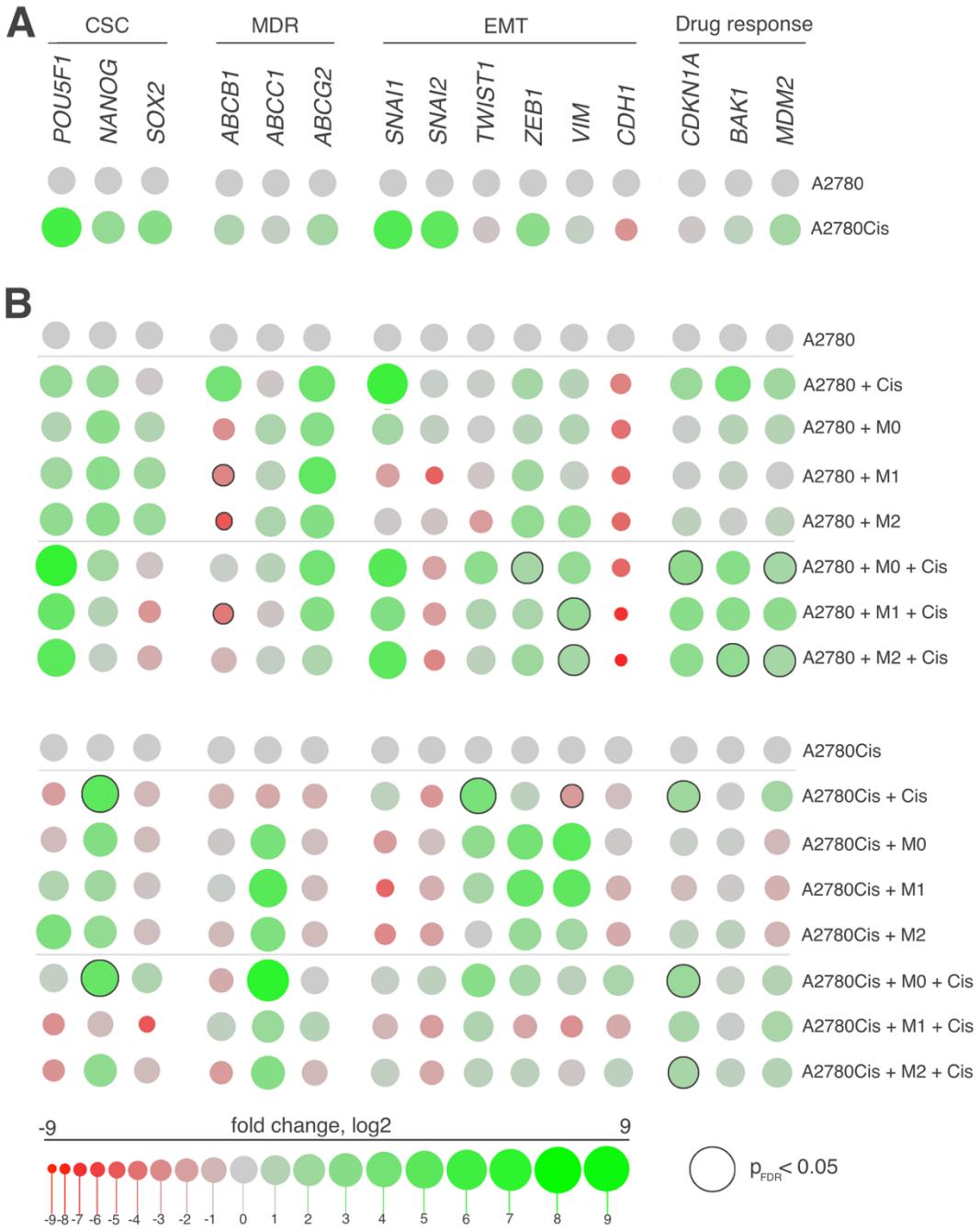

Figure 17. Stemness, drug-resistance and EMT marker expression profile in cancer cells. A. Profiling of selected genes in cisplatin-sensitive versus -resistant cell line. B. Profiling of selected genes in cancer cells upon treatment with 2 μM cisplatin or upon 48 h transwell co-culture with THP-1-derived macrophages in presence of cisplatin (2 μM). The log2 transformed relative expression levels are depicted as color intensity and circle size variation. Each circle represents the mean relative expression value from two independent experiments with two technical repeats, normalized to the expression level in A2780 (A) or the corresponding untreated cell line (B). The border indicates statistical significance (two-tailed unpaired Student's t-test with FDR correction $p<0.05$). CSC – cancer stem cells, MDR – multidrug resistance, EMT – epithelial-mesenchymal transition.

4.3.5. Macrophage mRNA expression profile upon co-culture with ovarian cancer cells

We aimed to dissect how cisplatin and OC cells of different platinum resistance status contribute to molecular characteristics of macrophages. We differentiated a monocytic cell line THP-1 into M0 macrophages by PMA and later polarized them to M1- (LPS+IFNγ) or M2- (IL-4+IL-13) type. To confirm the phenotype of these macrophages, we measured the mRNA levels of specific M1/M2 markers and selected five significantly upregulated genes of each phenotype for further monitoring (Figure 18 A). The expression of these markers was examined in macrophages in the co-culture system with cancer cells.

We observed the increase of M2-related markers in both M0- and M1-type macrophages under co-culture with cancer cells conditions (Figure 18 B). Additionally, a significant decrease in the expression of M1-related markers in M1-type macrophages was noted.

In M0-type macrophages, cisplatin increased the upregulation of M1 marker *IL6* and M2 markers *CLEC7A, MRC1 CCL22* expression. Co-culture with cell lines induced the upregulation of *CLEC7A*, and this increase also remained significant in combination with cisplatin. Altogether, both cell lines induced several significant modifications of M2 markers. Adding a drug to co-culture with A2780Cis did not influence the trends of expression, however, in co-culture with A2780, adding cisplatin resulted in synergy and upregulated even more M2 macrophage markers.

In M1-type macrophages, cisplatin downregulated expression of *CD274, IL-6*, and *HLA-DRA*, without inducing M2-type markers. Both cell lines influenced at least two M2-related genes, among them, *CCL22,* and decreased M1 markers, such as *CD274* and *HLA-DRA*. Adding cisplatin to co-culture with A2780 did not affect the expression profile, however, in co-culture with A2780Cis, it induced the *MRC1* expression.

In M2-type macrophages, the magnitude of changes in gene expression was less evident. Occasional changes in the expression of M1-related markers were noted, e.g., upregulation of *IL-6* and *TNF* in co-culture with A2780. *CD163*

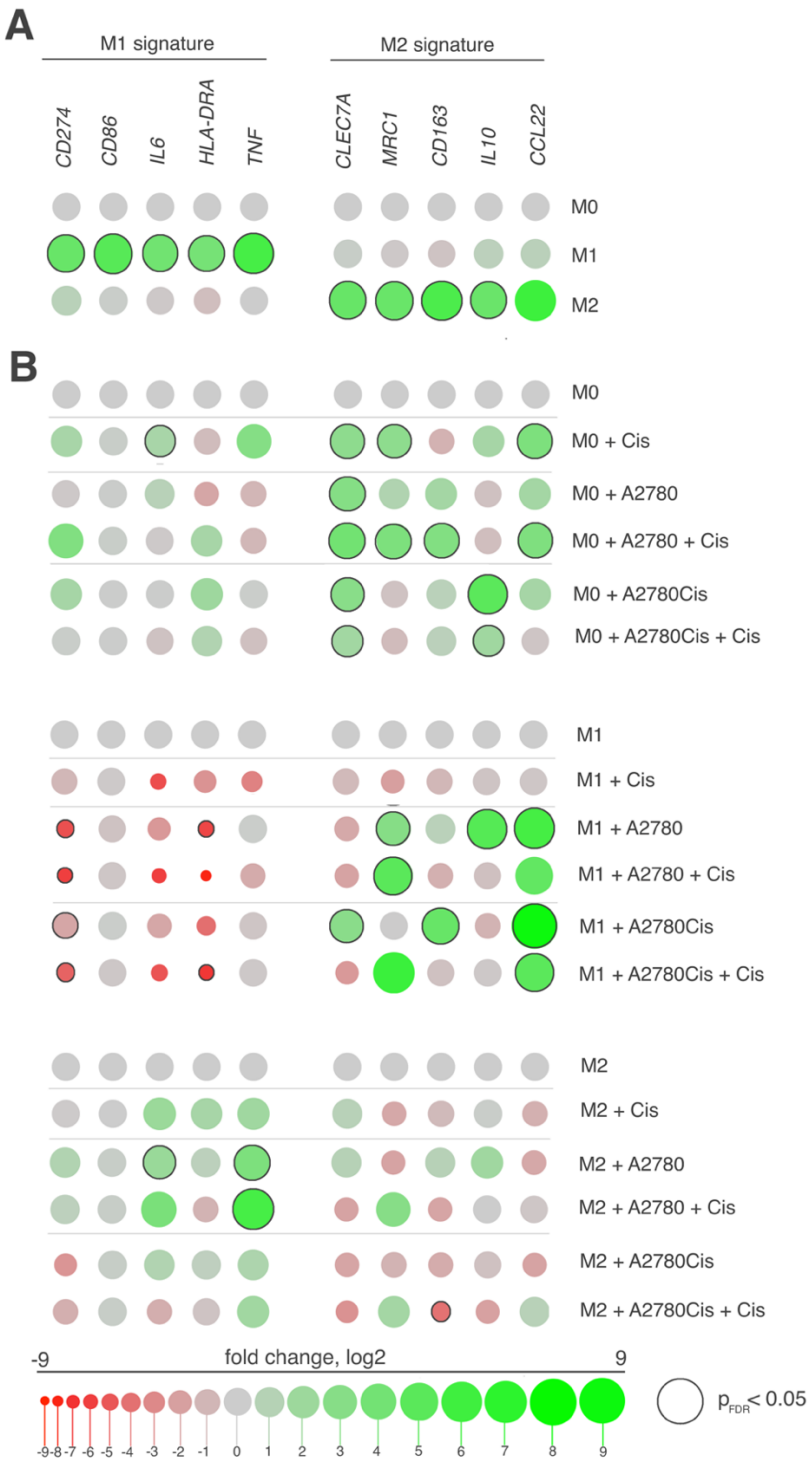

Figure 18. M1/M2 markers expression profile in macrophages. A. Profiling of selected genes in PMA-differentiated and M1 or M2 polarized macrophages. B. Profiling of selected genes in macrophages in response to chemotherapy or upon co-culture with tumor cells. The log2 transformed relative expression levels are depicted as color intensity and circle size variation. Each circle represents the mean relative expression value from two independent experiments with two technical repeats, normalized to the expression level in M0-like (A) or corresponding macrophage type (B). The border indicates statistical significance (two-tailed unpaired Student's t-test with FDR correction $p<0.05$).

was significantly downregulated in co-culture with A2780Cis in presence of cisplatin.

Altogether, we prove that ovarian cancer cells, independent of their cisplatin resistance status, tend to polarize M0 or M1 macrophages into M2-like type.

4.3.6. Discussion

Although the role of host stromal cells in tumor development is indisputable, the full picture and magnitude of microenvironmental regulation of cancer-related processes and, in particular, tumor response to chemotherapy is not yet fully understood. We developed and characterized a cisplatin-resistant A2780Cis cell line, which, together with the parental A2780 cell line, served as models representing different clinical scenarios of OC resistance development. After molecular and functional characterization of these cell lines, we established an indirect co-culture system with THP-1-derived macrophages, and studied their bidirectional interaction, with an extra focus on chemotherapy-induced changes. To our knowledge, this is the first report analyzing the crosstalk between macrophages and OC cells of different sensitivity in the presence of a chemotherapeutic agent.

Pulse-treatment of cancer cells with increasing drug concentrations resulted in generating A2780Cis cell line, which was 3.5-fold more resistant to cisplatin. Changes in cellular morphology served as an endpoint for generation of resistant cell lines, as well as a reason for focusing on EMT-related features [176]. Continuous drug treatment caused not only the morphology shift from rounded epithelial-like to spindle-shaped mesenchymal-like cells but also significant changes in gene expression profile. Cisplatin-resistant A2780Cis cell line exhibited the downregulation of *CDH1* and upregulation of EMT transcription regulators SNAI1, SNAI2, and ZEB1 at mRNA level. Also, A2780Cis retained increased migratory capacity. Cisplatin as previously shown to induce EMT *in vitro* after long-term treatment [177,178]. We hypothesized that the activation of EMT-related processes could result in the emergence of

stemness properties. TFs Oct3/4, Nanog, and Sox2, were first reported as master pluripotency network regulators in embryonic stem cells [179], also shown to be involved in cancer biology and upregulated in CSCs [180]. We observed the increase in mRNA level of these TFs together with high clonogenic potential in A2780Cis. Cytostatic drugs were shown to induce the stem cell markers in OC cells in the short term [181,182], as well as selectively enrich for CSCs under continuous drug treatment [183]. By treating A2780 with cisplatin, we already noted that even a single dose of the drug may cause a significant change towards activating EMT, CSC, MDR profile, as previously reported [181,184]. The transcriptional adjustment may be a sign of chemotherapy adaptation [185], as seen in resistant cells upon treatment with cisplatin. Together, the evidence for drug-induced cell plasticity and proliferation in A2780Cis provides a rationale for studying its role in tumor-stroma interplay and shaping of the TME.

We also found the significantly increased levels of Th1/Th2 cytokines (TNFα, IL-2, -4, -5, -6, -10, -13) in A2780Cis in comparison to cisplatin-sensitive A2780. The chemotherapy-promoted cytokine secretion increase was already shown in several short-term treatments *in vitro* studies [186,187]. We suggest that intense cytokine production in cisplatin-resistant cells may reflect the immunogenicity of cisplatin. Cytokine secretion as the hallmark of drug-induced immunogenic cell death mostly concerns Th1 type cytokines: IFNγ, TNFα, and, in some cases, IL-6 [188]. In our study we also noted the significant increase of Th2 cytokines, making A2780Cis an intriguing candidate for studying macrophage polarization.

However, different chemotherapeutic agents may induce distinct responses in monocytes/macrophages, which can either augment or antagonize the activity of the drug (likely in a tumor type-dependent manner) [189]. Here, we used human leukemic monocyte cell line THP-1 to differentiate monocytes into macrophages. Although THP-1-derived macrophages may not entirely reflect the actual TAMs, this cell line is stable, well-characterized [190,191] and thus suitable for studying the crosstalk with cancer cells *in vitro*. We polarized

PMA-differentiated M0 macrophages either with LPS+IFNγ or IL-4+IL-13 to obtain M1- or M2-like cells with characteristic mRNA expression signature, consistent with previous reports [190,192]. We judged the ability of OC cells to induce polarization based on the changes in the gene expression profile of co-cultured macrophages, compared to control M1- or M2-like cells. Ovarian cancer or stem-like cancer cells were previously reported to polarize macrophages into M2 phenotype [162,172,193]. In this study, upon chemotherapy treatment and co-culture with cancer cells, we also noticed the induction of M2-like transcriptional changes in M0 or M1 macrophages. These findings suggest that OC cells tend to induce M2-like mRNA profile independent of their platinum sensitivity status. However, we simultaneously observed that upon co-culture with macrophages, cisplatin-sensitive A2780 cell line displayed the most pronounced mRNA expression alterations, such as upregulation of stemness-related TFs and downregulation of E-cad coding gene. Besides, the combination of macrophages and cisplatin in co-culture resulted in additional upregulation of genes, coding for Oct3/4, ABCC1, Snail, ZEB1, Vimentin, which suggested that cisplatin and macrophages co-act to potentiate EMT-related processes in cancer cells, in accordance with Yu et al who reported similar effects in epithelial cells [194]. Strikingly, we observed that THP-1 derived macrophages were able to induce the changes in A2780 cells mRNA profile to a similar extent as chemotherapy, however, in some cases these alterations were of the inverse character. Based on these observations, we propose that although short-term co-culture with macrophages does not influence the ovarian cancer cells' cisplatin resistance level or the drug response-related gene expression, it already induces the changes in CSC, MDR and EMT-related gene expression profile. These alterations may promote the early development of potentially less sensitive cancer cell sub-clones, which can be accountable for therapy failure. Besides, it may explain why all co-culture systems resulted in the induction of M2-like macrophage transcriptome changes. We suggest that the macrophage-promoted EMT-induction in cancer cells and

M2-like macrophage polarization in co-culture are simultaneous processes, both leading to the formation of the immunosuppressive TME.

Although TAMs-mediated EMT regulation was *in vitro* shown to occur in cell lines of different origin [139–141], the underlying mechanisms of these interactions are still unclear. Several studies emphasized that TAMs promote EMT and CSC-like properties in cells via TGF-β1-induced EMT [141,195,196]. Other studies reported the TLR4/IL-10 signaling axis in macrophages acts as M2-promoting stimulus [197] as well as a tool for EMT induction in pancreatic cancer cells [140]. More, Dijkgraf et al. reported that cisplatin-induced macrophage skewing towards M2 was reflected by their production of IL-10 [172]. Our results add another evidence supporting the existence of this mechanism. We showed that stem-like colon cancer cells produce and secrete more IL-10 than the non-stem-like cells. Also, we detected IL-10-related changes in both components of indirect co-culture system upon the treatment with cytotoxic drugs: an increase in *IL-10* mRNA in M0 macrophages when treated with cisplatin, as well as the elevated production of IL-10 in cisplatin-resistant OC cells.

The broad spectrum of macrophage variety *in vivo* also has to be taken into account. For example, analysis of global gene expression profile in human ovarian carcinoma ascites-associated macrophages revealed mixed-polarization phenotypes unrelated to the M1/M2 classification [198]. In resistant OC cells we detected the elevated production of both Th1 and Th2 cytokines. Nevertheless, upregulation of M2-type-related genes was prevailing in co-culture. However, in different settings (cancer cells versus chemotherapy drugs versus the combination of both) both polarized and pre-polarized M2 macrophages did not maintain the stable mRNA expression profile, and, under certain conditions, even upregulated some of the M1 markers.

In conclusion, we provide evidence about the bidirectional interplay between macrophages and cancer cells. We report that OC cells, independent of their cisplatin resistance status, tend to polarize M0 or M1 macrophages into M2-like type. Alongside, macrophages can induce EMT and cellular stemness

properties in cisplatin-sensitive, but not -resistant, cells. Both cell types act towards tumor promotion and development of immunosuppressive microenvironment. Although we analyzed only the short-term indirect co-cultures, our findings provide the rationale for further functional investigations of early immune TME formation *in vivo*.

4.4. Development of immune tumor microenvironment in iBIP2 mouse model of melanoma

4.4.1. Rationale

In the previous chapters we reported that cancer cells are actively participating in the shaping of the immune tumor microenvironment. We have shown that, through the secretion of soluble factors, cancer cells can facilitate the M2 type polarization of macrophages and promote the immunosuppression. However, the *in vitro* co-culture reflects only one example of heterotypic interactions in a strictly controlled environment. The full picture of the development of immune TME would allow for better classification of tumors based on their immune phenotype and tailoring of precise treatment.

Tumor-specific mutations result in the emergence of neoantigens, recognizable by the immune system [6,199]. From the immunological point of view, cancers can be perceived as immunologically 'hot' or 'cold', meaning the high or the low level of infiltration with immune cells, and especially T lymphocytes [200]. Immune 'cold' tumors have highly vascular stroma and lack the immune infiltrate. Immune 'hot' tumors are usually generously infiltrated, and can be further subdivided into the immune-excluded (T lymphocytes gather around the tumor parenchyma) or inflamed (T lymphocytes penetrate the tumor parenchyma) subtype [7,11].

However, the dynamics of formation of the immune TME is frequently disregarded as too challenging to execute in patients. The preclinical tumor models often fail to faithfully represent the human tumors, especially if they are based on transplantable tumors or immune compromised mice. The need for

murine tumor models recapitulating the genetic lesions in human cancer resulted in derivation of genetically engineered mouse models, expressing the oncogene in a given tissue under specific conditions [201]. Here, we aimed to **characterize the formation of immune tumor microenvironment during melanoma tumor development in iBIP2 mouse model.** iBIP2 is a genetically engineered mouse model of melanoma, expressing V600E-mutated *BRAF* in melanocytes. Using mass cytometry (2.20.), we carried out the quantitative and qualitative immune TME analysis at the different points of melanoma tumors development (2.19.) in the iBIP2 model (2.16.).

4.4.2. Characteristics of iBIP2 mouse model of melanoma

IBIP2 tumor model is a genetically engineered Tet-inducible murine model for BRAF V600E mutated-melanoma with human BRAF transgene (Figure 19), that makes it a good candidate for studying targeted therapies for advanced melanoma. Previous research revealed that, similar to the clinical situation, iBIP2 tumors tend to respond to BRAF and MEK inhibitors, however, after some point (usually 21-28 day after the beginning of the treatment), the tumors start to relapse and become incurable [119].

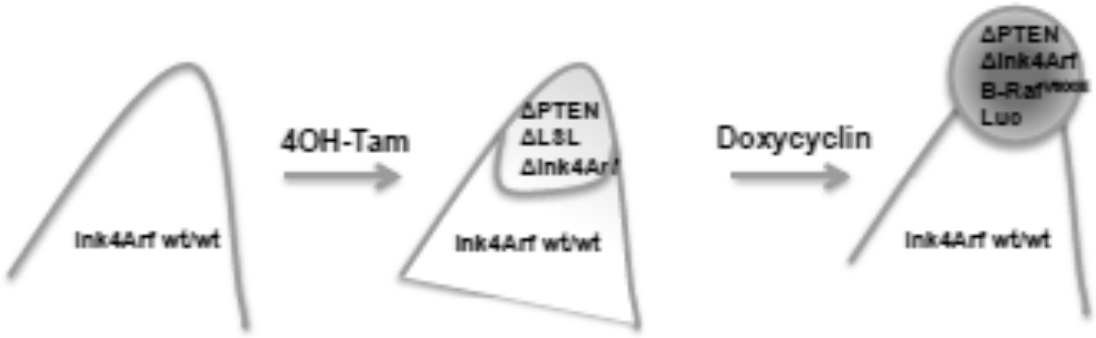

Figure 19. A schematic representation of tumor induction in the iBIP2 mouse model. Upon topical application of tamoxifen, Cdkn2a and Pten are specifically deleted only in the treated melanocytes, and rtTA is activated. Subsequent administration of doxycycline activates the BRAF V600E transgene only in melanocytes, in which the LSL-Stop-rtTA cassette, as well as Cdkn2a and Pten, were co-deleted. Courtesy of Hanahan Lab.

The IF staining on paraffin-fixed tumor sections revealed that developed iBIP2 tumors are heavily infiltrated with immune cells (as marked by CD45 staining) (Figure 20).

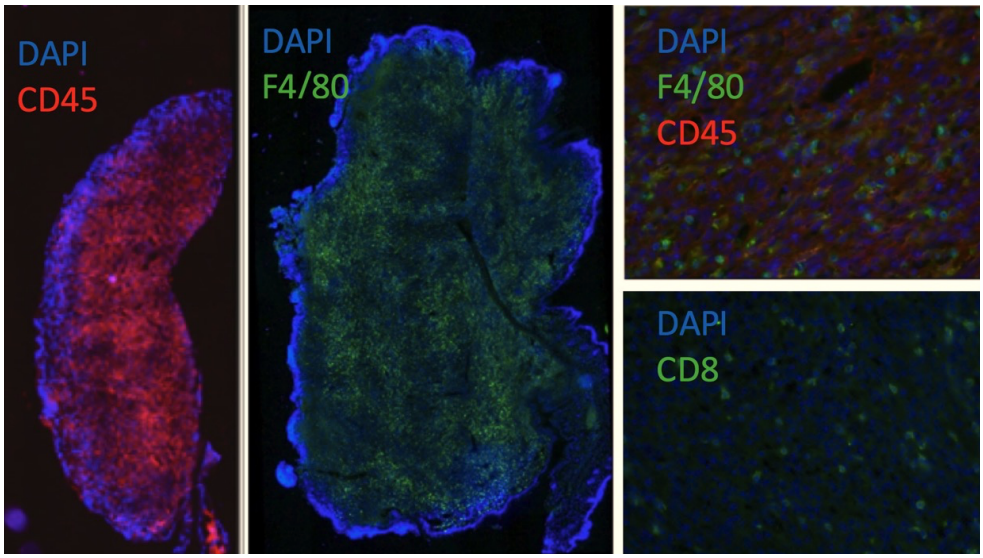

Figure 20. Immunofluorescent staining of immune cells in iBIP2 tumors. General immune infiltration (CD45), macrophages (F4/80), and CD8 T lymphocytes in tissue section are shown to massively infiltrate melanoma tumor in the iBIP2 model. Courtesy of Hanahan Lab.

Out of the immune cells, macrophages were abundant (as marked by F4/80 marker). The presence of intraepithelial CD8+ cells was also observed, suggesting that iBIP2 tumors may represent the inflamed immune phenotype, which is characterized by infiltration of TME by T cells that are not functioning properly. Nevertheless, the abundance of macrophages and other non-lymphoid immune cells may imply the existence of the immunosuppressive microenvironment in this model. As iBIP2 tumors initiate form BRAF V600E mutation, which results in neoantigen expression and possibly T cell priming, we hypothesized that antitumor immunity in iBIP2 microenvironment is to some extent present. This encouraged us to look into the formation of the iBIP2 immune TME during the course of time.

4.4.3. Immune microenvironment profiling during tumor development

We collected the samples of the mouse ear skin before tumor induction and 1 week after induction, prior to any neoplastic changes were

macroscopically visible (Figure 21). Also, we collected the samples of tumors of different sizes: <10 mm^3 (dot), 10-50 mm^3 (small), 50-100 mm^3 (medium), and >100 mm^3 (big). For each group, we collected 7 samples. All samples were enzymatically digested and subjected to mass cytometric analysis of immune TME.

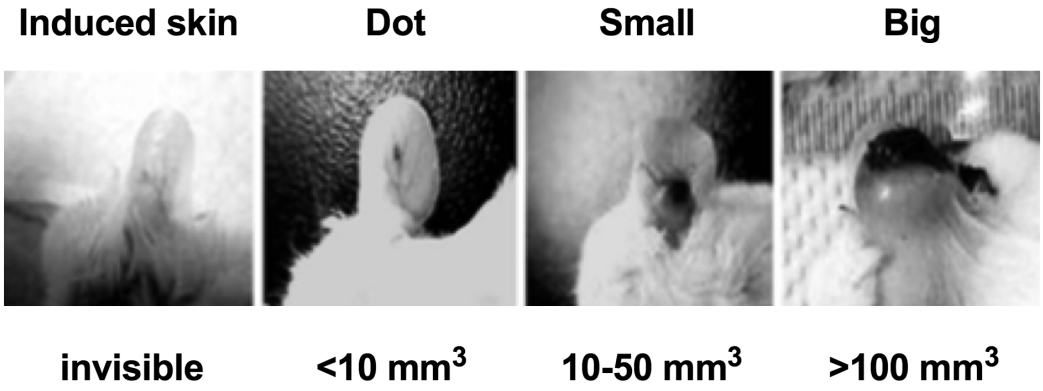

Figure 21. Macroscopical development of melanomas in the ear skin in the iBIP2 model. Courtesy of Hanahan Lab.

We identified main immune cell populations in tumors based on their surface phenotype markers expression (Figure 22). We observed a great influx of immune cells during tumor development to the visible dot size, with already a significant increase in CD45+ cells even after 1 week of induction. After the tumor develops, the level of immune infiltration stays stable, reaching 60-65%. These findings highlight the role of immune milieu during early steps of tumor development as well as its functional contribution in the developed tumor bulk.

We did not observe significant changes in the proportions of lymphoid cells. The general increase of immune cells implies a gradual influx of both T and B lymphocytes, which make up for 14-18% or 5-10% of the immune cells, respectively.

In myeloid cell compartment, we observed a significant influx of MDSCs in the period between induction and formation of a visible lesion. Independent of tumor size, the MDSC infiltration remains about 15-20% of the immune cells.

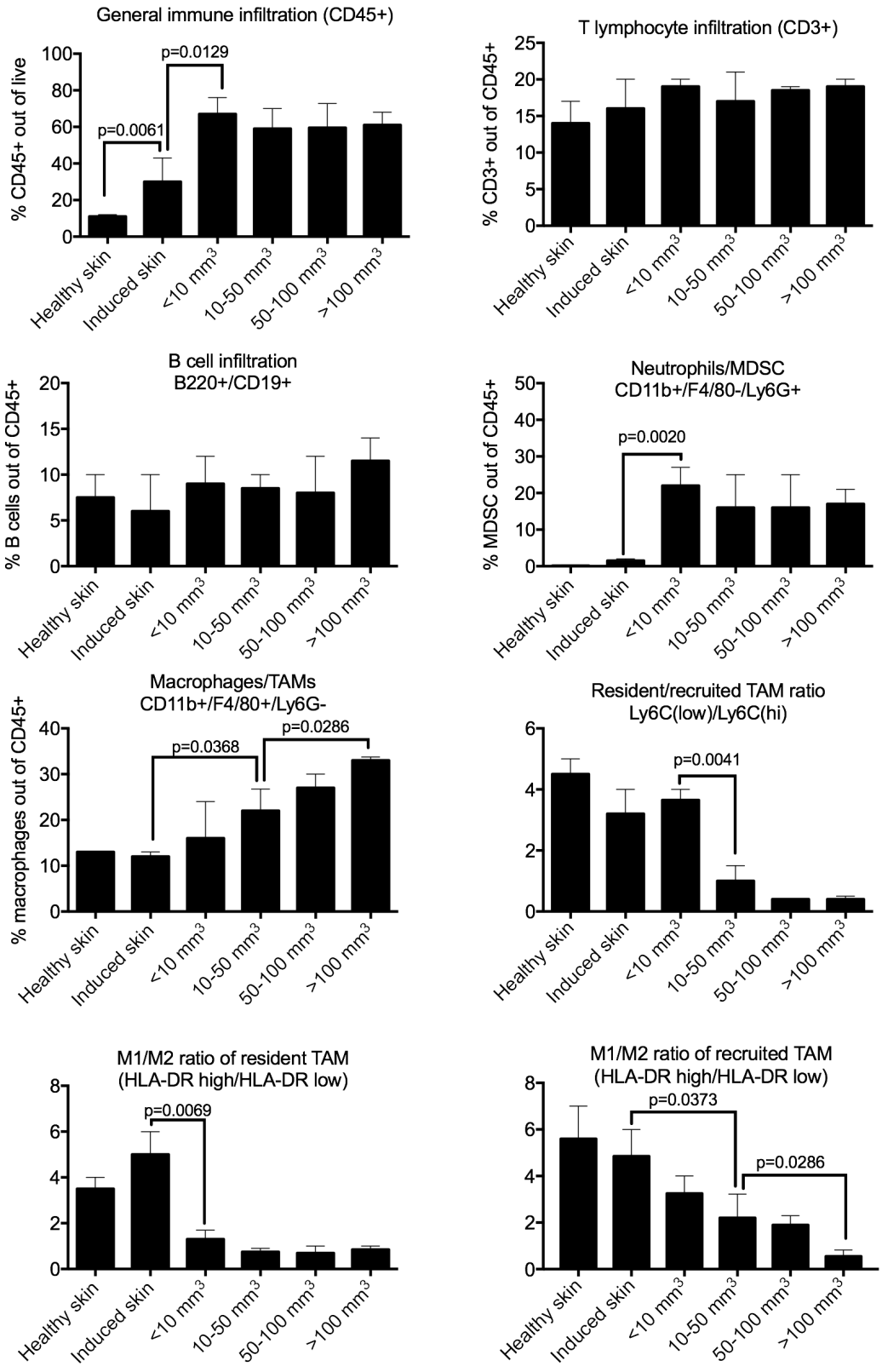

Figure 22 Immune microenvironment profile during tumor development. Mass cytometry quantification of different immune cell subsets in healthy or induced skin, as well as in tumors of different sizes. Bar graphs are shown as mean ± SD, n=7 for each group. Mann-Whitney test was used for comparison.

Macrophages make up about 12% of immune cells in the healthy or induced skin. However, tumor development results in a significantly increased proportion of macrophages, which vary between 15 and 30%, depending on tumor size. As expected, the ratio of resident to recruited macrophages gradually decreases, proving that tumors are able to attract circulating monocytes and convert them to TAMs. This process is most prominent during the initial growth of tumor bulk, as there is a significant difference between tumors of <10 mm^3 and tumors of 10-50 mm^3. The ratio of antitumor (M1) and tumor-promoting (M2) macrophages is higher in skin samples than in tumor tissue, meaning that the tumor either re-polarizes the M1 macrophages into M2 type or creates a microenvironment that promotes the M2-polarization of newly-recruited monocytes. In the case of resident macrophages, it is likely a re-polarization process, as the M1/M2 macrophage ratio drops suddenly during the early tumor formation when the macrophage influx is minimal. However, the rapid decrease of M1/M2 ratio suggests the parallel establishment of the immunosuppressive microenvironment. Similarly, tumors are able to recruit the undifferentiated monocytes and polarize them into the M2 subtype.

4.4.4. Discussion

Studies have shown that the activation of oncogenes or loss of tumor suppressor genes have a critical effect on the formation of the TME [202]. Commonly mutated genes, resulting in the neoantigens, can actively participate in recruiting, activation, or modulation of the immune system. This partly explains the inter- and intra-tumoral heterogeneity in immune infiltration and activation. It was shown *in vitro* that BRAF V600E mutation promotes the stromal cell-mediated immunosuppression by induction of IL-1 [203]. Other than that, studies thoroughly investigating the development of the immune TME under BRAF mutation are scarce. Genetically engineered mouse models that closely mimic the genetics and biology of human cancers, and thorough analysis of their TME, are necessary to better understand the dynamics of immune cell recruitment.

Here, we assessed the and immune microenvironment composition in BRAF V600E-driven genetically engineered mouse model of melanoma. The iBIP transgenic mouse model, described in [119], closely resembles human samples in terms of the molecular response od BRAF inhibition. Despite its initial response to targeted therapy, drug resistance emerges at a median of 32 days and iBIP tumors relapse. IBIP2 model, described in [204], is a refined version of the iBIP model, which is driven by tamoxifen- and doxycycline-inducible Cdkn2a and Pten deletion and BRAF V600E expression in skin melanocytes. The response of iBIP2 to BRAF inhibitors is comparable to the iBIP model (unpublished personal data). Therefore, it reliably reflects the clinical scenario of advanced melanoma which develops resistance to BRAF and MEK inhibitors and requires secondary targeting. Insights from studies in such mouse models can potentially translate to clinics and facilitate the design of human clinical trials.

Immune cells make up for more than a half of all cells in a developed iBIP2 tumors. The most prominent immune microenvironment changes observed during the development of iBIP2 tumors concerned the myeloid compartment. We found that the growth of palpable neoplasia was accompanied by a sharp influx of MDSCs. An increase of tumor bulk was followed by the recruitment of circulating monocytes and polarizing them into M2 TAMs.

On the basis of the current evidence, our data reveals the gradually developing abundant immunosuppressive microenvironment in iBIP2 mouse model of BRAF-mutated melanoma. These findings provide a rationale for further immunotherapeutic targeting od immune TME in this tumor model, representing the inflamed immune phenotype.

4.5. Checkpoint blockade in iBIP2 mouse model of melanoma

4.5.1. Rationale

Dysfunction of one or more steps of the cancer-immunity cycle destabilizes the immune-mediated control of tumor growth and causes immune

escape and tumor outgrowth [10]. Immunotherapy aims to repair the malfunctioning phase of cancer-immunity cycle and facilitate the antitumor immune response. In the previous chapter we found out that the melanoma tumors in iBIP2 mouse model are abundantly infiltrated with immune cells, including T lymphocytes, and therefore represent the tumors with inflamed immune phenotype.

In inflamed phenotype-bearing cancers, tumor cells are able to escape the immunological destruction by expressing the ligands for inhibitory receptors on T lymphocytes [10,200]. Most prominent examples of such receptors are CTLA-4 and PD-1, both acting as checkpoints for T cell activation [101,205]. Inhibition of these checkpoints with specific blocking antibodies unleashes the antitumor immune response. Checkpoint blockade has made a breakthrough in cancer immunotherapy, as it provides a durable response, likely due to the memory of the adaptive immune system, which translates into long-term survival for some patients. The first checkpoint inhibitor, anti-CTLA-4 antibody (ipilimumab) was approved by the FDA in 2011 for the treatment of metastatic melanoma. Since then, several others, targeting PD-1 or PD-L1, also received approval for treatment of cancers of other localizations, while many are still ongoing clinical trials [206,207]. The most successful clinical example is the treatment of advanced melanoma with both anti-CTLA-4 and anti-PD-1. Due to separate mechanisms, this combination reached the clinical response in 50% of patients [108].

Although melanoma is one of the cancer types best targeted by checkpoint blockade, many patients are refractory to therapy. The mechanisms of resistance to immunotherapy cover tumor cell intrinsic (the absence of antigenic proteins, the absence of antigen presentation, insensibility to T cells) as well as tumor cell extrinsic (absence of T cells, other inhibitory immune or immunosuppressive cells) factors [109]. However, recent studies revealed that even if melanoma tumors present as good candidates for checkpoint blockade (high infiltration with PD-1 expressing tumor-specific T cells at baseline), they do not always respond well to therapy [112,208], suggesting the existence of

other mechanisms, impeding the effective T cell response in those patients. Characterization of gene expression profile of anti-PD-1-resistant patients revealed the local upregulation of genes, associated with monocyte/macrophage/MDSCs and their immunosuppressive effects (IL-10, CCL2), together with genes responsible for EMT, angiogenesis, and wound healing. This innate resistance signature was observed in tumors of different localizations [209]. Immunosuppressive cell subsets, a dark horse of the TME, are potential modulators of immune activity against a tumor [210,211]. Myeloid cells are known to be involved in tumor cell invasion and are usually negatively correlated with prognosis, therefore, they deserve further attention as both the reason of immunotherapy resistance and a potential target.

Here, we aimed to **address the mechanisms of response and resistance to checkpoint blockade with anti-CTLA-4 and anti-PD-1 in the iBIP2 mouse model.** We carried out a pre-clinical trial with checkpoint inhibitors anti-CTLA-4, anti-PD-1, and their combination (2.18.). We pre-selected tumors based on their initial volume for assessing the short-term effect of checkpoint blockade on immune TME using mass cytometry (2.19., 2.20.). We then continued with long-term checkpoint blockade trial, where we evaluated the treatment efficacy by monitoring tumor growth (2.17.) and investigated the immune microenvironment alterations in mice with different types of outcome (2.19., 2.20.).

4.5.2. Short-term checkpoint blockade trial in tumors of different sizes

Immune TME profiling of iBIP2 tumors revealed the heavy immune infiltration of both lymphoid and myeloid lineages. Therefore, iBIP2 tumors most likely represent the inflamed immune phenotype. The immunotherapeutic strategy for management of tumors with similar features usually relies on invigorating and engaging T lymphocytes by using checkpoint inhibitors. Anti-CTLA-4 or anti-PD-1 blocking antibodies unlock the inhibitory signals between tumor cells and T lymphocytes and promote the antitumor immune response.

We decided to analyze the initial changes of the immune microenvironment after one dose of a checkpoint inhibitor or their combination. To investigate the influence of initial tumor size, if any, we carefully selected mice with tumors less than <50 mm^3 (small) and >100 mm^3 (big), and challenged them with one injection of anti-CTLA-4 (100 μg per mouse intraperitoneally), anti-PD-1 (250 μg per mouse intraperitoneally), their combination, or corresponding quantities of IgG isotype (n=6 mice per each group). We collected the tumors on the day 3 after the drug injection. The results of immune microenvironment profiling are in Figure 23.

We observed no difference in total immune infiltration proportion in none of the groups, confirming that tumors maintain a uniform immune infiltration level, which accounts for more than half of the tumor bulk and therefore may impede tumor shrinking during successful targeted or immune therapy.

There were no significant differences in B lymphocyte infiltration level, although in small tumors checkpoint blockade tended to decrease B cell proportion, whereas in large tumors the opposite trend was seen.

We noticed a significant increase in NK and dendritic cells in double-treated tumors of both size groups, in comparison to IgG control. These observations suggest the reinforcement of innate immunity killer and antigen-presenting cells in response to combination checkpoint inhibition therapy.

The myeloid compartment of small and big tumors distinctively responded to checkpoint blockade. While anti-CTLA-4 treatment does not change the proportion of MDSCs in tumors, anti-PD-1 as well as the combination of anti-CTLA-4 and anti-PD-1 significantly decreases the MDSCs infiltration level in small, but not in big tumors. Similarly, in small tumors treated with the combination of checkpoint inhibitors, there are significantly fewer macrophages, whereas in big tumors the macrophage infiltration level remains constant. Interestingly, the level of M1 macrophages in control and treated small size tumors was stable, and only the proportion of M2 macrophages was decreasing, indicating that checkpoint blockade treatment affects the

recruitment of monocytes and M2-polarization capacity in tumors of relatively smaller size.

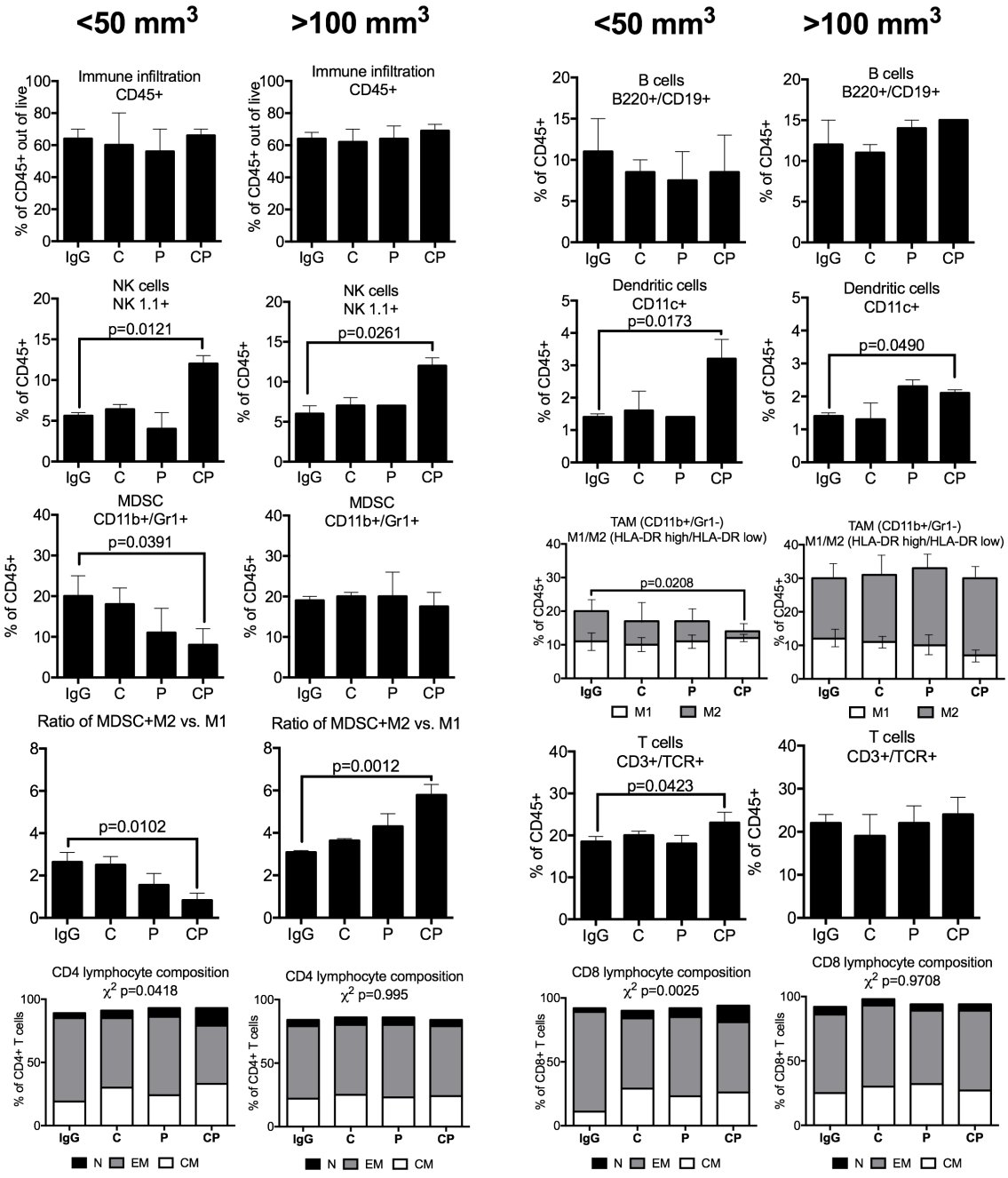

Figure 23. Immune microenvironment profile after one dose of checkpoint blockade. Mass cytometry quantification of different immune cell subsets in iBIP2 tumors of <50 mm^3 and >100 mm^3 sizes after one injection (day 3) of anti-CTLA-4, anti-PD-1 or their combination (day 3). Control mice were injected with IgG isotype. Bar graphs are shown as mean ± SD, n=6 for each group. Mann-Whitney test was used for comparison. C – anti-CTLA-4 group; P – anti-PD-1 group; CP – anti-CTLA-4 plus anti-PD-1 group. N – naïve T cells, EM – effector/effector memory T cells, CM – central memory T cells.

However, larger tumors did not respond in the same way. They initially had a higher proportion of macrophages in their immune infiltrate, and M2 subtype was prevailing. We also noticed the significant decrease of the M1 macrophage level in double-treated tumors in comparison to IgG control ($p=0.0312$).

The ratio of immunosuppressive (MDSC + M2 macrophages) versus antitumor (M1 macrophages) myeloid cells in small tumors (potential responders to checkpoint blockade) is significantly lower in tumors treated with anti-PD-1 alone ($p=0.0407$) or its combination with anti-CTLA-4 in comparison with IgG control tumors. Oppositely, single or combined checkpoint blockade results in a higher proportion of immunosuppressive myeloid cells in large tumors and thus contribute to their lack of response.

Last but not least, the direct effect of checkpoint blockade is releasing the inhibitory switch on T lymphocytes. CTLA-4 blockade allows for activation and proliferation of more T cell clones while PD-1 pathway blockade restores the activity of antitumor T cells. As shown in the previous section, IBIP2 tumors are characterized by considerable T cell infiltration, with a CD4/CD8 ratio ranging from 1 to 1.5. Treatment with one dose of both checkpoint inhibitors induces a small yet prominent increase in T cell infiltration level in small-sized tumors, while in large-sized tumors we did not observe this effect. Besides, the proportions between naïve (N), effector memory (EM) and central memory (CM) subsets in both CD4 and CD8 cells were constant is large tumors, whereas in small tumors there was a considerable increase in naïve and central memory CD4 and CD8 T lymphocytes after dual checkpoint inhibitor treatment.

The above findings suggest that the immune microenvironment in small tumors, characterized with a lower quantity of macrophages and higher M1/M2 ratio in comparison to larger size tumors, is associated with better response to dual checkpoint inhibition with anti-CTLA4 and anti-PD1. One dose of combination treatment decreases the ratio of immunosuppressive to antitumor myeloid cells and attracts naïve T lymphocytes.

4.5.3. Long-term checkpoint blockade trial

Having characterized the nature of immune TME in small (<50 mm^3) and large (>100 mm^3) iBIP2 mouse melanoma tumors after one dose of checkpoint inhibitors, we set up a trial aiming to assess the combined effect of anti-CTLA-4 and anti-PD-1 on the smaller (responsive) tumors on a longer run. The treatment group (n=12) received intraperitoneal injections of 100 μg of anti-CTLA-4 and 250 μg of anti-PD-1 every 3 days, while the control group (n=6) was challenged with respective quantities of corresponding IgG isotype antibodies. We involved only mice with tumor volume ranging from 20 to 60 mm^3. The distribution of tumor volumes did not differ between groups.

Out of 12 mice treated with checkpoint inhibitors combination, three individuals (Figure 24) did not respond to treatment from the very beginning and thus were classified as non-responders. All three non-responding tumors, together with IgG samples were collected on day 14. Four treated tumors were collected in response phase on the day 14 too, and five initially responding tumors were collected at the progression phase on the day 37.

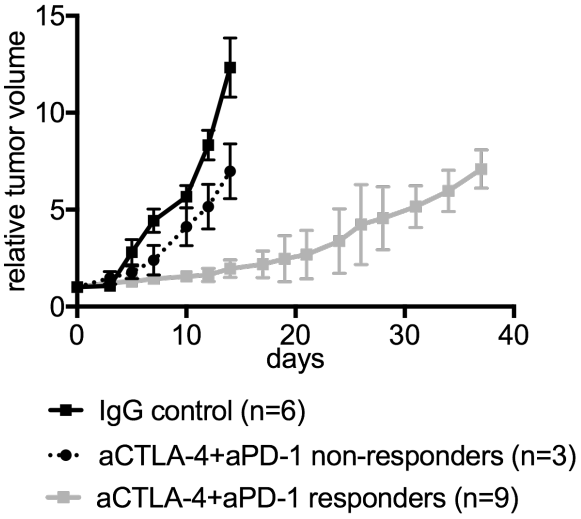

Figure 24. Long-term growth profiles for iBIP2 tumors, treated with double checkpoint blockade. Mice were treated with anti-CTLA-4 and anti-PD-1 combination. Control group was injected with IgG isotype. Growth curves are presented as mean ± SD over time.

We examined the quantitative differences in T cells, macrophages and MDSC infiltration in control, non-responding and responding tumors on day 14, as well as in initially responding, but progressing tumors on day 37 (Figure 25). The level of CD45+ immune infiltration was 60-65% and did not differ between groups (p=0.623). We found increased levels of T lymphocytes in responding

tumors, in comparison to control as well as to progression samples. T cell level in progressing samples was similar to the non-responding group.

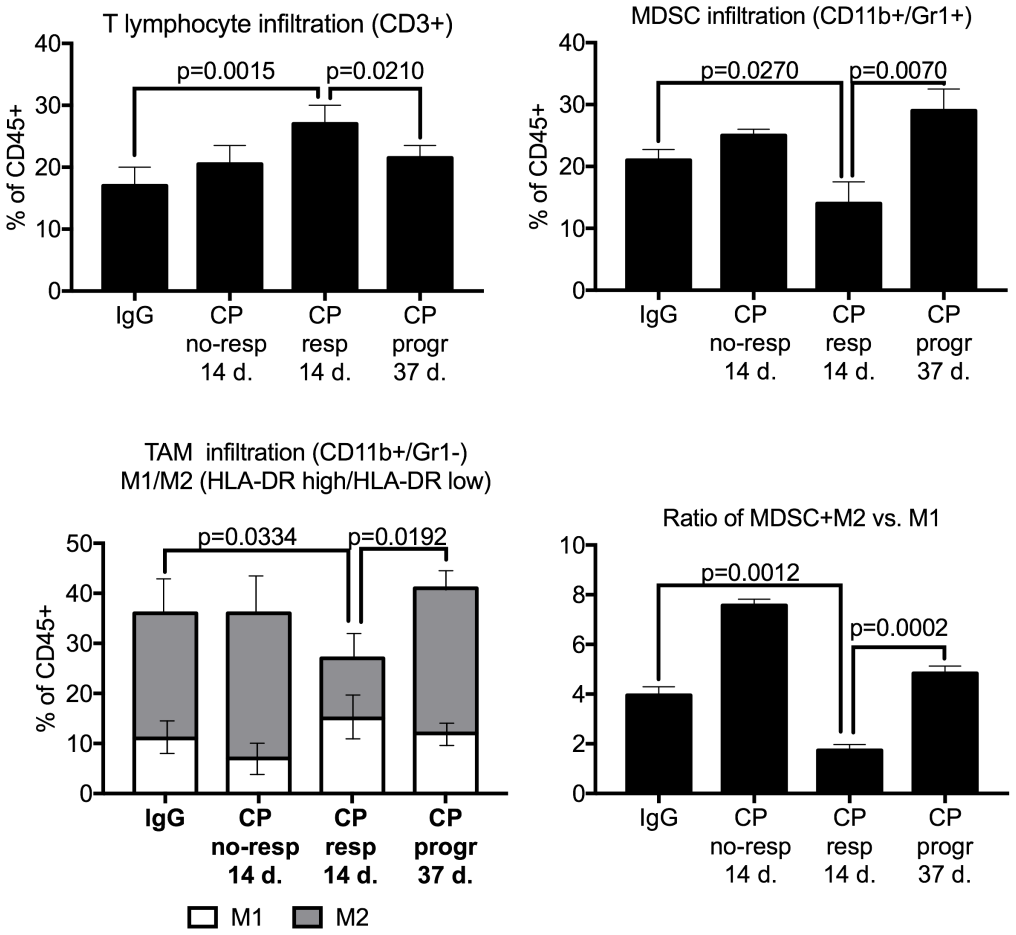

Figure 25. Immune microenvironment profile of non-responding, responding, and relapsing tumors during longitudinal checkpoint blockade treatment. Mass cytometry quantification of different immune cell subsets in control, responding and non-responding iBIP2 tumors on day 14 of double checkpoint blockade, as well as in relapsing tumors on day 37 of double checkpoint blockade. Bar graphs are shown as mean ± SD. Mann-Whitney test was used for comparison. CP – anti-CTLA-4 plus anti-PD-1 combination treatment.

The MDSC infiltration was significantly lower in responding samples than in control, non-responding, or progressing tumors. Similar trends were observed in TAM infiltration. However, the level of M1 macrophages did not correlate with total macrophage level. Although the responding tumors had the lowest count out of all groups, the proportion of M1 macrophages in these tumors was the highest. The ratio of immunosuppressive (MDSC+M2) versus

antitumor (M1) cells revealed that on day 14, non-responding tumors contain the greatest proportion on immunosuppressive cells (ratio=7.5), in comparison with control (ratio=4), whereas in responding tumors the M1 macrophages partly compensate for the immunosuppressive effect of MDSC and M2 macrophages (ratio=1.5). However, immunosuppressive myeloid cells again infiltrate tumors during the relapse phase (ratio=4.5).

The above findings suggest that although initially some small-sized tumors respond well to the combination of anti-CTLA-4 and anti-PD-1, eventually they progress. The increased proportion of immunosuppressive to antitumor myeloid cells is characteristic to both non-responding as well as responding yet progressing tumors and thus may contribute to the development of resistance to checkpoint blockade.

4.5.4. Discussion

Anti-CTLA-4 and anti-PD-1 immune checkpoint inhibitors have shown an extraordinary clinical activity in several types of cancer and are revolutionizing the medical oncology. Although both act as inhibitory T cell receptors, fundamental functional differences exist between CTLA-4 and PD-1. CTLA-4 is competing with CD28 for interaction with CD80/86 on antigen presenting cells, while PD-1 acts directly via PD-L1/PD-L2 interaction. Blocking of CTLA-4 affects the immune priming phase in lymph nodes and allows the activation and proliferation of T cells while simultaneously reducing Treg mediated immunosuppression. Blocking the PD-1 affects the effector phase and restores the activity of peripheral antitumor T cells [102]. Blocking both receptors usually results in the synergistic effect, although the mechanisms of this synergy are not completely clear. In the ideal scenario, it would induce the proliferation of high numbers of T cells early in the immune response, restore the activity of exhausted intratumoral T cells, and reduce the effect of Tregs [102,212]. The superior effect of the anti-CTLA-4 and anti-PD-1 combination over the monotherapy was shown in various preclinical [213–215] and clinical trials [107,108]. In our study we observed the same phenomenon – the

combination treatment more effectively promoted the microenvironment alterations in comparison to a single checkpoint inhibitor.

However, we observed a heterogeneous response to double checkpoint blockade which we found to be associated with the distribution of the initial tumor size. Preclinical trials, especially the ones involving immunotherapy and showing the outstanding effect and significant tumor shrinking, regularly receive the critique for being flawed and challenging in translation into clinical trials [216,217]. A recent systematic analysis showed that most of the studies pre-select the mice for tumor size (usually less than 100 mm^3) to report slowed or delayed growth. Regression of tumors larger than 200 mm^3 was observed only after passive antibody or adoptive T cell therapy. Very few studies used large tumors which could be representative of clinically relevant tumors [218]. Tumor burden was found to be associated with anti-PD-1 response in stage IV melanomas – the bigger the tumor, the more T cell reactivation was needed, and treatment failure arisen due to the inadequate magnitude of elicited immune effect [219]. Other researchers also emphasized an imbalance between the strength of immune response and baseline tumor size as the potential explanation of unsuccessful immunotherapy and suggested that the ratio of tumor mutation burden to tumor burden as a measure to predict the clinical benefit of checkpoint blockade [220]. Our findings in BRAF-mutated melanoma model agree with the above hypotheses, as we have provided evidence for the exponential growth of the proportion of total CD45+ cell infiltration during the early tumor formation. Immune cells, other than T lymphocytes, comprise a significant portion of tumor bulk and may physically dilute the effect of checkpoint blockade-activated cells in bigger tumors.

In clinical immunotherapy trials, a triple pattern of response is usually observed: initial and prolonged response, innate resistance or acquired resistance [109,211]. When we pre-selected for smaller tumors in long term double checkpoint inhibitor trial, we still observed the immediate resistance in 25% tumors. However, although the significant part of tumors responded, they eventually relapsed, resulting in a median of 21 days of prolonged time to

progression in comparison to intrinsically resistant tumors. Numerous resistance mechanisms are proposed and investigated. Large part of them concern T cells, e.g. insufficient generation of tumor-specific T cells, which are associated with the magnitude tumor mutational load and emergence of neoantigens [6,211]. Although our study model harbors BRAF V600E mutation in skin melanocytes, and thus by default presents a neoantigen, we did not investigate how many of the tumor-infiltrating T cells are mutated BRAF specific. The initial T cell infiltration was present and comparable in small (responding) and large (non-responding) tumors. However, only smaller tumors experienced the checkpoint blockade-generated influx of T cells, out of which there were large numbers of naïve and central memory T cells. Larger tumors did not respond to checkpoint blockade in terms of T cell numbers or proportions between naïve and memory lymphocytes. Besides, the intratumoral expression of CTLA-4 and PD-1 [221,222], which were present in considerable quantities in iBIP2 tumors, distinct predictive circulating biomarkers were proposed to evaluate the response to checkpoint blockade, namely the increase of CD4 and CD8 central memory T cells in response to anti-CTLA-4, and increase in NK cells for anti-PD1 therapy [223]. We observed the significant changes in these subtypes in response to a single dose of a combination checkpoint blockade.

Even in the case of successful neoantigen presentation and T cell activation, the inhospitable TME can impair the antitumor immune response. High levels of immune suppressive cytokines or metabolites, and recruitment of immunosuppressive cells (MDSC, M2 macrophages, Tregs promote the immune escape. Immune suppressive TME prevents antitumor cytotoxic and Th1-directed T cell activities [109,224]. The subtle baseline difference of the M1/M2 macrophage ratio, together with tumor size, was a marker for response to a single dose of combined anti-CTLA4 and anti-PD1 checkpoint inhibitors. After a single injection, smaller tumors with prevailing M1 TAMs were able to retain their number, along with a significant decrease in the M2 TAM and MDSCs. In larger tumors, double checkpoint blockade did not change the proportion of MDSCs but increased the proportion of M2 TAMs. At progression, the

proportion of T cells and myeloid cells in tumors were comparable to the ones of initially non-responding tumors, suggesting that immunosuppressive myeloid cells may account for both intrinsic and acquired resistance in this mouse model.

Given their abundance and immunosuppressive properties in the TME, macrophages and MDSCs are proposed as therapeutic targets to enhance the efficacy of checkpoint blockade [225,226]. Depletion of MDSC has been experimentally shown to enhance antitumor immune response [227]. Low levels of circulating MDSCs were also shown to be a positive predictor of ipilimumab treatment in metastatic melanoma patients [228]. Another immunosuppressive myeloid cell type, macrophages, were shown to impede CD8 T cells from reaching the tumor cells [229] or even directly limit PD-1 blockade by removing anti-PD-1 antibodies from PD-1 positive CD8 T cells in an FCγR-dependent manner [230]. However, in certain context macrophages cooperate with T cells to promote tumor regression [231]. Therefore, rather than the depletion, the reprogramming macrophages from M2 to T-cell migration supportive M1 could be another goal to overcome resistance to checkpoint blockade [232]. However, in iBIP2 model, the combined use of anti-PD-1 and anti-CSF1R did not inhibit melanoma growth, and blocking antibody failed to deplete or repolarize tumorigenic macrophages in transgenic melanoma, making IBIP2 model refractory to TAM elimination or repolarization by anti-CSF1R, oppositely to transplantable melanoma model [204]. The reason for this lack of response could be the myeloid cell-dependent mechanisms of response in this tumor model. Currently, a lot of clinical trials, combining checkpoint blockade with depletion of macrophages or, more rarely, MDSCs are ongoing [109]. A better understanding of microenvironment-driven resistance and effective co-targeting of immunosuppressive myeloid cells could translate to the clinical improvement of response to immunotherapy.

On the basis of the current evidence, our data confirms that gradually developing immunosuppressive microenvironment is a reason behind intrinsic as well as acquired resistance to immunotherapy, and encourages the use of immunosuppressive (MDSC+M2) to antitumor (M1) myeloid cell ratio in tumor

as a marker of response to double checkpoint blockade with anti-CTLA4 and anti-PD-1. Although our findings were limited to only one mouse model and did not take into account the effect of Tregs, taken together they provide the rationale for assessing the myeloid compartment in the immune TME at baseline as well as during, and after the treatment.

4.6. Immune tumor infiltration and serum chemokine profiling in ovarian cancer patients

4.6.1. Rationale

In the previous chapters we demonstrated the dynamics of immune TME formation during the development of BRAF-driven melanoma in mouse model, and highlighted the importance of immune TME during response to treatment. However, as iBIP2 mouse model represents a homogeneous inflamed phenotype tumor population, we were next interested in exploring more heterogeneous patient population and translating our previous findings for discovery of novel treatment targets or therapy biomarkers.

We chose to investigate the ovarian cancer, as its molecular analysis revealed the underlying genomic instability, DNA repair defects and copy number alterations, that may result in formation of neoantigens [233]. Moreover, several independent groups revealed the heterogeneity of OC based on gene and miRNA expression patterns and reported four largely overlapping molecular subtypes: C1/mesenchymal, C2/immunoreactive, C4/differentiated, C5/proliferative [233,234].

However, the current standard of care for OC does not yet include the state-of-the-art molecular and immunology findings, although recent studies emphasized an active role of the stromal TME in the pathogenesis of OC and presented evidence for association of molecular subtypes and survival [235,236], in particular that the immunoreactive molecular subtype-bearing patients, characterized by the elevated mRNA expression of chemokines, MHC class I/II, PD-L1, and IRF7, have a better prognosis than the other subtypes

[237]. These findings emphasize the role of immune system in OC, previously suggested by Coukos and colleagues [238], who showed TILs correlate with increased overall survival in OC patients.

The cross-talk between cancer and immune cells is orchestrated by cytokine and chemokine network, which can act both locally and systemically [239]. The circulating cytokines and chemokines reflect the TME [240]. We therefore aimed to **examine the immune phenotype of OC tumors and select the potential systemic markers reflecting the immune infiltration profile**. We used the K-means clustering to determine the immune phenotype of TCGA patient dataset (2.23.). By analyzing the mRNA expression data, we assigned a specific gene expression signature for each immune phenotype, and selected a set of chemokines for further analysis. From the 40 OC patients cohort (2.21.), we collected preoperative serum samples (2.22.) and surgically removed tumor tissue (2.22.). We next performed tumors immune infiltration measurement by flow cytometry (2.26.), histology staining (2.24.) and qPCR (2.27.). After classifying OC patients based on their tumor immune infiltration, we measured their level of intratumoral and circulating chemokines (2.25.) to select the combination allowing to predict the immune-infiltrated tumors.

4.6.2. Clustering ovarian tumors from TCGA dataset into distinct immune phenotypes

First, we aimed to classify patients from TCGA dataset based on their immune phenotypes. As there are no histology data available for TCGA tumors, we aimed to cluster them solely by their mRNA expression. Based on the previous research [241] and ovarian cancer-related literature search, we selected a set of immune phenotypes-related genes, covering the areas of immune response, angiogenesis, immune and non-immune stroma. We used mRNA data from 489 patients from the TCGA dataset. Supervised K-means clustering analysis revealed three clusters of patients with differential gene expression (Figure 26). These clusters reflected the immune phenotypes arising from cancer-immunity cycle and were termed accordingly. Patients of immune-desert

(D) cluster had high expression of angiogenesis-related genes and low expression of immune or stroma-related genes. In immune-excluded (E) cluster, there was a high expression of genes related to a non-immune reactive stroma. Samples from inflamed (I) cluster were characterized with high expression of inflammation and immune-response related genes. Both excluded and inflamed tumors had variable expression of immune stroma-representing genes.

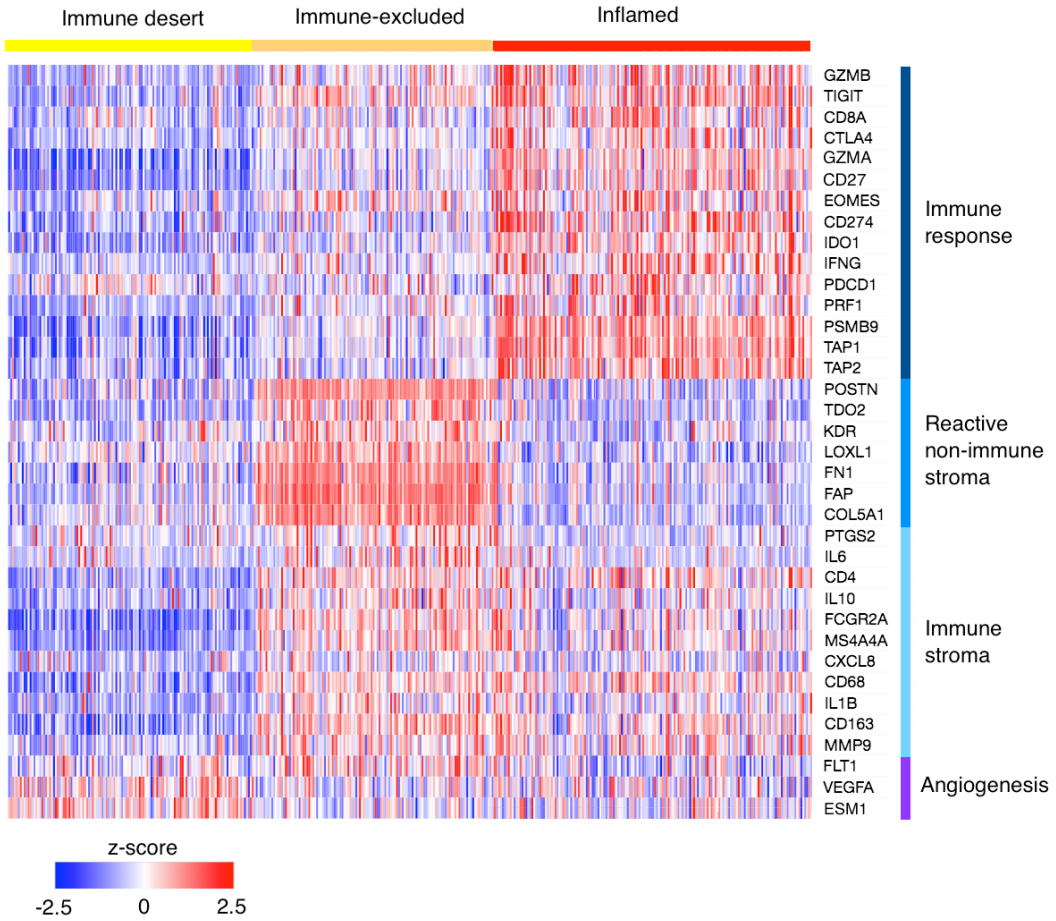

Figure 26. Tumor immune gene signature analysis. Heatmap showing the microarray expression (z-score) of genes of interest (rows) in 489 pre-treated tumors of TCGA dataset patients (columns). Supervised k-means clustering was applied to cluster tumors intro three distinct immune phenotypes (immune desert, immune-excluded, and inflamed), based on their expression of the genes related to immune response, reactive non-immune stroma, immune stroma, and angiogenesis

Survival analysis revealed that tumors clustered as immune-excluded have worst RFS and OS, whereas the prognosis of inflamed and deserted tumors is similar (not shown).

By analyzing the mRNA expression of genes, related to immune cell

recruitment and communication, CSC, EMT and MDR (not used for clustering), we found the immune phenotype-unique expression patterns (Table 4).

Table 4. Unique transcriptional profile in tumors of different immune phenotypes. In TCGA dataset (microarray data) we identified the significantly upregulated genes of interest, that are common for tumors of excluded phenotype, inflamed phenotype, or for both of them. For significance, Mann-Whitney test with FDR correction was used.

Excluded + Inflamed					
Gene	**Function**	**p**	**Gene**	**Function**	**p**
CCL2	IMM	<0.0001	*CCL4*	IMM	<0.0001
CCL3	IMM	<0.0001	*CCL11*	IMM	<0.0001
CCL20	IMM	0.0271	*IL18*	IMM	0.0045
Excluded			**Inflamed**		
Gene	**Function**	**p**	**Gene**	**Function**	**p**
CSF3	IMM	0.0033	*CCL1*	IMM	0.0023
CXCL1	IMM	0.0003	*CCL5*	IMM	<0.0001
CXCL5	IMM	0.0003	*CCL17*	IMM	0.0438
CXCL8	IMM	0.0048	*CLEC7A*	IMM	<0.0001
ICAM1	IMM	0.0001	*CSF2*	IMM	0.0013
IL1B	IMM	<0.0001	*CXCL9*	IMM	<0.0001
MARCO	IMM	<0.0001	*CXCL10*	IMM	<0.0001
MMP3	STR	<0.0001	*CXCL11*	IMM	<0.0001
CTNNB1	CSC	0.0048	*HLA-DRA*	IMM	<0.0001
NOTCH1	CSC	<0.0001	*STAT1*	IMM	<0.0001
CDH2	EMT	<0.0001	*NANOG*	CSC	0.0129
SNAI1	EMT	<0.0001	*POU5F1*	CSC	0.0020
SNAI2	EMT	<0.0001	*SOX2*	CSC	0.0104
TWIST1	EMT	<0.0001	*ABCB1*	MDR	0.0019
VIM	EMT	<0.0001	*ABCG2*	MDR	0.0003
ZEB1	EMT	<0.0001	*PCNA*	MDR	0.0202

ANG – angiogenesis, CSC – cancer stem cells, EMT – epithelial-mesenchymal transition, IMM – immune system, STR – stroma.

Both immune-related subtypes, excluded and inflamed, are characterized with upregulated mRNA of macrophage-attracting chemokines CCL2, CCL3, CCL4, eosinophils-attracting CCL11, Treg-attracting CCL20, and DC-attracting IL-18. Also, excluded tumors have a phenotype-specific high expression of neutrophil/MDSC attracting CXCL1, CXCL5, CXCL8, CSF3. Inflamed tumors

are characterized by high expression of activated T lymphocyte attractants CXCL9, CXCL10, CXCL11, CCL5, Treg attractant CCL17, as well as macrophage-attracting CCL1 and CSF2. Both immune-related subtypes have increased expressions of both M1 (IL-1β in excluded, HLA-DRA in inflamed) and M2 macrophage (MARCO in excluded, CLEC7A in inflamed) markers. Interestingly, the mRNA levels of classical EMT- and CSC-related TFs are mutually exclusive in excluded (EMT high, CSC low) and inflamed (EMT low, CSC high) tumors.

4.6.3. Classifying ovarian tumors based on their immune infiltration

Having revealed the specific chemokine landscapes in immune infiltrated (excluded and inflamed) ovarian tumors from TCGA dataset, we hypothesized that local and systemic chemokine milieu could serve as a biomarker and help subtyping the ovarian tumors.

For this, we analyzed the immune infiltration in tumors from 40 patients diagnosed with OC of stage III (90%) or IV (10%). We grouped the patients into inflamed and non-inflamed tumor groups, based on three parameters: TILs in tumor sections, immune response-related gene expression in tumor tissue, and CD3+ positive cell count in the tumor (Figure 27).

H&E-stained tumor tissue sections were evaluated by a pathologist for the presence or absence of TILs (Figure 27 A), resulting in 21 TIL-positive and 19 TIL-negative samples.

Immune response-related gene expression was measured with qPCR, and clustered into high-expression (18 samples) and low expression (22 samples) clusters (Figure 27 B).

The percentage of CD3+ cells in tumors was evaluated with flow cytometry on freshly digested tumor tissue samples. Gating for living cells and CD45+ was applied. A cutoff of 3% of CD3+ cells was applied to divide the study population into 18 samples with high and 22 samples with low immune infiltration in the tumor (Figure 27 C).

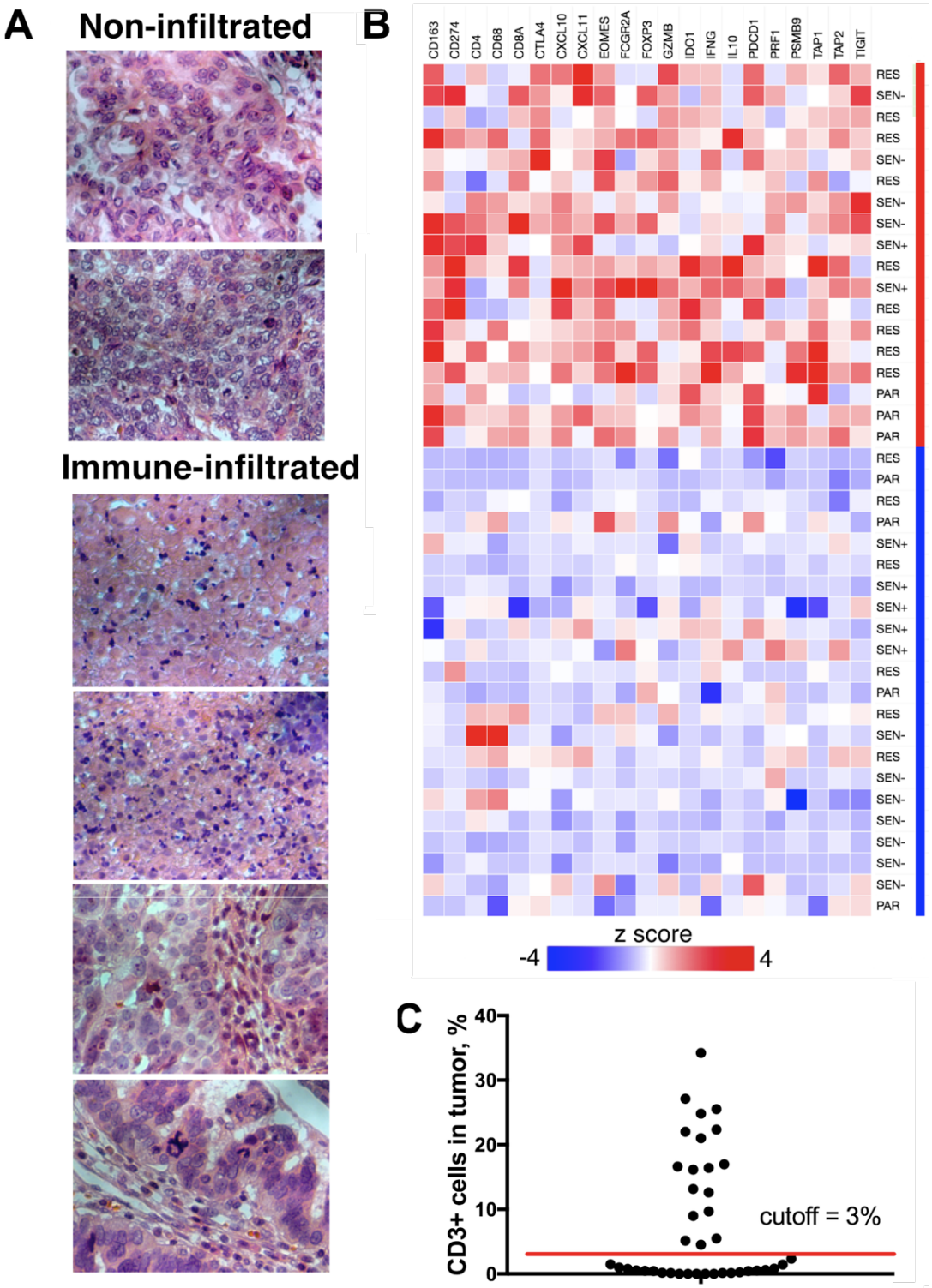

Figure 27. Selection of immune-infiltrated tumors. We grouped the patients based on three independent evaluations. Tumors were classified as immune-infiltrated if intraepithelial or stromal T lymphocytes were detected in H&E stained tissues (A). Patients were clustered based on the tumoral mRNA expression levels of immune response-related genes, as measured with qPCR (B). Level of CD3+ cells was evaluated under flow cytometer and a cutoff of 3% was applied to distinguish immune-infiltrated tumors (C). Patients were assigned to the immune-infiltrated group if positive for at least two factors

We assigned the patients into the immune-infiltrated group if they were positive for at least two factors out of three: >3% of infiltration with CD3+, presence of TILs in tumor sections, or inclusion in highly expressed immune-related gene cluster. Out of 25 samples, characterized by at least one positive inflammation-related factor, only 12% did not overlap with other factors, and thus were assigned to the non-infiltrated group, together with the rest of the samples, which did not qualify for the immune-infiltrated group. Finally, we ended up with 22 patients in the immune-infiltrated and 18 in the non-infiltrated group (Table 5). The median age, stage, and survival did not differ between groups.

Table 5. Overview of patients characteristics based on their immune infiltration in tumor (n=40).

	Immune-infiltrated	**Non-infiltrated**	**P value**
N	22	18	
Age			0.561
median	66	67	
range	46-76	32-74	
Stage			0.938
III	20 (91%)	16 (89%)	
IV	2 (9%)	2 (11%)	
RFS			0.4102
Median, months	7.2	18.6	
OS			0.7110
Median, months	NR	NR	

RFS – recurrence-free survival, OS – overall survival, NR – not reached

Notably, the general CD45+ infiltration level (measured by flow cytometry) was 38% in immune-infiltrated group versus 16% in non-infiltrated group (p=0.0038). CD3+ infiltration was 13% versus 2.5% (p=0.0052), respectively. Infiltration with myeloid cells (determined from sample scatter profile) was 19% versus 13 % (p=0.0112), respectively.

After grouping the patients into immune infiltrated and non-infiltrated groups, we determined their intratumoral concentration of chemokines, earlier

identified in TCGA dataset as specific to immune excluded and/or inflamed subtypes: CCL2, -3, -4, -5, -11, -17, -20, CXCL1, -5, -8, -9, -10, -11. We observed the increased level of CCL3, CCL4, CCL5, CXCL9, CXCL10, and CXCL11 (Figure 28) in tumors belonging to the immune-infiltrated group in comparison to tumors in the non-infiltrated group.

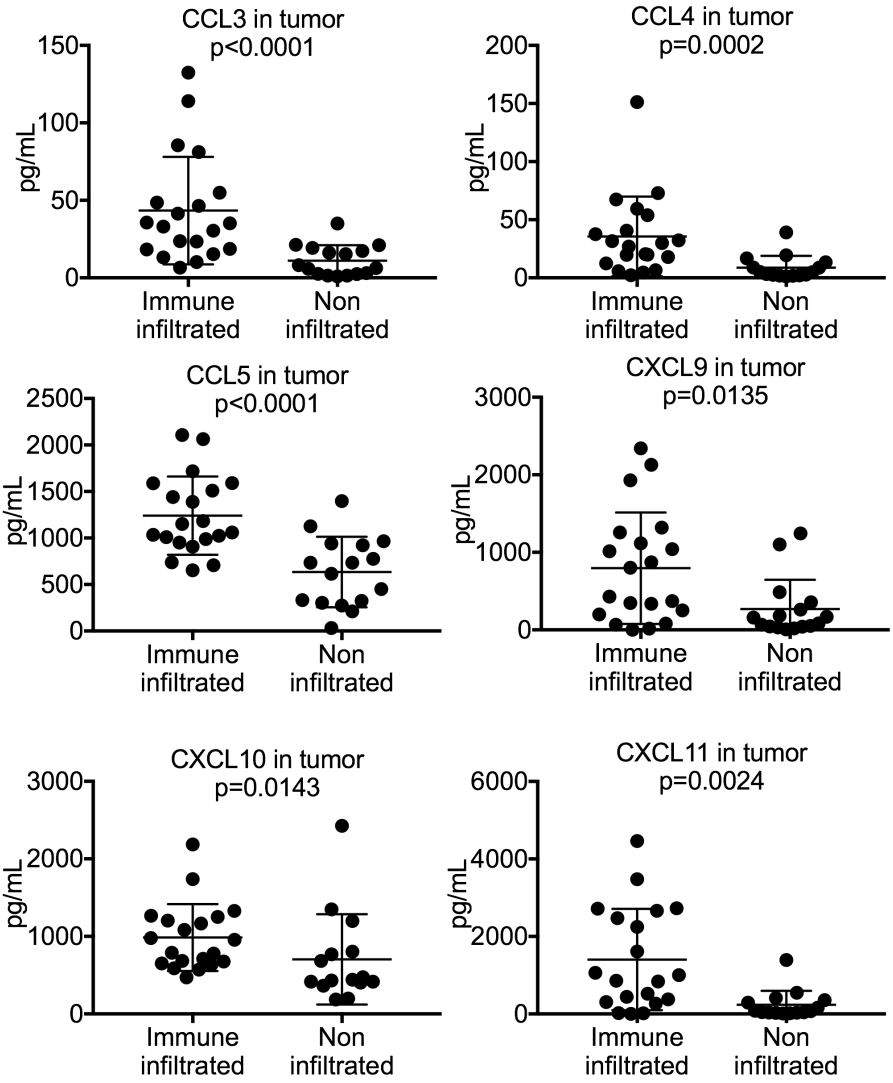

Figure 28. Levels of intratumoral chemokines in immune-infiltrated and non-infiltrated tumors. The concentration of chemokines is normalized to total protein concentration in tumor lysate. Scatter plots include mean and standard deviation. Differences in cytokine levels were identified by Mann-Whitney-U-test.

4.6.4. Detection of immune-infiltrated tumors with the circulating CXCL9+CXCL10

The differential levels of chemokines in immune infiltrated and non-

infiltrated tumors encouraged us to examine the difference in preoperative patient serum. We noted the differences in serum level of CXCL11, CCL2, CXCL10, and CXCL9. The levels of these chemokines were higher in the serum of patients in the infiltrated group in comparison to the non-infiltrated group (Table 6), correspondingly with the trends seen in tumors.

Table 6. Overview of circulating chemokine levels and their performance metrics in patients with immune-infiltrated versus non-infiltrated tumors. Differences in cytokine levels were identified by Mann-Whitney-U-test. AUC and sensitivity at given specificity were calculated from receiver operating characteristic curve.

	Immune-infiltrated (n=22) mean (range) pg/ml	Non-infiltrated (n=18) mean (range) pg/ml	p	AUC	cutoff pg/ml	SE %	SP %	CUI +	CUI -
CXCL11	870 (120-5740)	406 (36-1457)	0.0330	0.709	983	30	94	0.26	0.49
CCL2	1796 (649-3744)	864 (193-2269)	0.0006	0.825	2134	30	94	0.26	0.49
CXCL10	1625 (217-4988)	667 (124-2187)	0.0003	0.841	1410	40	94	0.36	0.52
CXCL9	190 (10-953)	44 (10-174)	0.0006	0.846	147	45	94	0.41	0.54
Combo CXCL9 CXCL10	-	-	-	0.900	-	70	94	0.75	0.74

AUC – area under the curve, SE – sensitivity, SP – specificity, CUI – clinical utility

To evaluate the predictive value of serum chemokines, we carried out the ROC curve analysis to calculate the cutoff, area under the curve (AUC) and sensitivity at clinically relevant specificity. At 94% specificity, the sensitivity of single chemokines varied between 30% and 45%. Taken alone, these cytokines exhibited poor positive and fair negative clinical utility, despite good AUC values. Out of possible combinations, a CXCL9+CXCL10 classifier proved to be the best: with 70% sensitivity and 94% specificity it resulted in good positive and negative clinical utility for discrimination of patients with inflamed tumors. CXCL9+CXCL10 had improved AUC in comparison to CXCL9 alone (Figure 29).

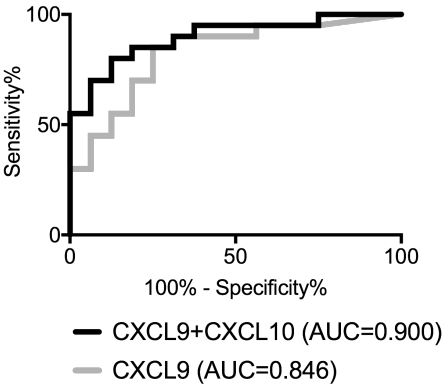

Figure 29. ROC curves of circulating chemokines as detectors of patients with immune-infiltrated tumors. ROC - receiver operating characteristic, AUC – area under the curve - was calculated from the ROC curve

Although the actual RFS curves of patients from immune-infiltrated and non-infiltrated patients did not differ significantly (p=0.4102), patients with elevated serum levels of CXCL9+CXCL10 had significantly worse RFS and were 2.4 likely to progress that patients with low serum levels of CXCL9+CXCL10 (Figure 30). No association with OS was observed.

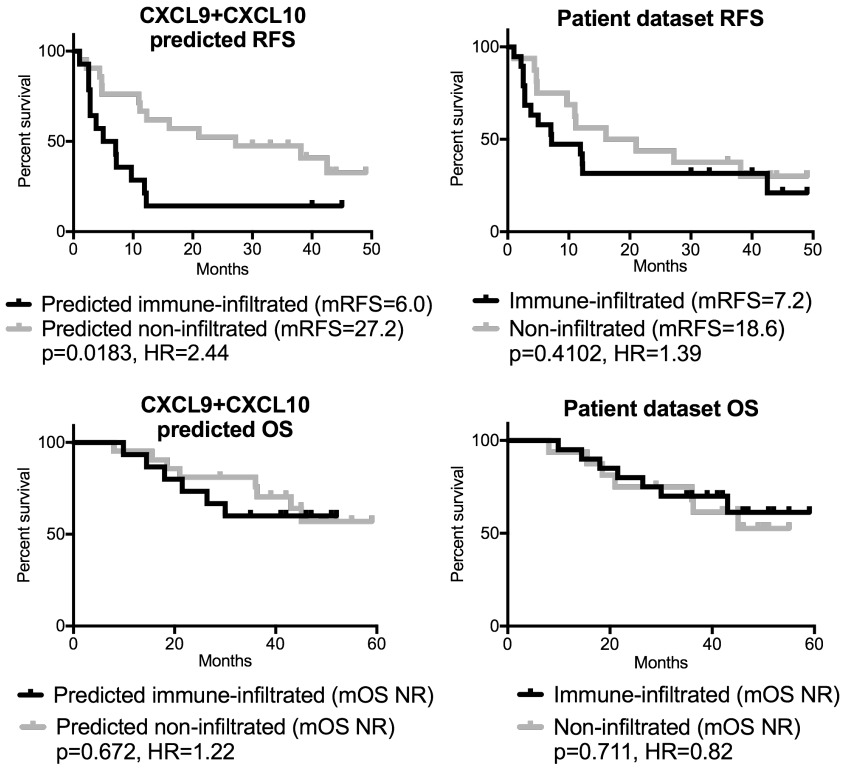

Figure 30. Predictive value of CXCL9+CXCL10. Recurrence-free and overall survival estimates for patients with immune-infiltrated or non-infiltrated tumors, as predicted with preoperative circulating CXCL9+CXCL10, compared to actual survival of our study patients' with immune-infiltrated or non-infiltrated tumors. mRFS – median recurrence-free and mOS – median overall survival is given in months and was calculated from Kaplan Meier survival curves. Log-rank test p-value and hazard ratio (HR) for recurrence or death are shown.

4.6.5. Discussion

The cancer-immunity cycle summarizes the stepwise processes required to yield anticancer T cell response [7] and distinguishes three immune infiltration phenotypes together with potentially suitable immunotherapeutic strategies for each of them. Using the specific immune-phenotype oriented set of genes on TCGA dataset, we were able to classify tumors into the immune desert, immune excluded or inflamed subtype. Further transcriptomic analysis revealed that immune-excluded subtype is characterized by the high expression of neutrophil/MDSC-attracting chemokines and EMT-related TFs. The inflamed subtype is characterized by the high expression of T cell-attracting chemokines and CSC-related TFs. Both immune-excluded and inflamed tumors express high levels of macrophage-recruiting factors. These findings suggest that each immune phenotype manifests its specific chemokines, that can mediate the cross-talk of various cell types.

Studies demonstrated that the signaling components and metabolites of the TME can gain access to the bloodstream [240,242]. Therefore, we hypothesized that chemokines in cancer patient serum may reflect the immune TME status in a given tumor, and therefore is a relevant and convenient approach for discovery of novel biomarkers, which can be beneficial for the personalized management of complex diseases such as recurrent ovarian cancer.

We found the increased levels of circulating CXCL9 and CXC10 in the sera of patients with immune-infiltrated tumors. Together with their receptor CXCR3, these cytokines can act both as tumor suppressing and promoting factors, depending on their source. CXCL9 and CXCL10 recruit T and B lymphocytes, NK, and NKT cells [243]. However, their prognostic impact is rather contradictory. We propose CXCL9+CXCL10 classifier for discrimination of patients with stronger immune infiltration in tumors. Also, these chemokines can potentially select patients with higher risk to experience early recurrence. Although in OC intratumoral CXCL9 and CXCL10 correlate with better OS [244], the levels of these chemokines were shown to be associated with worse

prognosis in several other cancers [245–250]. The complexity of surrounding TME can explain the differences in observed outcomes, as the tumor-dependent factors can shift the microenvironment from immune activating to immune suppressing. Also, CXCL9 and CXCL10 chemokines can recruit both CTLs and Tregs, as shown in ovarian cancer *in vitro* and in murine models [251,252]. In our study, elevated circulating chemokine levels reflected the overall T lymphocyte infiltration. However, gene expression analysis revealed the presence of both antitumoral (increased expression of CD8, IFNγ, granzymes, eomesodermin) and immunosuppressive (increased expression of FoxP3, CTLA-4, PD-L1, IL-10, CD163) T cells-associated processes in inflamed tumors. These findings suggest the presence of both CTLs and Tregs, often in the same tumor. CTL/Treg ratio can determine the prognosis of OC patients [253]. Another reason for the contradictory prognostic role of CXCL9 and CXCL10 are their splice variants, that can act antagonistically, as shown in hepatocellular carcinoma and OC [254–256].

One of the crucial cancer-immunity cycle stages, trafficking and retaining of effector T cells in the tumor, is shown to be mediated by CXCL9 and CXCL10 [7]. More, the expression of these cytokines, together with IFNγ and granzymes, correlates strongly with the expression of PD-L1 in the tumor, suggesting the potential benefit of checkpoint blockade [257]. The successful clinical trials in melanoma and RCC reported the association of intratumoral CXCL9 and CXCL10 in TILs with clinical benefit from adoptive T cell therapy [258], ipilimumab [259,260], pembrolizumab [261], as well as the increase of circulating CXCL9 and CXCL10 during treatment with nivolumab [262,263]. The early phase checkpoint inhibitor trials in OC demonstrated a durable antitumor response in some patients (reviewed in [264]). We also detected increased mRNA expression of CTLA-4, PD-L1, IFNg, granzyme B, and CXCL10 in histologically-confirmed immune-infiltrated tumors with increased serum CXCL9+CXCL10 level. The relatively short RFS of these patients indicates them as potential candidates for immunotherapy. So far, the results of checkpoint inhibition in OC are promising regarding the poor sensitivity of

platinum-resistant OC to other conventional chemotherapy agents [264,265]. Therefore, modulation of TME in patients selected with the help of accurate predictive biomarkers may be an encouraging means for improving the OC management and survival. However, the presence of Tregs has to be acknowledged too, as it may impact the choice and strategy of further immunotherapy treatment.

In conclusion, we confirm the existence of specific chemokine expression patterns in different immune phenotypes of OC and suggest that immune-infiltrated tumors can be preoperationally characterized by the elevated levels of circulating CXCL9+CXCL10, that reflect the increased expression of other inflammatory chemokines in tumor tissue. Despite the exploratory nature of this study, our findings provide background for further investigations of the clinical performance of multiple chemokine combinations as patients stratification tools for better OC management.

4.7. Prediction of disease recurrence in ovarian cancer patients

4.7.1. Rationale

Current situation in OC management remains unsatisfactory as the overall survival has hardly improved over the past decades [266,267]. OC nearly always presents with advanced disease and therefore accounts for low overall survival [268]. Standard-of-care treatment for primary OC is cytoreductive surgery followed by 6 cycles of adjuvant chemotherapy with carboplatin and paclitaxel. OC tumors are initially responsive to platinum-based chemotherapy, however, the majority of patients eventually experience the tumor recurrence [269]. As the effectiveness of second-line chemotherapy regimens for OC is limited [270], the multiplex categorization of patients, incorporating the recent discoveries of molecular genetics, is suggested for future patient stratification in clinical trials [271]. In the previous chapter we confirmed the existence of three immune phenotypes in TCGA dataset, each with specific gene expression

pattern, highlighting the relevance of the immune system in OC development and, potentially, in response to treatment.

The role of the immune system in the development of chemoresistance and recurrence of OC remains elusive. The primary evidence for association of immune cells and chemosensitivity in OC was recently reported from *in vitro* and mouse model studies, which demonstrated the ability of CD8+ T cells to alter the metabolism of cytostatic drugs in fibroblasts [272] or negative regulation of PD-L1 on CD8+ T cells [273] to abrogate chemoresistance. However, dual nature of the immune system is often exploited by tumor cells to create local immune suppression [274] and promote chemoresistance [275]. Cytokines and chemokines form the extensive networks regulating the processes of antitumor immune response and tumor-induced immunosuppression, therefore they present as convenient candidates for the discovery of novel biomarkers as the basis for rational treatment decisions.

Despite frequent recurrence and limited effective treatment options, the selection of reliable prognostic and predictive biomarkers in OC, especially those of immune origin, remains limited [276]. Here, we aimed to **evaluate the potential of systemic cytokines as predictive markers of ovarian cancer recurrence.** From the 40 OC patients cohort (2.21.), we collected preoperative serum samples (2.22.). We determined the preoperative level of circulating chemokines in sera of patients and aligned them with the treatment outcome (2.25.). We selected the best circulating chemokine combination allowing to predict the patient's response to treatment.

4.7.2. Monitoring disease course in ovarian cancer patients

All patients involved in this study (n=40) were diagnosed with OC of stage III (90%) or IV (10%). After the complete resection of tumor foci, all patients completed 6 cycles of adjuvant chemotherapy with carboplatin and paclitaxel. The median follow up time was 46 months. The patients were regularly tested for the blood CA125 level. Recurrence was confirmed by radiological imaging. 73% of patients (n=29) experienced the recurrence of

primary disease during the follow-up period with a median recurrence-free survival (RFS) equal to 11.1 months. An overview of patients clinical characteristics is presented in Table 7.

Table 7. Overview of patients characteristics based on their treatment outcome (n=40).

	Recurrent	Non-recurrent	P value
N	29	11	
Age			0.217
median	63	67	
range	32-76	32-74	
Stage			0.109
III	25 (86%)	11 (100%)	
IV	4 (14%)	0 (0%)	
RFS			<0.0001
Median, months	7.1	NR	
OS			0.0054
Median, months	43.0	NR	

RFS – recurrence-free survival, OS – overall survival, NR – not reached

4.7.3. Detection of recurrence-prone tumors with the circulating CCL4+CCL20+CXCL1

We hypothesized that profiling circulating inflammatory cytokines could help unveil the role of inflammation in OC response to chemotherapy. We examined if our chemokines of interest, specified in the previous chapter are differentially expressed in serum in recurrent and non-recurrent patients (Table 8).

To evaluate the predictive value of serum chemokines, we carried out the ROC curve analysis to calculate the cutoff, area under the curve (AUC) and sensitivity at clinically relevant specificity. Among single chemokines, CCL4 had the best sensitivity (62%) and fair positive clinical utility (CUI) at a cutoff of 20 pg/ml. Combining two or more chemokines into a single classifier resulted in improved sensitivity. The combination of CCL4+CCL20+CXCL1 had good positive and fair negative clinical utility. ROC curves for CCL4 and best combination classifier are shown in Figure 31.

Table 8. Overview of circulating chemokine levels and their performance metrics in recurrent versus non-recurrent patients. Differences in cytokine levels were identified by Mann-Whitney-U-test. AUC and sensitivity at given specificity were calculated from receiver operating characteristic curve.

	REC (n=29) mean (range) pg/ml	NON (n=11) mean (range) pg/ml	p	AUC	cutoff pg/ml	SE %	SP %	CUI +	CUI -
CCL20	46 (2.5-357)	12 (2.5-61)	0.006	0.794	32	31	91	0.27	0.30
CXCL1	2058 (118-7542)	1105 (46-3632)	0.015	0.762	2028	42	91	0.39	0.34
CCL3	9.0 (2.8-31.3)	3.8 (2.3-5.8)	0.007	0.787	5.2	54	91	0.50	0.39
CCL4	28 (7.6-126)	14 (6.7-20)	0.016	0.758	20	62	91	0.58	0.42
Combo CCL4 CCL20 CXCL1	-	-	-	0.854	-	81	91	0.77	0.58

REC – recurrent, NON – non-recurrent, AUC – area under curve, SE – sensitivity, SP – specificity, CUI – clinical utility

The combination of CCL4+CCL20+CXCL1 could also predict RFS and overall survival (OS), reflecting the trends of our study population, as well as TCGA patient population (Figure 32).

Figure 31. ROC curves of circulating chemokines as detectors of recurrence-prone patients. ROC - receiver operating characteristic, AUC – area under the curve - was calculated from the ROC curve

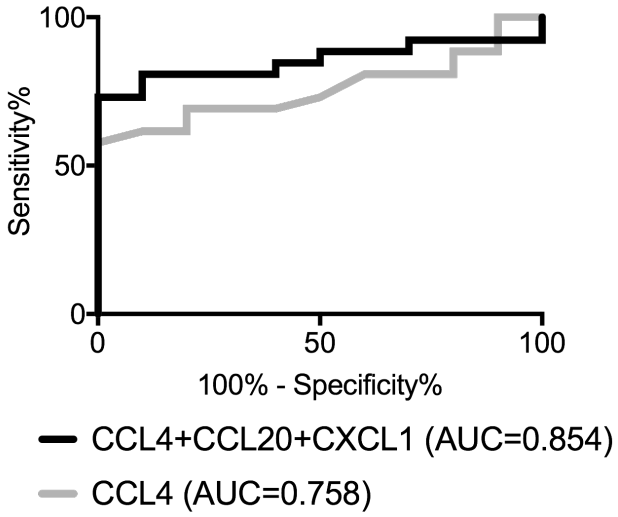

Elevated serum levels of CCL4+CCL20+CXCL1 resulted in four-times higher risk to recur as well as significantly worse survival prognosis. The predicted median RFS and OS was comparable to median RFS and OS of patients included in the TCGA dataset.

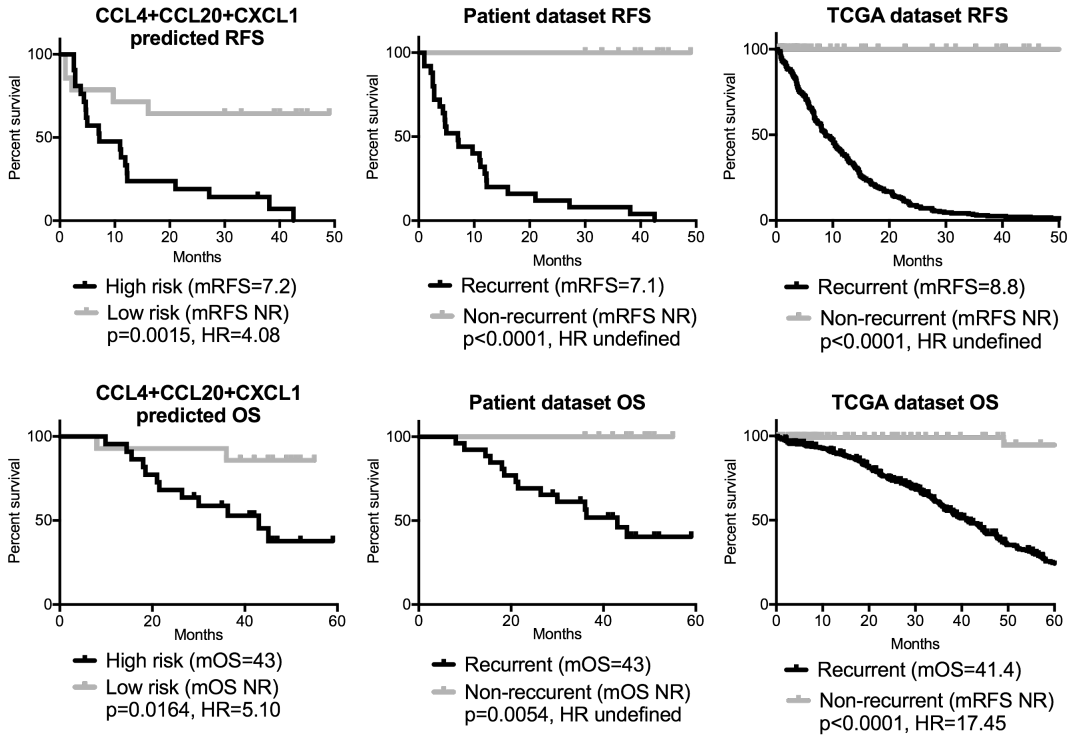

Figure 32. Predictive value of CCL4+CCL20+CXCL1. Recurrence-free and overall survival estimates for patients with high risk or low risk of recurrence as predicted with CCL4+CCL20+CXCL1, compared to actual survival in recurrent versus non-recurrent patients in our study and TCGA datasets. mRFS – median recurrence-free and mOS – median overall survival is given in months and was calculated from Kaplan Meier survival curves. Log-rank test p-value and hazard ratio (HR) for recurrence or death are shown.

4.7.4. Discussion

Resistance to platinum-based chemotherapy remains the major cause of recurrence of OC. There are no clinically useful biomarkers to predict the chemotherapy outcome ahead of treatment. Since OC is often driven by somatic and germline mutations, attempts to classify tumors as treatment-sensitive or -resistant were usually focusing on tumor gene expression profiling and resulted in multiple predictive gene expression algorithms [277–279]. Our previous findings, showing that the soluble circulating factors to some extent reflect the TME, encouraged us to address the preoperative serum chemokine level as potential predictive biomarkers for ovarian cancer.

So far, the attempts to discover the circulating biomarkers of chemoresistance were mostly limited to classical OC markers of recurrence

monitoring. CA-125 was shown to be a positive response predictor if present at lower levels at the time of diagnosis [280], however, other studies contradict this finding [281] or emphasize another OC marker – HE4 - to be more specific in preoperative prediction of platinum sensitivity [282,283]. The lack of reliable preoperative biomarkers of recurrence emerges from the complexity of chemoresistance development process, which in turn depends on multiple factors such as intrinsic genetic and epigenetic alterations, the cell metabolism as well as the tumor immune infiltration, and even the host immunity [284,285]. The idea that the elements of complex TME contribute to responsiveness and resistance to chemotherapy suggests the rationale for systemic analysis of soluble mediators. Platinum-based drugs and mitotic inhibitors taxols are able to increase the expression of NFκB-dependent chemokines and thus promote the acquired chemoresistance [286,287]. We hypothesized that recurrence-prone tumors may exhibit altered levels of serum chemokines already at diagnosis. We detected the increased levels of CCL4, CXCL1, CCL20 chemokines in patients, who later experienced disease recurrence. These cytokines were shown to have pleiotropic effects in cancer development and response to treatment. Increased levels of circulating CXCL1 in ovarian carcinomas versus benign pelvic masses imply its role as a marker in early OC detection [288], which may be attributable to its capability to induce OC cells proliferation by transactivation of EGFR and induction of MAPK signaling, as shown *in vitro* [289]. CXCL1 participates in endothelial-carcinoma-myeloid signaling network by its ability to recruit neutrophils that release VEGF-A and promote angiogenesis *in vivo*. More, recruited neutrophils/MDSCs promote cancer cell survival [290]. Chemotherapy-induced TNF-α increases the expression of CXCL1, amplifying the loop and causing chemoresistance [291]. CCL20, similarly to CXCL1, is also expressed in response to EGF and TNF-α [292] and has a pro-metastatic effect, inducing proliferation, migration, and adhesion of tumor cells [293,294]. Besides, CCL20 recruits CD34+ derived dendritic cells and Tregs [295,296]. An interesting mechanism was proposed in esophageal squamous cell carcinoma study, which showed that CCL4 and CCL20 recruit functionally different T

lymphocyte subsets, CTLs and Tregs, respectively. High level of CCL20 was associated with worse prognosis, whereas increased CCL4 correlated with better overall survival [297]. Correlation of increased intratumoral CCL4 and CD8+ TILs was also reported in OC [298]. Altogether, the increased levels of CCL4+CCL20+CXCL1 in recurrent patients' serum suggest the existence of a dichotomous immune milieu in chemoresistant OC patients where anti-tumor effects of CCL4 are overshadowed by tumor-promoting properties of CCL20.

In conclusion, we propose a combination of circulating preoperative CCL4+CCL20+CXCL1 chemokines as a predictive biomarker for evaluating OC recurrence. Although our findings are rather descriptive, they provide the background for their further mechanistic investigation as well as validation of the biomarker combination in a larger population.

4.8 Overview of findings and their translational relevance

In this study, we have approached the crosstalk of cancer and immune system at local and systemic levels during the processes of tumor development and response to treatment.

The surrounding immune microenvironment in the tumor can polarize the immune response from antitumor to tumor promoting. The goal of immune-based therapies is to balance the host immunity in a way that it destroys cancer cells. Here, we investigated the frequently underestimated balance between immunogenic and tolerogenic properties of tumor antigen-matured DCs, *in vitro* differentiated from monocytes. We demonstrated that maturation with cancer cell lysate results in development of typical mature DC surface phenotype, as well as considerable production of IL-12 and overall T cell stimulation. However, cancer cell lysate also indirectly promoted the expression of tolerogenic marker CD85k, on DCs, as well as their secretion of immunosuppressive cytokines and consecutive Treg induction. These features can be further addressed to improve the anticancer effect of DCs in clinical trials. The cancer cell-induced tolerogenicity of DCs suggests the presence of

immunosuppressive components in the lysate of cancer cells of different histological origins.

We next aimed to dissect how cancer cells of a single origin, varying in their differentiation level and stemness capacity, can affect another type of monocyte-derived myeloid cells, macrophages, in terms of inducing their M1/M2 polarization. Our findings, summarized in Figure 33, suggest the novel hypothesis, relating the cancer cell stemness potential and macrophage polarization abilities. We found that stem-like colon cancer cell lines, characterized by the higher mRNA expression of CSC and EMT markers in comparison to non-stem-like cells are able to induce the acquisition of the representative M2-like surface marker expression profile in differentiated PBMC-derived macrophages. The possible mechanism behind this polarization is the significantly increased secretion of Th2 cytokines IL-10 and IL-13 in stem-like cell line HCT116 and COLO320 in comparison to non-stem-like cell lines HT29, SW620 and NCI-H508. Nevertheless, other soluble factors or extracellular vesicles, not addressed in this study, could also account for increased M2-like polarization ability in stem-like cells.

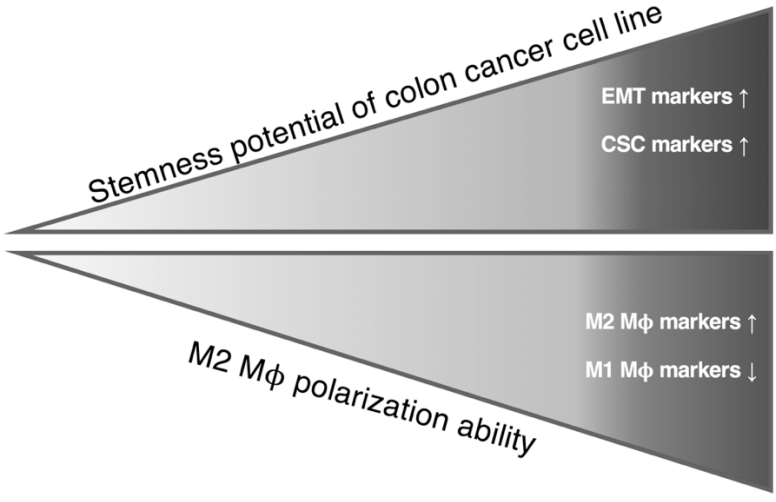

Figure 33. The relationship between stemness potential of colon cancer cells and their macrophage polarization ability. Our findings suggest that macrophages, conditioned with the medium of cells expressing high levels of CSC and EMT markers, were more prone to acquire M2-like phenotype. Cancer wells with higher stemness potential secrete more Th2 type cytokines. CSC – cancer stem cells, EMT – epithelial-mesenchymal transition, Mϕ - macrophage.

After demonstrating the unidirectional effect of cancer cell secretome on macrophage polarization, we next aimed to analyze the bidirectional interplay between these two cell types. By co-culturing the macrophages and ovarian cancer cells in the drug resistance background, we show that, independently of the initial platinum resistance level, cancer cells act towards inducing the M2-like phenotype in macrophages (Figure 34). In resistant cancer cells, this may be determined by the acquisition of molecular and functional EMT- and stemness-related properties, as well as increased production of immunomodulatory cytokines. In platinum-sensitive cells, EMT- and stemness-related transcriptional profile is upregulated upon the co-culture with macrophages. We hypothesize that these alterations may promote the early development of resistant cancer cell sub-clones. Together, these findings suggest that macrophage-promoted EMT-induction in cancer cells and M2-like macrophage polarization in co-culture are the results of cancer and immune cells collaboration towards the creation of immunosuppressive microenvironment.

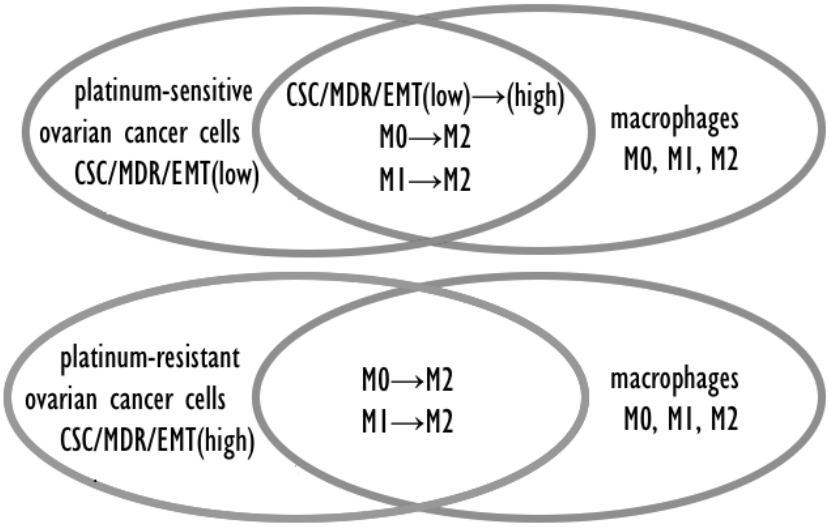

Figure 34. The crosstalk of ovarian cancer cells and macrophages. Independently on the platinum resistance status, co-culture of ovarian cancer cells and macrophages results in macrophages polarization into M2-like phenotype. Platinum-resistant cancer cells retain their high expression of CSC/MDR/EMT markers. Platinum-sensitive cells upregulate the level of CSC/MDR/EMT upon the co-culture with macrophages. CSC – cancer stem cells, EMT – epithelial-mesenchymal transition, MDR – multidrug resistance.

The M2-like macrophage polarization observed in *in vitro* crosstalk studies, representing the early process of tumor formation encouraged us to analyze the dynamics of immune microenvironment formation during development of melanoma tumors *in vivo*. During tumor development in BRAF V600E mutation-driven iBIP2 mouse model, we observed a gradual reprogramming of the immune microenvironment from antitumor-oriented (prevalence of M1 macrophages) to immunosuppression-oriented (prevalence of M2 macrophages). As iBIP2 tumors are massively infiltrated with immune cells, we considered using checkpoint blockade as a suitable immune-targeting melanoma treatment. We found that tumor size as well as the level of immunosuppressive myeloid cells are related to intrinsic and acquired resistance to anti-CTLA-4 and anti-PD-1 combination and therefore are potential targets to improve the efficacy of immunotherapy (Figure 35).

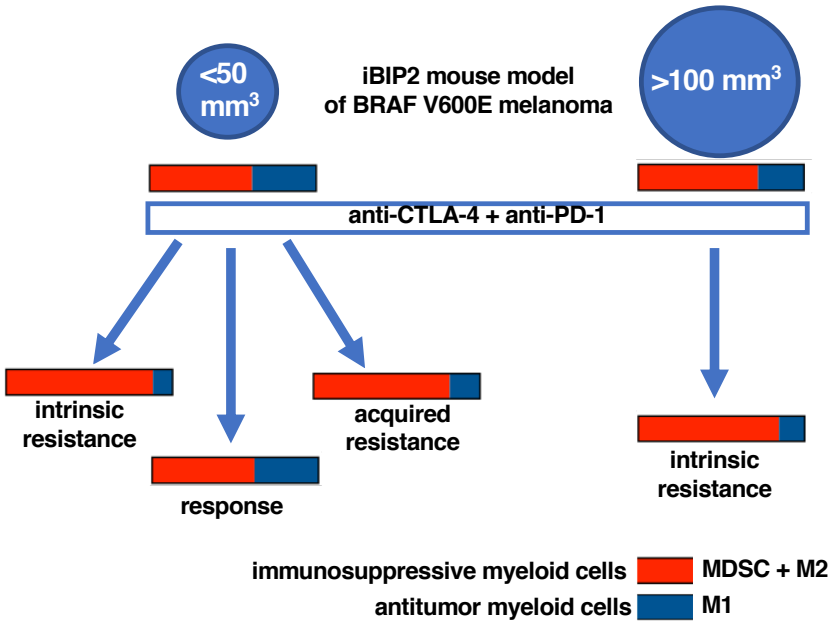

Figure 35. Dynamics of immunosuppressive to antitumor myeloid cell ratio in response to treatment with checkpoint blockade. The immunosuppressive microenvironment renders large tumors unresponsive to double checkpoint blockade. Roughly 25% of smaller tumors are initially unresponsive to checkpoint blockade. Initially responsive tumors eventually acquire resistance mechanisms and relapse. We suggest that both intrinsic and acquired resistance are associated with high (>4) immunosuppressive to antitumor myeloid cell ratio. MDSC – myeloid-derived suppressor cell, M – macrophage.

We propose the intratumoral ratio of immunosuppressive (MDSC + M2 macrophages) to antitumor (M1 macrophages) as a marker of response to double checkpoint blockade.

After showing that the qualitative and quantitative analysis of immune microenvironment presents as a valuable approach for tumor characterization and monitoring the response to therapy, we were encouraged to translate these findings for ovarian cancer. The unsatisfactory clinical outcome of patients with advanced OC urges the search for novel prognostic and predictive biomarkers, and therefore dictated the exploratory nature of this study. We first classified ovarian tumors based on their immune phenotype. For this, we used TCGA dataset patients, which were clustered into immune-desert (non-infiltrated) and -excluded or inflamed subtypes (immune-infiltrated) based on their mRNA expression. We assigned a specific chemokine expression pattern for immune-infiltrated phenotypes. We next translated the *in silico* results into the dataset of ovarian cancer patients, for which we had collected sera and tumor samples.

After classifying patients based on their tumor immune infiltration, we showed that preoperative circulating CXCL9+CXCL10 chemokine combination reflects the level of immune infiltration in ovarian tumors (Figure 36 A). Also, after classifying patients based on their response to primary treatment with platinum-based chemotherapy, we suggested that the increased preoperative levels of circulating CCL4+CCL20+CXCL1 chemokine combination in OC patients serum is associated with shorter RFS and OS (Figure 36 B). Further validations on a larger scale are needed to confirm that these chemokine combinations could successfully model the outcome in other patient populations. Also, determining the exact source and function of these chemokines in ovarian cancer setting is necessary for dissecting and targeting the tumor microenvironment.

In summary, our study provides the evidence for the elements of the immune system to be actively involved in shaping the tumor microenvironment and serving as predictive biomarkers or therapeutic targets. As we used different tumor models, the direct translation of discussed findings from one model to

another would require additional validation. However, the general principles and hypotheses introduced in this study, such as stemness-induced macrophage polarization, macrophage-induced EMT, the ratio of immunosuppressive and antitumor myeloid cells or immune-phenotype specific chemokine expression patterns, could be applied for cancers of other localizations.

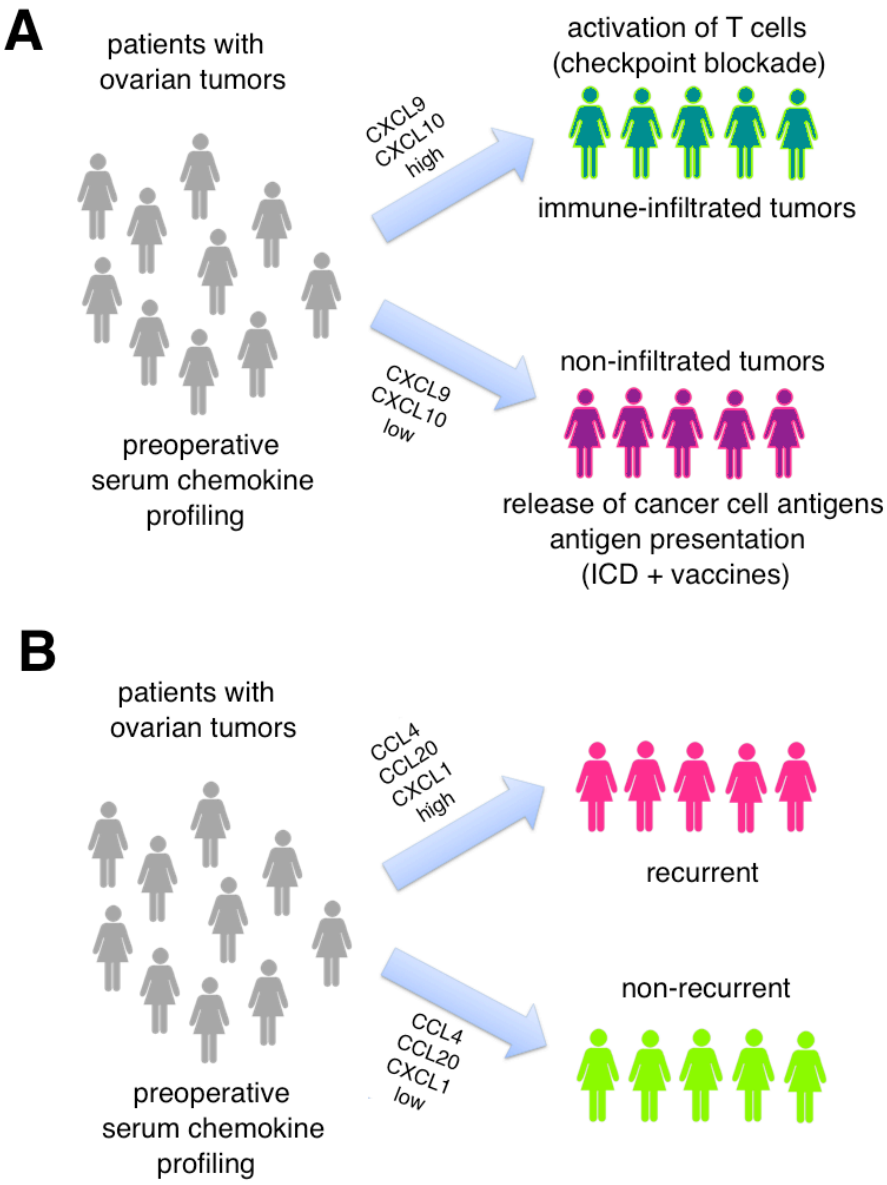

Figure 36. Proposed biomarkers combinations. A. Circulating CCL4+CCL20+CXCL1 combination serves for distinguishing of disease recurrence-prone patients. B. Circulating CXCL9+CXCL10 combination serves for distinguishing of patients with immune-infiltrated tumors. Both groups could further benefit from different types of immunotherapy. ICD – immunogenic cell death.

CONCLUSIONS

1. Although maturation with cancer cell lysate induces a typical mature dendritic cell surface phenotype, as well as a considerable production of IL-12 and overall T cell stimulation, it may also promote a mixed Th1/Th2 type antitumor response and thus render dendritic cells more tolerogenic.
2. The pronounced expression of stemness features in colon cancer cells increases their ability to induce M2-like macrophage polarization. Stem-like cells express significantly more IL-10 and IL-13 than the non-stem-like cells.
3. Ovarian cancer cells, independent of their cisplatin resistance status, tend to polarize M0 or M1 macrophages into M2-like type. Alongside, macrophages can induce EMT and stemness properties in cisplatin-sensitive, but not -resistant, cells.
4. iBIP2 mouse model of melanoma represents the inflamed tumor phenotype, characterized by the gradually developing abundant immunosuppressive microenvironment.
5. The high tumoral ratio of immunosuppressive myeloid cells (MDSC + M2-like macrophages) to antitumor myeloid cells (M1-like macrophages) is a marker of insensitivity to checkpoint blockade with anti-CTLA-4 and anti-PD-1 in iBIP2 mouse model of BRAF-mutated melanoma.
6. Inflamed and immune-excluded ovarian cancer phenotypes are characterized by the expression of the specific sets of chemokines. High preoperative levels of circulating CXCL9+CXCL10 chemokine combination in ovarian patients serum can distinguish immune-infiltrated tumors.
7. High preoperative levels of circulating CCL4+CCL20+CXCL1 chemokine combination in ovarian cancer patients serum can predict the recurrence of the disease.

PUBLICATIONS

Research articles, directly related to the scope of the doctoral dissertation, published in journals with a citation index (IF) in the Clarivate Analytics Web of Science platform.

Published

1. **Mlynska A**, Povilaityte E, Zemleckaite I, Zilionyte K, Strioga M, Krasko J, Dobrovolskiene N, Peng MW, Intaite B, Pasukoniene V. Platinum sensitivity of ovarian cancer cells does not influence their ability to induce M2-type macrophage polarization. *American Journal of Reproductive Immunology*. 2018:e12996. Epub ahead of print.

2. Dobrovolskiene N, Pasukoniene V, Darinskas A, Krasko JA, Zilionyte K, **Mlynska A**, Gudleviciene Z, Miseikyte-Kaubriene E, Schijns V, Lubitz W, Kudela P, Strioga M. Tumor lysate-loaded Bacterial Ghosts as a tool for optimized production of therapeutic dendritic cell-based cancer vaccines. *Vaccine*. 2018;36:4171-4180.

Submitted

3. **Mlynska A**, Salciuniene G, Zilionyte K, Garberyte S, Strioga M, Intaite B, Barakauskiene A, Lazzari G, Dobrovolskiene N, Krasko JA, Pasukoniene V. Chemokine profiling in ovarian cancer patients serum reveals candidate biomarkers for recurrence and immune infiltration. *Under review in Oncology Reports.*

The results of this thesis were presented in 11 international conferences as oral and poster presentations.

Other publications, not directly related to the scope of the doctoral dissertation, in journals with a citation index in the Clarivate Analytics Web of Science platform.

Published

1. Krasko JA, Zilionyte K, Darinskas A, Dobrovolskiene N, **Mlynska A**, Riabceva S, Zalutsky I, Derevyanko M, Kulchitsky V, Karaman O, Fedosova N, Smychych TV, Didenko G, Chekhun V, Strioga M, Pasukoniene V. Post-operative unadjuvanted therapeutic xenovaccination with chicken whole embryo vaccine suppresses distant micrometastases and prolongs survival in a murine Lewis lung carcinoma model. *Oncology Letters*. 2018;15:5098-5104.

2. Liubaviciute A, Krasko JA, **Mlynska A**, Lagzdina J, Suziedelis K, Pasukoniene V. Evaluation of low-dose proton beam radiation efficiency in MIA PaCa-2 pancreatic cancer cell line vitality and H2AX formation. *Medicina (Kaunas)*. 2015;51:302-6.

3. Strioga M, Darinskas A, Pasukoniene V, **Mlynska A**, Ostapenko V, Schijns V. Xenogeneic therapeutic cancer vaccines as breakers of immune tolerance for clinical application: to use or not to use? *Vaccine*. 2014;32:4015-24.

4. Pasukoniene V, **Mlynska A**, Steponkiene S, Poderys V, Matulionyte M, Karabanovas V, Statkute U, Purviniene R, Krasko JA, Jagminas A, Kurtinaitiene M, Strioga M, Rotomskis R. Accumulation and biological effects of cobalt ferrite nanoparticles in human pancreatic and ovarian cancer cells. *Medicina (Kaunas)*. 2014;50:237-44.

ACKNOWLEDGEMENTS

I am deeply grateful to people who contributed to making this thesis possible:

To my supervisor Dr. Vita Pašukonienė for her endless enthusiasm and trust in me. Vita, you are the inspiration to all of us. To my colleagues in ImunoLab who always provided the most enjoyable immunosupportive microenvironment. To Karolina and Neringa for our motivation-boosting rituals. To Marius for sharing his extensive knowledge. To all colleagues in the National Cancer Institute that I had the pleasure to work with. To doctor Birutė Intaitė for her goodwill and management of patient sample collection. To doctor Aušrinė Barakauskienė for her invaluable help with tumor histology evaluation. To my students who contributed to this work.

To the Hanahan Lab in EPFL, and especially to my supervisor Dr. Krisztian Homicsko, who believed in me and offered me to join his projects - the time I spent in Switzerland was one of the most challenging yet rewarding periods of my scientific path. To my chouchou Mei for always having my back in the lab. To Sylvie, Stephan, and Bruno for their help with mouse trials. To all people I was honored to work with - for broadening my horizons in many fields.

To the Department of Biochemistry and Molecular Biology at Vilnius University, my Alma Mater where I was first introduced to the spectacular world of life sciences. Special thanks to my first scientific supervisor Assoc. Prof. Elena Bakienė for her constant support and attention through the last decade, and Prof. Edita Sužiedėlienė for her kindness and professional guidance through the thesis preparation process.

To my family and friends, who are still taking me as I am despite all the PhD craze. For the endless love and support which I received more than I felt I deserved, and for giving me space and solitude when I needed it.

CURRICULUM VITAE

Agata Mlynska (1988-09-29)

Laboratory of Immunology
National Cancer Institute
Santariškių st. 1, LT-08660, Vilnius, Lithuania

Email: **agata.mlynska@gmail.com**
Tel: +370 677 34601
LinkedIn: https://www.linkedin.com/in/agata-mlynska-79355a1b/
ResearchGate: https://www.researchgate.net/profile/Agata_Mlynska
ORCID ID: 0000-0002-3646-0258

Education:

- PhD studies in biochemistry, Vilnius University, 2013-2018
  Thesis: *The role of systemic and local immunity in tumor development and response to treatment*
- Biochemistry, M.Sc, Vilnius University, 2010-2012
  Thesis: *Methylation of IGF2BP1 gene in human leukemia cell lines*
- Biochemistry, B.Sc, Vilnius University, 2006-2010
  Thesis: *Investigation of phototoxic action of carbocyanine dye TICS No.150 on prokaryotic and tumor cells*

Research experience:

- Junior researcher, National Cancer Institute, 2011-present
- Doctoral assistant, École polytechnique fédérale de Lausanne, 2014-2017
- Graduate student, Vilnius University Hospital Santaros Klinikos, 2010-2012
- Trainee, Oslo University Hospital, 2010
- Undergraduate student, Vilnius University, 2009-2010

Scientific production: an author of 6 papers with citation index; a presenter in 11 international scientific conferences.
Projects: participation in 8 research projects (including 3 ongoing).
Certifications: Advanced flow cytometry; Laboratory animal science (FELASA B category); Good manufacturing practice (GMP).
Awards: SCIEX Swiss scientific exchange Scholarship; Best poster award in THE COINS 2016 conference
Membership: Lithuanian Society for Immunology

REFERENCES

1. Hanahan D, Weinberg RA. Hallmarks of cancer: the next generation. Cell. 2011;144:646–74.

2. Hanahan D, Coussens LM. Accessories to the crime: functions of cells recruited to the tumor microenvironment. Cancer Cell. 2012;21:309–22.

3. Kreso A, Dick JE. Evolution of the cancer stem cell model. Cell Stem Cell. 2014;14:275–91.

4. Jayachandran A, Dhungel B, Steel JC. Epithelial-to-mesenchymal plasticity of cancer stem cells: therapeutic targets in hepatocellular carcinoma. J Hematol Oncol. 2016;9:74.

5. Bussard KM, Mutkus L, Stumpf K, Gomez-Manzano C, Marini FC. Tumor-associated stromal cells as key contributors to the tumor microenvironment. Breast Cancer Res. 2016;18:1–11.

6. Schumacher TN, Schreiber RD. Neoantigens in cancer immunotherapy. Science. 2015;348:69-74.

7. Chen DS, Mellman I. Oncology meets immunology: the cancer-immunity cycle. Immunity. 2013;39:1–10.

8. Dunn GP, Old LJ, Schreiber RD. The three Es of cancer immunoediting. Annu Rev Immunol. 2004;22:329–60.

9. Swann JB, Smyth MJ. Immune surveillance of tumors. J Clin Invest. 2007;117:1137–46.

10. Kim R. Cancer immunoediting: from immune surveillance to immune escape. Immunology. 2007;121:1-14.

11. Chen DS, Mellman I. Elements of cancer immunity and the cancer-immune set point. Nature. 2017;541:321-330.

12. Fridman WH, Zitvogel L, Sautès-Fridman C, Kroemer G. The immune contexture in cancer prognosis and treatment. Nat Rev Clin Oncol. 2017;14:717–34.

13. Lyons YA, Wu SY, Overwijk WW, Baggerly KA, Sood AK. Immune cell profiling in cancer: molecular approaches to cell-specific identification. NPJ Precis Oncol. 2017;1:26.

14. Syn NLX, Yong WP, Goh BC, Lee SC. Evolving landscape of tumor molecular profiling for personalized cancer therapy: a comprehensive review. Expert Opin Drug Metab Toxicol 2016;12:911–22.

15. Yang Y. Cancer immunotherapy: harnessing the immune system to battle cancer. J Clin Invest. 2015;125:3335-7.

16. Peto J. Cancer epidemiology in the last century and the next decade. Nature. 2001;411:390–5.

17. Hanahan D, Weinberg RA. The hallmarks of cancer. Cell. 2000;100:57–70.

18. Siddiqa A, Marciniak RA. Targeting the hallmarks of cancer. Cancer Biol Ther. 2008;7:740-1.

19. Mokhtari RB, Homayouni TS, Baluch N, Morgatskaya E, Kumar S, Das B, et al. Combination therapy in combating cancer. Oncotarget. 2017;8:38022-38043.

20. Nowell PC., Nowell PCC. The clonal evolution of tumor cell populations. Science. 1976;194:23–8.

21. Fisher R, Pusztai L, Swanton C. Cancer heterogeneity: Implications for targeted therapeutics. Br J Cancer. 2013;108:479–85.

22. Gerlinger M, Rowan AJ, Horswell S, Larkin J, Endesfelder D, Gronroos E, et al. Intratumor heterogeneity and branched evolution revealed by multiregion sequencing. N Engl J Med. 2012;366:883–92.

23. Jamal-Hanjani M, Wilson GA, McGranahan N, Birkbak NJ, Watkins TBK, Veeriah S, et al. Tracking the evolution of non–small-cell lung cancer. N Engl J Med. 2017;376:2109–21.

24. Turajlic S, Xu H, Litchfield K, Rowan A, Horswell S, Chambers T, et al. Deterministic evolutionary trajectories influence primary tumor growth: TRACERx Renal. Cell. 2018;173:595–610.

25. Meacham CE, Morrison SJ. Tumor heterogeneity and cancer cell plasticity. Nature. 2013;501:328–37.

26. Batlle E, Sancho E, Francí C, Domínguez D, Monfar M, Baulida J, et al. The transcription factor Snail is a repressor of E-cadherin gene expression in epithelial tumour cells. Nat Cell Biol. 2000;2:84–

9.

27. van Niekerk G, Davids LM, Hattingh SM, Engelbrecht A-M. Cancer stem cells: a product of clonal evolution? Int J Cancer. 2017;140:993–9.

28. Li J, Li J, Chen B. Oct4 was a novel target of Wnt signaling pathway. Mol Cell Biochem. 2012;361:233–40.

29. Xu C, Xie D, Yu S-C, Yang X-J, He L-R, Yang J, et al. β-Catenin/POU5F1/ SOX2 transcription factor complex mediates IGF-I receptor signaling and predicts poor prognosis in lung adenocarcinoma. Cancer Res. 2013;73:3181–9.

30. van Schaijik B, Davis PF, Wickremesekera AC, Tan ST, Itinteang T. Subcellular localisation of the stem cell markers OCT4, SOX2, NANOG, KLF4 and c-MYC in cancer: a review. J Clin Pathol. 2018;71:88–91.

31. Kozar S, Morrissey E, Nicholson AM, van der Heijden M, Zecchini HI, Kemp R, et al. Continuous clonal labeling reveals small numbers of functional stem cells in intestinal crypts and adenomas. Cell Stem Cell. 2013;13:626–33.

32. Zomer A, Ellenbroek SIJ, Ritsma L, Beerling E, Vrisekoop N, Van Rheenen J. Intravital imaging of cancer stem cell plasticity in mammary tumors. Stem Cells. 2013;31:602–6.

33. Batlle E, Clevers H. Cancer stem cells revisited. Nat Med. 2017;23:1124–34.

34. Shibue T, Weinberg RA. EMT, CSCs, and drug resistance: the mechanistic link and clinical implications. Nat Rev Clin Oncol. 2017;14:611–29.

35. Shih JY, Yang PC. The EMT regulator slug and lung carcinogenesis. Carcinogenesis. 2011;32:1299–304.

36. Clark AG, Vignjevic DM. Modes of cancer cell invasion and the role of the microenvironment. Curr Opin Cell Biol. 2015;36:13–22.

37. Bierie B, Pierce SE, Kroeger C, Stover DG, Pattabiraman DR, Thiru P, et al. Integrin-β4 identifies cancer stem cell-enriched populations of partially mesenchymal carcinoma cells. Proc Natl Acad Sci . 2017;114:E2337–46.

38. Zhou P, Li B, Liu F, Zhang M, Wang Q, Liu Y, et al. The epithelial to mesenchymal transition (EMT) and cancer stem cells: Implication for treatment resistance in pancreatic cancer. Mol Cancer. 2017;28:52.

39. Nieto MA, Huang RYYJ, Jackson RAA, Thiery JPP. EMT: 2016. Cell. 2016;166:21–45.

40. Shackleton M, Quintana E, Fearon ER, Morrison SJ. Heterogeneity in cancer: cancer stem cells versus clonal evolution. Cell. 2009;138:822–9.

41. Albini A, Bruno A, Gallo C, Pajardi G, Douglas M, Dallaglio K, et al. Cancer stem cells and the tumor microenvironment: interplay in tumor heterogeneity. Connect Tissue Res. 2015;56:414-25.

42. Madar S, Goldstein I, Rotter V. "Cancer associated fibroblasts" - more than meets the eye. Trends Mol Med. 2013;19:447–53.

43. Gascard P, Tlsty TD. Carcinoma-associated fibroblasts: orchestrating the composition of malignancy. Genes Dev. 2016;30:1002–19.

44. Raica M, Cimpean AM, Ribatti D. Angiogenesis in pre-malignant conditions. Eur J Cancer. 2009;45:1924–34.

45. Fouad YA, Aanei C. Revisiting the hallmarks of cancer. Am J Cancer Res. 2017;7:1016–36.

46. Ribeiro AL, Okamoto OK. Combined effects of pericytes in the tumor microenvironment. Stem Cells Int. 2015;2015:868475.

47. Nagy JA, Chang SH, Shih SC, Dvorak AM, Dvorak HF. Heterogeneity of the tumor vasculature. Semin Thromb Hemost. 2010;36:321–31.

48. Tammela T, Alitalo K. Lymphangiogenesis: molecular mechanisms and future promise. Cell. 2010;140:460–76.

49. Gardner A, Ruffell B. Dendritic Cells and Cancer Immunity. Trends Immunol. 2016;37:855–65.

50. Ma Y. Dendritic cells in the cancer microenvironment. J Cancer. 2013;4:36–44.

51. Dieu-Nosjean MC, Goc J, Giraldo NA, Sautès-Fridman C, Fridman WH. Tertiary lymphoid

structures in cancer and beyond. Trends Immunol. 2014;35:571–80.

52. Spranger S, Dai D, Horton B, Gajewski TF. Tumor-residing Batf3 dendritic cells are required for effector T cell trafficking and adoptive T cell therapy. Cancer Cell. 2017;31:711–723.

53. Tran Janco JM, Lamichhane P, Karyampudi L, Knutson KL. Tumor-infiltrating dendritic cells in cancer pathogenesis. J Immunol. 2015;194:2985–91.

54. Reiser J, Banerjee A. Effector, memory, and dysfunctional CD8 + T cell fates in the antitumor immune response. J Immunol Res. 2016;2016:1–14.

55. Kiraz Y, Baran Y, Nalbant A. T cells in tumor microenvironment. Tumor Biol. 2016;37:39–45.

56. Burkholder B, Huang RY, Burgess R, Luo S, Jones VS, Zhang W, et al. Tumor-induced perturbations of cytokines and immune cell networks. Biochim Biophys Acta. 2014;1845:182–201.

58. Disis ML. Immune regulation of cancer. J Clin Oncol. 2010;28:4531–8.

59. Mantovani A, Sica A, Sozzani S, Allavena P, Vecchi A, Locati M. The chemokine system in diverse forms of macrophage activation and polarization. Trends Immunol. 2004;25:677–86.

60. Ruffell B, Affara NI, Coussens LM. Differential macrophage programming in the tumor microenvironment. Trends Immunol. 2012;33:119–26.

61. Bingle L, Brown NJ, Lewis CE. The role of tumour-associated macrophages in tumour progression: implications for new anticancer therapies. J Pathol. 2002;196:254–65.

62. Biswas SK, Mantovani A. Macrophage plasticity and interaction with lymphocyte subsets: cancer as a paradigm. Nat Immunol. 2010;11:889–96.

63. Qian BZ, Pollard JW. Macrophage diversity enhances tumor progression and metastasis. Cell. 2010;141:39–51.

64. Noy R, Pollard JW. Tumor-associated macrophages: from mechanisms to therapy. Immunity. 2014;41:49–61.

65. Umansky V, Blattner C, Gebhardt C, Utikal J. The role of myeloid-derived suppressor cells (MDSC) in cancer progression. Vaccines. 2016;4:36.

66. Gabrilovich DI. Myeloid-derived suppressor cells. Cancer Immunol Res. 2017;5:3–8.

67. Pahl J, Cerwenka A. Tricking the balance: NK cells in anti-cancer immunity. Immunobiology. 2017;222:11–20.

68. Yuen GJ, Demissie E, Pillai S. B Lymphocytes and cancer: a love–hate relationship. Trends in Cancer. 2016;2:747–57.

69. Sarvaria A, Madrigal JA, Saudemont A. B cell regulation in cancer and anti-tumor immunity. Cell Mol Immunol. 2017;14:662-674.

70. Lu P, Weaver VM, Werb Z. The extracellular matrix: a dynamic niche in cancer progression. J Cell Biol. 2012;196:395–406.

71. Wang M, Zhao J, Zhang L, Wei F, Lian Y, Wu Y, et al. Role of tumor microenvironment in tumorigenesis. J Cancer. 2017;8:761–73.

72. Lee S, Margolin K. Cytokines in cancer immunotherapy. Cancers (Basel). 2011;3:3856–93.

73. Dranoff G. Cytokines in cancer pathogenesis and cancer therapy. Nat Rev Cancer. 2004;4:11–22.

74. Lippitz BE. Cytokine patterns in patients with cancer : a systematic review. Lancet Oncol. 2013;14:e218–28.

75. Nagarsheth N, Wicha MS, Zou W. Chemokines in the cancer microenvironment and their relevance in cancer immunotherapy. Nat. Rev. Immunol. 2017;17:559–72.

76. Fridman WH, Pagès F, Sautès-Fridman C. The immune contexture in human tumours: impact on clinical outcome. Nat Rev Cancer. 2012;12:298–306.

77. Mantovani A, Allavena P, Sica A, Balkwill F. Cancer-related inflammation. Nature. 2008;454:436–44.

78. Coussens LM, Werb Z. Inflammation and cancer. Nature. 2002;420:860–7.

79. Landskron G, Fuente M De, Thuwajit P, Thuwajit C, Hermoso MA. Chronic inflammation and

cytokines in the tumor microenvironment. J Immunl Res. 2014;2014:149185.

80. Heemskerk B, Kvistborg P, Schumacher TNM. The cancer antigenome. EMBO J. 2013;32:194–203.

81. Vinay DS, Ryan EP, Pawelec G, Talib WH, Stagg J, Elkord E, et al. Immune evasion in cancer: Mechanistic basis and therapeutic strategies. Semin Cancer Biol. 2015;35:S185–98.

82. Hegde PS, Karanikas V, Evers S. The where, the when and the how of immune monitoring for cancer immunotherapies. Clin Cancer Res. 2016;22:1865–75.

83. Lanitis E, Dangaj D, Irving M, Coukos G. Mechanisms regulating T-cell infiltration and activity in solid tumors. Ann Oncol. 2017;28:xii18-xii32.

84. Restifo N, Dudley M, Rosenberg SA. Adoptive immunotherapy for cancer: harnessing the T cell response. Nat Rev Immunol. 2012;12:269–81.

85. Richardson MA, Ramirez T, Russell NC, Moye LA. Coley toxins immunotherapy: a retrospective review. Altern Ther Health Med. 1999;5:42–7.

86. Morales A, Eidinger D, Bruce AW. Intracavitary Bacillus Calmette-Guerin in the treatment of superficial bladder tumors. J Urol. 1976;116:180–2.

87. Dudley ME, Wunderlich JR, Shelton TE, Even J, Rosenberg SA. Generation of tumor-infiltrating lymphocyte cultures for use in adoptive transfer therapy for melanoma patients. J Immunother. 2003;26:332–42.

88. Kalos M, Levine BL, Porter DL, Katz S, Grupp SA, Bagg A JC. T cells with chimeric antigen receptors have potent antitumor effects and can establish memory in patients with advanced leukemia. Sci Transl Med. 2011;3:95ra73.

89. Song W, Musetti S, Huang L. Nanomaterials for cancer immunotherapy. Biomaterials. 2017;148:16–30.

90. Schuster M, Nechansky A, Kircheis R. Cancer immunotherapy. Biotechnol J. 2006;1:138–47.

91. Mellman I, Coukos G, Dranoff G. Cancer immunotherapy comes of age. Nature. 2011;480:480–9.

92. Kantoff PW, Higano CS, Shore ND, Berger ER, Small EJ, Penson DF, et al. Sipuleucel-T immunotherapy for castration-resistant prostate cancer. N Engl J Med. 2010;363:411–22.

93. Banchereau J, Palucka K. Immunotherapy: cancer vaccines on the move. Nat Rev Clin Oncol. 2018;15:9-10.

94. Kranz LM, Diken M, Haas H, Kreiter S, Loquai C, Reuter KC, et al. Systemic RNA delivery to dendritic cells exploits antiviral defence for cancer immunotherapy. Nature. 2016;534:396–401.

95. Rosenberg SA, Yang JC, Sherry RM, Kammula US, Hughes MS, Phan GQ, et al. Durable complete responses in heavily pretreated patients with metastatic melanoma using T-cell transfer immunotherapy. Clin Cancer Res. 2011;17:4550–7.

96. D'Aloia MM, Zizzari IG, Sacchetti B, Pierelli L, Alimandi M. CAR-T cells: The long and winding road to solid tumors review. Cell Death Dis. 2018;9:282.

97. Roberts ZJ, Better M, Bot A, Roberts MR, Ribas A. Axicabtagene ciloleucel, a first-in-class CAR T cell therapy for aggressive NHL. Leuk Lymphoma. 2018;59:1785-96.

98. Neelapu SS, Locke FL, Bartlett NL, Lekakis LJ, Miklos DB, Jacobson CA, et al. Axicabtagene ciloleucel CAR T-cell therapy in refractory large B-cell lymphoma. N Engl J Med. 2017;377:2531-44.

99. Irving M, de Silly RV, Scholten K, Dilek N, Coukos G. Engineering chimeric antigen receptor T-cells for racing in solid tumors: don't forget the fuel. Front Immunol. 2017;8:267.

100. Guo Y, Feng K, Wang Y, Han W. Targeting cancer stem cells by using chimeric antigen receptor-modified T cells: a potential and curable approach for cancer treatment. Protein Cell. 2018;9:516-26.

101. Krummel MF, Allison JP. CD28 and CTLA-4 have opposing effects on the response of T cells to stimulation. J Exp Med. 1995;182:459–65.

102. Buchbinder EI, Desai A. CTLA-4 and PD-1 pathways similarities, differences, and implications of their inhibition. Am J Clin Oncol. 2016;39:98–106.

103. Hodi FS, O'Day SJ, McDermott DF, Weber RW, Sosman JA, Haanen JB, et al. Improved survival with ipilimumab in patients with metastatic melanoma. N Engl J Med. 2010;363:711–23.

105. Keir ME, Butte MJ, Freeman GJ, Sharpe AH. PD-1 and its ligands in tolerance and immunity. Annu Rev Immunol. 2008;26:677–704.

105. Weber J, Mandala M, Del Vecchio M, Gogas HJ, Arance AM, Cowey CL, et al. Adjuvant nivolumab versus ipilimumab in resected stage III or IV melanoma. N Engl J Med. 2017;377:1824-1835.

106. Fuchs CS, Doi T, Jang RW, Muro K, Satoh T, Machado M, et al. Safety and efficacy of pembrolizumab monotherapy in patients with previously treated advanced gastric and gastroesophageal junction cancer. JAMA Oncol. 2018;4:e180013.

107. Postow MA, Chesney J, Pavlick AC, Robert C, Grossmann K, McDermott D, et al. Nivolumab and ipilimumab versus ipilimumab in untreated melanoma. N Engl J Med. 2015;372:2006–17.

108. Larkin J, Chiarion-Sileni V, Gonzalez R, Grob JJ, Cowey CL, Lao CD, et al. Combined nivolumab and ipilimumab or monotherapy in untreated melanoma. N Engl J Med. 2015;373:23–34.

109. Sharma P, Hu-Lieskovan S, Wargo JA, Ribas A. Primary, adaptive, and acquired resistance to cancer immunotherapy. Cell. 2017;168:707–23.

110. Topalian SL, Hodi FS, Brahmer JR, Gettinger SN, Smith DC, McDermott DF, et al. Safety, activity, and immune correlates of anti–PD-1 antibody in cancer. N Engl J Med. 2012;366:2443–54.

111. Hamid O, Sosman JA, Lawrence DP, Sullivan RJ, Ibrahim N, Kluger HM, et al. Clinical activity, safety, and biomarkers of MPDL3280A, an engineered PD-L1 antibody in patients with locally advanced or metastatic melanoma (mM). J Clin Oncol. 2013;31:9010.

112. Tumeh PC, Harview CL, Yearley JH, Shintaku IP, Taylor EJM, Robert L, et al. PD-1 blockade induces responses by inhibiting adaptive immune resistance. Nature. 2014;515:568–71.

113. Gajewski TF. The next hurdle in cancer immunotherapy: Overcoming the non-T-cell-inflamed tumor microenvironment. Semin Oncol. 2016;42:663–71.

114. Van Allen EM, Miao D, Schilling B, Shukla SA, Blank C, Zimmer L, et al. Genomic correlates of response to CTLA-4 blockade in metastatic melanoma. Science. 2015;350:207–11.

115. Spranger S, Luke JJ, Bao R, Zha Y, Hernandez KM, Li Y, et al. Density of immunogenic antigens does not explain the presence or absence of the T-cell–inflamed tumor microenvironment in melanoma. Proc Natl Acad Sci. 2016;113:E7759–68.

116. McDermott M, Eustace AJ, Busschots S, Breen L, Crown J, Clynes M, et al. In vitro development of chemotherapy and targeted therapy drug-resistant cancer cell lines: a practical guide with case studies. Front Oncol. 2014;4:40.

117. Yan XD, Li M, Yuan Y, Mao N, Pan LY. Biological comparison of ovarian cancer resistant cell lines to cisplatin and taxol by two different administrations. Oncol Rep. 2007;17:1163–9

118. Smith M, Young H, Hurlstone A, Wellbrock C. Differentiation of THP1 cells into macrophages for transwell co-culture assay with melanoma cells. Bio Protocol. 2015;5:e1638.

119. Kwong LN, Boland GM, Frederick DT, Helms TL, Akid AT, Miller JP, et al. Co-clinical assessment identifies patterns of BRAF inhibitor resistance in melanoma. 2015;125:1459-70.

120. Pfaffl MW. A new mathematical model for relative quantification in real-time RT-PCR. Nucleic Acids Res. 2001;29:45e–45.

121. Mitchell AJ. Sensitivity x PPV is a recognized test called the clinical utility index (CUI+). Eur J Epidemiol. 2011;26:251–2.

122. Richards DM, Hettinger J, Feuerer M. Monocytes and macrophages in cancer: development and functions. Cancer Microenviron. 2013;6:179–91.

123. Marigo I, Zilio S, Desantis G, Rô Me Galon J, Murray PJ, Bronte V, et al. T cell cancer therapy requires CD40-CD40L activation of tumor necrosis factor and inducible nitric-oxide-synthase-producing dendritic cells. Cancer Cell. 2016;30:377–90.

124. Rainone V, Martelli C, Ottobrini L, Biasin M, Borelli M, Lucignani G, et al. Immunological characterization of whole tumour lysate-loaded dendritic cells for cancer immunotherapy. PLoS One. 2016;11:e0146622.

125. Hubo M, Trinschek B, Kryczanowsky F, Tuettenberg A, Steinbrink K, Jonuleit H. Costimulatory molecules on immunogenic versus tolerogenic human dendritic cells. Front Immunol. 2013;4:82.

126. O'Neill DW, Adams S, Bhardwaj N. Manipulating dendritic cell biology for the active

immunotherapy of cancer. Blood. 2004;104:2235–46.

127. Strioga MM, Felzmann T, Powell DJ, Ostapenko V, Dobrovolskiene NT, Matuskova M, et al. Therapeutic dendritic cell-based cancer vaccines: the state of the art. Crit Rev Immunol. 2013;33:489–547.

128. Bellone G, Carbone A, Smirne C, Scirelli T, Buffolino A, Novarino A, et al. Cooperative induction of a tolerogenic dendritic cell phenotype by cytokines secreted by pancreatic carcinoma cells. J Immunol. 2006;177:3448–60.

129. Dong B, Dai G, Xu L, Zhang Y, Ling L, Sun L, et al. Tumor cell lysate induces the immunosuppression and apoptosis of mouse immunocytes. Mol Med Rep. 2014;10:2827–34.

130. Manavalan JS, Rossi PC, Vlad G, Piazza F, Yarilina A, Cortesini R, et al. High expression of ILT3 and ILT4 is a general feature of tolerogenic dendritic cells. Transpl Immunol. 2003;11:245–58.

131. Koski GK, Koldovsky U, Xu S, Mick R, Sharma A, Fitzpatrick E, et al. A novel dendritic cell-based immunization approach for the induction of durable Th1-polarized Anti-HER-2/neu responses in women with early breast cancer. J Immunother. 2012;35:54–65.

132. Sica A, Schioppa T, Mantovani A, Allavena P. Tumour-associated macrophages are a distinct M2 polarised population promoting tumour progression: potential targets of anti-cancer therapy. Eur J Cancer. 2006;42:717–27.

133. Lan C, Heindl A, Huang X, Xi S, Banerjee S, Liu J, et al. Quantitative histology analysis of the ovarian tumour microenvironment. Sci Rep. 2015;5:16317.

134. Pollard JW. Tumour-educated macrophages promote tumour progression and metastasis. Nat. Rev. Cancer. 2004;4:71–8.

135. Mantovani A, Schioppa T, Porta C, Allavena P, Sica A. Role of tumor-associated macrophages in tumor progression and invasion. Cancer Metastasis Rev. 2006;25:315–22.

136. Gil-Bernabé AM, Ferjančič Š, Tlalka M, Zhao L, Allen PD, Im JH, et al. Recruitment of monocytes/macrophages by tissue factor-mediated coagulation is essential for metastatic cell survival and premetastatic niche establishment in mice. Blood. 2012;119:3164–75.

137. Vlaicu P, Mertins P, Mayr T, Widschwendter P, Ataseven B, Högel B, et al. Monocytes/macrophages support mammary tumor invasivity by co-secreting lineage-specific EGFR ligands and a STAT3 activator. BMC Cancer. 2013;13:197.

138. Dhabekar G, Dandekar R, Kingaonkar A. Role of macrophages in malignancy. Ann Maxillofac Surg. 2011;1:150-4.

139. Su S, Liu Q, Chen J, Chen J, Chen F, He C, et al. A Positive feedback loop between mesenchymal-like cancer cells and macrophages is essential to breast cancer metastasis. Cancer Cell. 2014;25:605–20.

140. Liu CY, Xu JY, Shi XY, Huang W, Ruan TY, Xie P, et al. M2-polarized tumor-associated macrophages promoted epithelial-mesenchymal transition in pancreatic cancer cells, partially through TLR4/IL-10 signaling pathway. Lab Investig. 2013;93:844–54.

141. Fan QM, Jing YY, Yu GF, Kou XR, Ye F, Gao L, et al. Tumor-associated macrophages promote cancer stem cell-like properties via transforming growth factor-beta1-induced epithelial-mesenchymal transition in hepatocellular carcinoma. Cancer Lett. 2014;352:160–8.

142. Kalluri R, Weinberg RA. The basics of epithelial-mesenchymal transition. J Clin Invest. 2009;119:1420–8.

143. Ye X, Weinberg RA. Epithelial-mesenchymal plasticity: a central regulator of cancer progression. Trends Cell Biol. 2015;25:675–86.

144. Sadanandam A, Lyssiotis CA, Homicsko K, Collisson EA, Gibb WJ, Wullschleger S, et al. A colorectal cancer classification system that associates cellular phenotype and responses to therapy. Nat Med. 2013;19:619–25.

145. Budinska E, Popovici V, Tejpar S, D'Ario G, Lapique N, Sikora KO, et al. Gene expression patterns unveil a new level of molecular heterogeneity in colorectal cancer. J Pathol. 2013;231:63–76.

146. Roepman P, Schlicker A, Tabernero J, Majewski I, Tian S, Moreno V, et al. Colorectal cancer intrinsic subtypes predict chemotherapy benefit, deficient mismatch repair and epithelial-to-mesenchymal transition. Int J Cancer. 2014;134:552–62.

147. Marisa L, de Reyniès A, Duval A, Selves J, Gaub MP, Vescovo L, et al. Gene expression classification of colon cancer into molecular subtypes: characterization, validation, and prognostic value. PLoS Med. 2013;10:e1001453.

148. Cavnar MJ, Turcotte S, Katz SC, Kuk D, Gönen M, Shia J, et al. Tumor-associated macrophage infiltration in colorectal cancer liver metastases is associated with better outcome. Ann Surg Oncol. 2017;24:1835–42.

149. Koelzer VH, Canonica K, Dawson H, Sokol L, Karamitopoulou-Diamantis E, Lugli A, et al. Phenotyping of tumor-associated macrophages in colorectal cancer: Impact on single cell invasion (tumor budding) and clinicopathological outcome. Oncoimmunology. 2016;5:e1106677.

150. Gulubova M, Ananiev J, Yovchev Y, Julianov A, Karashmalakov A, Vlaykova T. The density of macrophages in colorectal cancer is inversely correlated to TGF-β1 expression and patients' survival. J Mol Histol. 2013;44:679–92.

151. Cui Y-L, Li H-K, Zhou H-Y, Zhang T, Li Q. Correlations of tumor-associated macrophage subtypes with liver metastases of colorectal cancer. Asian Pacific J Cancer Prev. 2013;14:1003–7.

152. Marech I, Ammendola M, Sacco R, Sammarco G, Zuccalà V, Zizzo N, et al. Tumour-associated macrophages correlate with microvascular bed extension in colorectal cancer patients. J Cell Mol Med. 2016;20:1373–80.

153. Edin S, Wikberg ML, Dahlin AM, Rutegård J, Öberg Å, Oldenborg P-A, et al. The distribution of macrophages with a M1 or M2 phenotype in relation to prognosis and the molecular characteristics of colorectal cancer. PLoS One. 2012;7:e47045.

154. Zhang W, Chen L, Ma K, Zhao Y, Liu X, Wang Y, et al. Polarization of macrophages in the tumor microenvironment is influenced by EGFR signaling within colon cancer cells. Oncotarget. 2016;7:75366-78.

155. Chen L, Wang S, Wang Y, Zhang W, Ma K, Hu C, et al. IL-6 influences the polarization of macrophages and the formation and growth of colorectal tumor. Oncotarget. 2018;9:17443–54.

156. Popěna I, Abols A, Saulite L, Pleiko K, Zandberga E, Jēkabsons K, et al. Effect of colorectal cancer-derived extracellular vesicles on the immunophenotype and cytokine secretion profile of monocytes and macrophages. Cell Commun Signal. 2018;16:17.

157. Baj-Krzyworzeka M, Mytar B, Szatanek R, Surmiak M, Weglarczyk K, Baran J, et al. Colorectal cancer-derived microvesicles modulate differentiation of human monocytes to macrophages. J Transl Med. 2016;14:36.

158. Mao F, Kang J-J, Cai X, Ding N-F, Wu Y-B, Yan Y-M, et al. Crosstalk between mesenchymal stem cells and macrophages in inflammatory bowel disease and associated colorectal cancer. Contemp Oncol (Pozn). 2017;21:91–7.

159. Sicco C Lo, Reverberi D, Balbi C, Ulivi V, Principi E, Pascucci L, et al. Mesenchymal stem cell-derived extracellular vesicles as mediators of anti-inflammatory effects: endorsement of macrophage polarization. Stem Cells Transl Med. 2017;6:1018–28.

160. Vasandan AB, Jahnavi S, Shashank C, Prasad P, Kumar A, Prasanna SJ. Human mesenchymal stem cells program macrophage plasticity by altering their metabolic status via a PGE2-dependent mechanism. Sci Rep. 2016;6:38308.

161. Takizawa N, Okubo N, Kamo M, Chosa N, Mikami T, Suzuki K, et al. Bone marrow-derived mesenchymal stem cells propagate immunosuppressive/ anti-inflammatory macrophages in cell-to-cell contact-independent and -dependent manners under hypoxic culture. Exp Cell Res. 2017;358:411–20.

162. Deng X, Zhang P, Liang T, Deng S, Chen X, Zhu L. Ovarian cancer stem cells induce the M2 polarization of macrophages through the PPARγ and NF-κB pathways. Int J Mol Med. 2015;36:449–54.

163. Sousa S, Brion R, Lintunen M, Kronqvist P, Sandholm J, Mönkkönen J, et al. Human breast cancer cells educate macrophages toward the M2 activation status. Breast Cancer Res. 2015;17:101.

164. Hollmén M, Roudnicky F, Karaman S, Detmar M. Characterization of macrophage--cancer cell crosstalk in estrogen receptor positive and triple-negative breast cancer. Sci Rep. 2015;5:9188.

165. Roszer T. Understanding the mysterious M2 macrophage through activation markers and effector mechanisms. Mediators Inflamm. 2015;2015:816460.

166. Shen D-W, Pouliot LM, Hall MD, Gottesman MM. Cisplatin resistance: a cellular self-defense mechanism resulting from multiple epigenetic and genetic changes. Pharmacol Rev. 2012;64:706–21.

167. Norouzi-Barough L, Sarookhani MR, Sharifi M, Moghbelinejad S, Jangjoo S, Salehi R. Molecular Mechanisms of Drug Resistance in Ovarian Cancer. J Cell Physiol. 2017;233:4546-62.

168. Chien J, Kuang R, Landen C, Shridhar V. Platinum-sensitive recurrence in ovarian cancer: the role of tumor microenvironment. Front Oncol. 2013;3:251.

169. Dauer P, Nomura A, Saluja A, Banerjee S. Microenvironment in determining chemo-resistance in pancreatic cancer: neighborhood matters. Pancreatology. 2017;17;7–12.

170. Baghdadi M, Wada H, Nakanishi S, Abe H, Han N, Wira EP, et al. Chemotherapy-induced IL34 enhances immunosuppression by tumor-associated macrophages and mediates survival of chemoresistant lung cancer cells. Cancer Res. 2016;76:6030–42.

171. Takeuchi S, Baghdadi M, Tsuchikawa T, Wada H, Nakamura T, Abe H, et al. Chemotherapy-derived inflammatory responses accelerate the formation of immunosuppressive myeloid cells in the tissue microenvironment of human pancreatic cancer. Cancer Res. 2015;75:2629–40.

172. Dijkgraaf EM, Heusinkveld M, Tummers B, Vogelpoel LTC, Goedemans R, Jha V, et al. Chemotherapy alters monocyte differentiation to favor generation of cancer-supporting M2 macrophages in the tumor microenvironment. Cancer Res. 2013;73:2480–92.

173. Ruffell B, Coussens LM. Macrophages and Therapeutic Resistance in Cancer. Cancer Cell. 2015;27:462–72.

174. Ozols RF, Masuda H, Grotzinger KR, Whang-Peng J, Louie KG, Knutsen T, et al. Characterization of a cis-diamminedichloroplatinum(II)-resistant human ovarian cancer cell line and its use in evaluation of platinum analogues. Cancer Res. 1987;47:414–8.

175. Singh A, Settleman J. EMT, cancer stem cells and drug resistance: An emerging axis of evil in the war on cancer. Oncogene. 2010;29:4741–51.

176. Moreno-Bueno G, Peinado H, Molina P, Olmeda D, Cubillo E, Santos V, et al. The morphological and molecular features of the epithelial-to-mesenchymal transition. Nat Protoc. 2009;4:1591–613.

177. Baribeau S, Chaudhry P, Parent S, Asselin É. Resveratrol inhibits cisplatin-induced epithelial-to-mesenchymal transition in ovarian cancer cell lines. PLoS One. 2014;9:e86987.

178. Li S, Zhang X, Zhang R, Liang Z, Liao W, Du Z, et al. Hippo pathway contributes to cisplatin resistant-induced EMT in nasopharyngeal carcinoma cells. Cell Cycle. 2017;16:1601–10.

179. Boyer LA, Lee TI, Cole MF, Johnstone SE, Levine SS, Zucker JP, et al. Core transcriptional regulatory circuitry in human embryonic stem cells. Cell. 2005;122:947–56.

180. Hadjimichael C, Chanoumidou K, Papadopoulou N, Arampatzi P, Papamatheakis J, Kretsovali A. Common stemness regulators of embryonic and cancer stem cells. World J Stem Cells. 2015;7:1150–84.

181. Wiechert A, Saygin C, Thiagarajan PS, Rao VS, Hale JS, Gupta N, et al. Cisplatin induces stemness in ovarian cancer. Oncotarget. 2016;7.

182. Xiong X, Arvizo RR, Saha S, Robertson DJ, McMeekin S, Bhattacharya R, et al. Sensitization of ovarian cancer cells to cisplatin by gold nanoparticles. Oncotarget. 2014;5:6453–65.

183. Ghosh RD, Ghuwalewala S, Das P, Mandloi S, Alam SK, Chakraborty J, et al. MicroRNA profiling of cisplatin-resistant oral squamous cell carcinoma cell lines enriched with cancer-stem-cell-like and epithelial-mesenchymal transition-type features. Sci Rep. 2016;6:23932.

184. Latifi A, Abubaker K, Castrechini N, Ward AC, Liongue C, Dobill F, et al. Cisplatin treatment of primary and metastatic epithelial ovarian carcinomas generates residual cells with mesenchymal stem cell-like profile. J Cell Biochem. 2011;112:2850–64.

185. Di Nicolantonio F, Mercer SJ, Knight LA, Gabriel FG, Whitehouse PA, Sharma S, et al. Cancer cell adaptation to chemotherapy. BMC Cancer. 2005;5.

186. Levina V, Su Y, Nolen B, Liu X, Gordin Y, Lee M, et al. Chemotherapeutic drugs and human tumor cells cytokine network. Int J Cancer. 2008;123:2031–40.

187. Edwardson DW, Boudreau J, Mapletoft J, Lanner C, Kovala AT, Parissenti AM. Inflammatory cytokine production in tumor cells upon chemotherapy drug exposure or upon selection for drug

resistance. PLoS One. 2017;12:e0183662.

188. Showalter A, Limaye A, Oyer JL, Igarashi R, Kittipatarin C, Copik AJ, et al. Cytokines in immunogenic cell death: applications for cancer immunotherapy. Cytokine. 2017;97:123–32.

189. De Palma M, Lewis CE. Macrophage regulation of tumor responses to anticancer therapies. Cancer Cell. 2013;23:277–86.

190. Genin M, Clement F, Fattaccioli A, Raes M, Michiels C. M1 and M2 macrophages derived from THP-1 cells differentially modulate the response of cancer cells to etoposide. BMC Cancer. 2015;15:577.

191. Li C, Levin M, Kaplan DL. Bioelectric modulation of macrophage polarization. Sci Rep. 2016;6:21044.

192. Tarique AA, Logan J, Thomas E, Holt PG, Sly PD, Fantino E. Phenotypic, functional and plasticity features of classical and alternatively activated human macrophages. Am J Respir Cell Mol Biol. 2015;53:676–88.

193. Zhang Q, Cai DJ, Li B. Ovarian cancer stem-like cells elicit the polarization of M2 macrophages. Mol Med Rep. 2015;11:4685–93.

194. Yu CC, Chien CT, Chang TC. M2 macrophage polarization modulates epithelial-mesenchymal transition in cisplatin-induced tubulointerstitial fibrosis. Biomed. 2016;6:29–34.

195. Bonde AK, Tischler V, Kumar S, Soltermann A, Schwendener RA. Intratumoral macrophages contribute to epithelial-mesenchymal transition in solid tumors. BMC Cancer. 2012;12:35.

196. Zhu L, Fu X, Chen X, Han X, Dong P. M2 macrophages induce EMT through the TGF-β/Smad2 signaling pathway. Cell Biol Int. 2017;41:960–8.

197. Banerjee S, Halder K, Bose A, Bhattacharya P, Gupta G, Mahapatra SK, et al. TLR signaling mediated differential histone modification at IL-10 and IL-12 promoter region leads to functional impairments in tumor associated macrophages. Carcinogenesis. 2011;32:1789-97.

198. Reinartz S, Schumann T, Finkernagel F, Wortmann A, Jansen JM, Meissner W, et al. Mixed-polarization phenotype of ascites-associated macrophages in human ovarian carcinoma: correlation of CD163 expression, cytokine levels and early relapse. Int J Cancer. 2014;134:32–42.

199. Efremova M, Finotello F, Rieder D, Trajanoski Z. Neoantigens generated by individual mutations and their role in cancer immunity and immunotherapy. Front Immunol. 2017;8:1679.

200. Spranger S. Mechanisms of tumor escape in the context of the T-cell-inflamed and the non-T-cell-inflamed tumor microenvironment. Int Immunol. 2016;28:383–91.

201. Budhu S, Wolchok J, Merghoub T. The importance of animal models in tumor immunity and immunotherapy. Curr Opin Genet Dev. 2014;24:46–51.

202. Wellenstein MD, de Visser KE. Cancer-cell-intrinsic mechanisms shaping the tumor immune landscape. Immunity. 2018;48:399–416.

203. Khalili JS, Liu S, Rodríguez-Cruz TG, Whittington M, Wardell S, Liu C, et al. Oncogenic BRAF(V600E) promotes stromal cell-mediated immunosuppression via induction of interleukin-1 in melanoma. Clin Cancer Res. 2012;18:5329–40.

204. Neubert NJ, Schmittnaegel M, Bordry N, Nassiri S, Wald N, Martignier C, et al. T cell-induced CSF1 promotes melanoma resistance to PD1 blockade. Sci Transl Med. 2018;10:eaan3311.

205. Ishida Y, Agata Y, Shibahara K, Honjo T. Induced expression of PD-1, a novel member of the immunoglobulin gene superfamily, upon programmed cell death. EMBO J. 1992;11:3887–95.

206. Abril-Rodriguez G, Ribas A. SnapShot: immune checkpoint inhibitors. Cancer Cell. 2017;31:848–848.

207. Mahmoudi M, Farokhzad OC. Cancer immunotherapy: wound-bound checkpoint blockade. Nat Biomed Eng. 2017,1:31.

208. Topalian SL, Taube JM, Anders RA, Pardoll DM. Mechanism-driven biomarkers to guide immune checkpoint blockade in cancer therapy. Nat. Rev. Cancer. 2016;16:275–87.

209. Hugo W, Zaretsky JM, Sun L, Song C, Moreno BH, Hu-Lieskovan S, et al. Genomic and transcriptomic features of response to anti-PD-1 therapy in metastatic melanoma. Cell. 2016;165:35–44.

210. Nowicki TS, Hu-Lieskovan S, Ribas A. Mechanisms of resistance to PD-1 and PD-L1 blockade. Cancer J. 2018;24:47–53.

211. Jenkins RW, Barbie DA, Flaherty KT. Mechanisms of resistance to immune checkpoint inhibitors. Br J Cancer. 2018;118:9–16.

273.

212. Intlekofer AM, Thompson CB. At the Bench: Preclinical rationale for CTLA-4 and PD-1 blockade as cancer immunotherapy. J Leukoc Biol. 2013;94:25–39.

213. Curran MA, Montalvo W, Yagita H, Allison JP. PD-1 and CTLA-4 combination blockade expands infiltrating T cells and reduces regulatory T and myeloid cells within B16 melanoma tumors. Proc Natl Acad Sci. 2010;107:4275–80.

214. Selby MJ, Engelhardt JJ, Johnston RJ, Lu LS, Han M, Thudium K, et al. Preclinical development of ipilimumab and nivolumab combination immunotherapy: mouse tumor models, in vitro functional studies, and cynomolgus macaque toxicology. PLoS One. 2016;11:e0161779.

215. Huang RY, Francois A, McGray AR, Miliotto A, Odunsi K. Compensatory upregulation of PD-1, LAG-3, and CTLA-4 limits the efficacy of single-agent checkpoint blockade in metastatic ovarian cancer. Oncoimmunology. 2016;6:e1249561.

216. Denayer T, Stïhrn T, Van Roy M. Animal models in translational medicine: Validation and prediction. New Horizons Transl Med. 2014;2:5–11.

217. Silberberg SD. Should clinicians care about preclinical animal research? Neurology. 2013;80:1072–3.

218. Wen FT, Thisted RA, Rowley DA, Schreiber H. A systematic analysis of experimental immunotherapies on tumors differing in size and duration of growth. Oncoimmunology. 2012;1:172–8.

219. Huang AC, Postow MA, Orlowski RJ, Mick R, Bengsch B, Manne S, et al. T-cell invigoration to tumour burden ratio associated with anti-PD-1 response. Nature. 2017;545:60–5.

220. Qin BD, Jiao XD, Zang YS. Tumor mutation burden to tumor burden ratio and prediction of clinical benefit of anti-PD-1/PD-L1 immunotherapy. Med Hypotheses. 2018;116:111–3.

221. Paulsen E-E, Kilvaer TK, Rakaee M, Richardsen E, Hald SM, Andersen S, et al. CTLA-4 expression in the non-small cell lung cancer patient tumor microenvironment: diverging prognostic impact in primary tumors and lymph node metastases. Cancer Immunol Immunother. 2017;66:1449-1461.

222. Maleki Vareki S, Garrigós C, Duran I. Biomarkers of response to PD-1/PD-L1 inhibition. Crit Rev Oncol Hematol. 2017;116:116–24.

223. Subrahmanyam PB, Dong Z, Gusenleitner D, Giobbie-Hurder A, Severgnini M, Zhou J, et al. Distinct predictive biomarker candidates for response to anti-CTLA-4 and anti-PD-1 immunotherapy in melanoma patients. J Immunother Cancer. 2018;6:18.

224. O'Donnell JS, Long G V., Scolyer RA, Teng MWL, Smyth MJ. Resistance to PD1/PDL1 checkpoint inhibition. Cancer Treat. Rev. 2017;52:71–81.

225. Mantovani A, Marchesi F, Malesci A, Laghi L, Allavena P. Tumour-associated macrophages as treatment targets in oncology. Nat Rev Clin Oncol. 2017;14:399–416.

226. Toor SM, Elkord E. Therapeutic prospects of targeting myeloid-derived suppressor cells and immune checkpoints in cancer. Immunol Cell Biol. 2018. Epub ahead of print.

227. Highfill SL, Cui Y, Giles AJ, Smith JP, Zhang H, Morse E, et al. Disruption of CXCR2-mediated MDSC tumor trafficking enhances anti-PD1 efficacy. Sci Transl Med. 2014;6:237ra67.

228. Meyer C, Cagnon L, Costa-Nunes CM, Baumgaertner P, Montandon N, Leyvraz L, et al. Frequencies of circulating MDSC correlate with clinical outcome of melanoma patients treated with ipilimumab. Cancer Immunol Immunother. 2014;63:247–57.

229. Peranzoni E, Lemoine J, Vimeux L, Feuillet V, Barrin S, Kantari-Mimoun C, et al. Macrophages impede CD8 T cells from reaching tumor cells and limit the efficacy of anti–PD-1 treatment. Proc Natl Acad Sci. 2018;115:E4041-50.

230. Arlauckas SP, Garris CS, Kohler RH, Kitaoka M, Cuccarese MF, Yang KS, et al. In vivo imaging reveals a tumor-associated macrophage-mediated resistance pathway in anti-PD-1 therapy. Sci Transl

Med. 2017;9:eaal3604.

231. Saha D, Martuza RL, Rabkin SD. Macrophage polarization contributes to glioblastoma eradication by combination immunovirotherapy and immune checkpoint blockade. Cancer Cell. 2017;32:253–267.

232. Schultze JL. Reprogramming of macrophages - new opportunities for therapeutic targeting. Curr Opin Pharmacol. 2016;26:10–5.

233. Bell D, Berchuck A, Birrer M, Chien J, Cramer DW, Dao F, et al. Integrated genomic analyses of ovarian carcinoma. Nature. 2011;474:609–15.

234. Tothill RW, Tinker A V., George J, Brown R, Fox SB, Lade S, et al. Novel molecular subtypes of serous and endometrioid ovarian cancer linked to clinical outcome. Clin Cancer Res. 2008;14:5198–208.

235. Verhaak RGW, Tamayo P, Yang J-Y, Hubbard D, Zhang H, Creighton CJ, et al. Prognostically relevant gene signatures of high-grade serous ovarian carcinoma. J Clin Invest. 2013;123:517–25.

236. Konecny GE, Wang C, Hamidi H, Winterhoff B, Kalli KR, Dering J, et al. Prognostic and therapeutic relevance of molecular subtypes in high-grade serous ovarian cancer. J Natl Cancer Inst. 2014;106:dju249.

237. Nelson BH. New insights into tumor immunity revealed by the unique genetic and genomic aspects of ovarian cancer. Curr Opin Immunol. 2015;33:93–100.

238. Hwang W-T, Adams SF, Tahirovic E, Hagemann IS, Coukos G. Prognostic significance of tumor-infiltrating T cells in ovarian cancer: a meta-analysis. Gynecol Oncol. 2012;124:192–8.

239. Mukaida N, Sasaki SI, Baba T. Chemokines in cancer development and progression and their potential as targeting molecules for cancer treatment. Mediators Inflamm. 2014:2014;170381.

240. Gnjatic S, Bronte V, Brunet LR, Butler MO, Disis ML, Galon J, et al. Identifying baseline immune-related biomarkers to predict clinical outcome of immunotherapy. J.Immunother Cancer. 2017;5:44.

241. McDermott DF, Huseni MA, Atkins MB, Motzer RJ, Rini BI, Escudier B, et al. Clinical activity and molecular correlates of response to atezolizumab alone or in combination with bevacizumab versus sunitinib in renal cell carcinoma. Nat Med. 2018;24:749-57.

242. Pitteri SJ, Kelly-Spratt KS, Gurley KE, Kennedy J, Buson TB, Chin A, et al. Tumor microenvironment-derived proteins dominate the plasma proteome response during breast cancer induction and progression. Cancer Res. 2011;71:5090–100

243. Tokunaga R, Zhang W, Naseem M, Puccini A, Berger MD, Soni S, et al. CXCL9, CXCL10, CXCL11/CXCR3 axis for immune activation – a target for novel cancer therapy. Cancer Treat. Rev. 2018;63:40–7.

244. Bronger H, Singer J, Windmüller C, Reuning U, Zech D, Delbridge C, et al. CXCL9 and CXCL10 predict survival and are regulated by cyclooxygenase inhibition in advanced serous ovarian cancer. Br J Cancer. 2016;115:553–63.

245. Mir MA, Maurer MJ, Ziesmer SC, Slager SL, Habermann T, Macon WR, et al. Elevated serum levels of IL-2R, IL-1RA, and CXCL9 are associated with a poor prognosis in follicular lymphoma. Blood. 2015;125:992–8.

246. Flores RJ, Kelly AJ, Li Y, Nakka M, Barkauskas DA, Krailo M, et al. A novel prognostic model for osteosarcoma using circulating CXCL10 and FLT3LG. Cancer. 2017;123:144–54.

247. Hong JY, Ryu KJ, Lee JY, Park C, Ko YH, Kim WS, et al. Serum level of CXCL10 is associated with inflammatory prognostic biomarkers in patients with diffuse large B-cell lymphoma. Hematol Oncol. 2017;35:480–6.

248. Bai M, Chen X, Ba YI. CXCL10/CXCR3 overexpression as a biomarker of poor prognosis in patients with stage II colorectal cancer. Mol Clin Oncol. 2016;4:23–30.

249. Toiyama Y, Fujikawa H, Kawamura M, Matsushita K, Saigusa S, Tanaka K, et al. Evaluation of CXCL10 as a novel serum marker for predicting liver metastasis and prognosis in colorectal cancer. Int J Oncol. 2012;40:560–6.

250. Specht K, Harbeck N, Smida J, Annecke K, Reich U, Naehrig J, et al. Expression profiling identifies genes that predict recurrence of breast cancer after adjuvant CMF-based chemotherapy. Breast Cancer Res Treat. 2009;118:45–56.

251. K. Au K, Peterson N, Truesdell P, Reid-Schachter G, Khalaj K, Ren R, et al. CXCL10 alters the tumour immune microenvironment and disease progression in a syngeneic murine model of high-grade serous ovarian cancer. Gynecol Oncol. 2017;145:436–45.

252. Redjimi N, Raffin C, Raimbaud I, Pignon P, Matsuzaki J, Odunsi K, et al. CXCR3+ T regulatory cells selectively accumulate in human ovarian carcinomas to limit type I immunity. Cancer Res. 2012;72:4351–60.

253. Sato E, Olson SH, Ahn J, Bundy B, Nishikawa H, Qian F, et al. Intraepithelial CD8+ tumor-infiltrating lymphocytes and a high CD8+/regulatory T cell ratio are associated with favorable prognosis in ovarian cancer. Proc Natl Acad Sci. 2005;102:18538–43.

254. Casrouge A, Decalf J, Ahloulay M, Lababidi C, Mansour H, Vallet-Pichard A, et al. Evidence for an antagonist form of the chemokine CXCL10 in patients chronically infected with HCV. J Clin Invest. 2011;121:308–17.

255. Rainczuk A, Rao JR, Gathercole JL, Fairweather NJ, Chu S, Masadah R, et al. Evidence for the antagonistic form of CXC-motif chemokine CXCL10 in serous epithelial ovarian tumours. Int J Cancer. 2014;134:530–41.

256. Ding Q, Lu P, Xia Y, Ding S, Fan Y, Li X, et al. CXCL9: evidence and contradictions for its role in tumor progression. Cancer Med. 2016;5:3246–59.

257. Peng W, Liu C, Xu C, Lou Y, Chen J, Yang Y, et al. PD-1 blockade enhances T-cell migration to tumors by elevating IFN-γ inducible chemokines. Cancer Res. 2012;72:5209–18.

258. Bedognetti D, Spivey TL, Zhao Y, Uccellini L, Tomei S, Dudley ME, et al. CXCR3/CCR5 pathways in metastatic melanoma patients treated with adoptive therapy and interleukin-2. Br J Cancer. 2013;109:2412–23.

259. Harlin H, Meng Y, Peterson AC, Zha Y, Tretiakova M, Slingluff C, et al. Chemokine expression in melanoma metastases associated with CD8+ T-cell recruitment. Cancer Res. 2009;69:3077–85.

260. Tarhini AA, Lin Y, Lin HM, Vallabhaneni P, Sander C, LaFramboise W, et al. Expression profiles of immune-related genes are associated with neoadjuvant ipilimumab clinical benefit. Oncoimmunology. 2016;6:e1231291.

261. Ayers M, Lunceford J, Nebozhyn M, Murphy E, Loboda A, Kaufman DR, et al. IFN- γ – related mRNA profile predicts clinical response to PD-1 blockade. J Clin Invest. 2017;127:2930–40.

262. Yamazaki N, Kiyohara Y, Uhara H, Iizuka H, Uehara J, Otsuka F, et al. Cytokine biomarkers to predict antitumor responses to nivolumab suggested in a phase 2 study for advanced melanoma. Cancer Sci. 2017;108:1022–31.

263. Choueiri TK, Fishman M, Escudier B, McDermott DF, Drake CG, Kluger HM, et al. Immunomodulatory activity of nivolumab in metastatic renal cell carcinoma. Clin Cancer Res. 2016;1:1–30.

264. Hamanishi J, Mandai M, Konishi I. Immune checkpoint inhibition in ovarian cancer. Int Immunol. 2016;28:339–48.

265. Hamanishi J, Mandai M, Ikeda T, Minami M, Kawaguchi A, Murayama T, et al. Safety and antitumor activity of Anti-PD-1 antibody, nivolumab, in patients with platinum-resistant ovarian cancer. J Clin Oncol. 2015;33:4015–22.

266. Sant M, Allemani C, Santaquilani M, Knijn A, Marchesi F, Capocaccia R, et al. EUROCARE-4. Survival of cancer patients diagnosed in 1995-1999. Results and commentary. Eur J Cancer. 2009;45:931–91.

267. Sant M, Chirlaque Lopez MD, Agresti R, Sánchez Pérez MJ, Holleczek B, Bielska-Lasota M, et al. Survival of women with cancers of breast and genital organs in Europe 1999-2007: results of the EUROCARE-5 study. Eur J Cancer. 2015;51:2191–205.

268. Bowtell DD, Böhm S, Ahmed AA, Aspuria P-J, Bast RC, Beral V, et al. Rethinking ovarian cancer II: reducing mortality from high-grade serous ovarian cancer. Nat Rev Cancer. 2015;15:668–79.

269. Matulonis UA, Sood AK, Fallowfield L, Howitt BE, Sehouli J, Karlan BY. Ovarian cancer. Nat Rev Dis Prim. 2016;2:1–22.

270. Pujade-Lauraine E, Combe P. Recurrent ovarian cancer. Ann Oncol. 2016;27:i63–5.

271. Alvarez RD, Matulonis UA, Herzog TJ, Coleman RL, Monk BJ, Markman M. Moving beyond the platinum sensitive/resistant paradigm for patients with recurrent ovarian cancer. Gynecol Oncol. 2016;141:405–9

272. Wang W, Kryczek I, Dostál L, Lin H, Tan L, Zhao L, et al. Effector T cells abrogate stroma-mediated chemoresistance in ovarian cancer. Cell. 2016;165:1092–105.

273. Xu S, Tao Z, Hai B, Liang H, Shi Y, Wang T, et al. miR-424(322) reverses chemoresistance via T-cell immune response activation by blocking the PD-L1 immune checkpoint. Nat Commun. 2016;7:11406.

274. Rabinovich GA, Gabrilovich D, Sotomayor EM. Immunosuppressive strategies that are mediated by tumor cells. Annu Rev Immunol. 2007;25:267–96.

275. Castells M, Thibault B, Delord JP, Couderc B. Implication of tumor microenvironment in chemoresistance: tumor-associated stromal cells protect tumor cells from cell death. Int J Mol Sci. 2012;13:9545–71.

276. Y Yang W-L, Lu Z, Bast RC. The role of biomarkers in the management of epithelial ovarian cancer. Expert Rev Mol Diagn. 2017;17:577–91.

277. Gevaert O, De Smet F, Van Gorp T, Pochet N, Engelen K, Amant F, et al. Expression profiling to predict the clinical behaviour of ovarian cancer fails independent evaluation. BMC Cancer. 2008;8;18.

278. Helleman J, Jansen MPHM, Span PN, Van Staveren IL, Massuger LFAG, Meijer-Van Gelder ME, et al. Molecular profiling of platinum resistant ovarian cancer. Int J Cancer. 2006;118:1963–71.

279. Gonzalez Bosquet J, Newtson AM, Chung RK, Thiel KW, Ginader T, Goodheart MJ, et al. Prediction of chemo-response in serous ovarian cancer. Mol Cancer. 2016;15:66.

280. Chung RK, Newtson AM, Mott SL, Gonzalez Bosquet J. Clinicopathological predictors of responsiveness in epithelial ovarian cancer: a preliminary institutional study. Proc Obstet Gynecol. 2015;5:6.

281. Masoumi-Moghaddam S, Amini A, Wei A-Q, Robertson G, Morris DL. Vascular endothelial growth factor expression correlates with serum CA125 and represents a useful tool in prediction of refractoriness to platinum-based chemotherapy and ascites formation in epithelial ovarian cancer. Oncotarget. 2015;6:28491–501.

282. Angioli R, Capriglione S, Aloisi A, Guzzo F, Luvero D, Miranda A, et al. Can HE4 predict platinum response during first-line chemotherapy in ovarian cancer? Tumor Biol. 2014;35:7009–15.

283. Chudecka-Głaz A, Cymbaluk-Płoska A, Wężowska M, Menkiszak J. Could HE4 level measurements during first-line chemotherapy predict response to treatment among ovarian cancer patients? PLoS One. 2018;13:e0194270.

284. Pogge von Strandmann E, Reinartz S, Wager U, Müller R. Tumor–host cell interactions in ovarian cancer: pathways to therapy failure. Trends in Cancer. 2017;3:137–48.

285. Senthebane DA, Rowe A, Thomford NE, Shipanga H, Munro D, Al Mazeedi MAM, et al. The role of tumor microenvironment in chemoresistance: to survive, keep your enemies closer. Int J Mol Sci. 2017;18:E1586.

286. de Visser KE, Jonkers J. Towards understanding the role of cancer-associated inflammation in chemoresistance. Curr Pharm Des. 2009;15:1844–53.

287. Szajnik M, Szczepanski MJ, Czystowska M, Elishaev E, Mandapathil M, Nowak-Markwitz E, et al. TLR4 signaling induced by lipopolysaccharide or paclitaxel regulates tumor survival and chemoresistance in ovarian cancer. Oncogene. 2009;28:4353–63.

288. Wang Q, Li D, Zhang W, Tang B, Li QQ, Li L. Evaluation of proteomics-identified CCL18 and CXCL1 as circulating tumor markers for differential diagnosis between ovarian carcinomas and benign pelvic masses. Int J Biol Markers. 2011;26:262–73.

289. Bolitho C, Hahn MA, Baxter RC, Marsh DJ. The chemokine CXCL1 induces proliferation in epithelial ovarian cancer cells by transactivation of the epidermal growth factor receptor. Endocr Relat Cancer. 2010;17:929–40.

290. Scapini P, Morini M, Tecchio C, Minghelli S, Di Carlo E, Tanghetti E, et al. CXCL1/macrophage inflammatory protein-2-induced angiogenesis in vivo is mediated by neutrophil-derived vascular endothelial growth factor-A. J Immunol. 2004;172:5034–40.

291. Acharyya S, Oskarsson T, Vanharanta S, Malladi S, Kim J, Morris PG, et al. A CXCL1 paracrine network links cancer chemoresistance and metastasis. Cell. 2012;150:165–78.

292. Son DS, Kabir SM, Dong Y, Lee E, Adunyah SE. Characteristics of chemokine signatures elicited by EGF and TNF in ovarian cancer cells. J Inflamm. 2013;10:25.

293. Marsigliante S, Vetrugno C, Muscella A. CCL20 induces migration and proliferation on breast epithelial cells. J Cell Physiol. 2013;228:1873–83.

294. Beider K, Abraham M, Begin M, Wald H, Weiss ID, Wald O, et al. Interaction between CXCR4 and CCL20 pathways regulates tumor growth. PLoS One. 2009;4:e5125.

295. Greaves DR, Wang W, Dairaghi DJ, Dieu MC, Saint-Vis B, Franz-Bacon K, et al. CCR6, a CC chemokine receptor that interacts with macrophage inflammatory protein 3-alpha and is highly expressed in human dendritic cells. J Exp Med. 1997;186:837–44.

296. Cook KW, Letley DP, Ingram RJM, Staples E, Skjoldmose H, Atherton JC, et al. CCL20/CCR6-mediated migration of regulatory T cells to the Helicobacter pylori-infected human gastric mucosa. Gut. 2014;63:1550–9.

297. Liu JY, Li F, Wang LP, Chen XF, Wang D, Cao L, et al. CTL- vs Treg lymphocyte-attracting chemokines, CCL4 and CCL20, are strong reciprocal predictive markers for survival of patients with oesophageal squamous cell carcinoma. Br J Cancer. 2015;113:747–55.

298. Zsiros E, Duttagupta P, Dangaj D, Li H, Frank R, Garrabrant T, et al. The ovarian cancer Chemokine landscape is conducive to homing of vaccine-primed and CD3/CD28-Costimulated T cells prepared for adoptive therapy. Clin Cancer Res. 2015;21:2840–50.

APPENDIXES

Appendix 1. Categorized list of genes of interest, together with forward (F) and reverse (R) qPCR primer sequences.

Gene	Protein	Primer sequence
HOUSEKEEPING		
GAPDH	GAPDH	F: AATCCCATCACCATCTTCCA R: TGGACTCCACGACGTACTCA
RLP13A	RLP13A	F: GAGGTATGCTGCCCCACAA R: GTGGGATGCCGTCAAACA
ANGIOGENESIS		
VEGFA	VEGF	F: GGAGGGCAGAATCATCACGAAG R: CACACAGGATGGCTTGAAGATG
KDR	KDR	F: GCAGGGGACAGAGGGACTTG R: GAGGCCATCGCTGCACTCA
ESM1	ESM-1	F: CTTGCTACCGCACAGTCTCA R: GCGTGGATTTAACCATTTCC
PECAM1	PECAM-1	F: CTGCTGACCCTTCTGCTCTGTTC R: GGCAGGCTCTTCATGTCAACACT
FLT1	VEGFR-1	F: TGCCGGGTTACGTCACCTA R: GTCCCAGATTATGCGTTTTCCAT
DRUG RESPONSE		
ABCB1	ABCB1	F: GATCTGTGAACTCTTGTTTTCA R: GAAGAGAGACTTACATTAGGC
ABCC1	ABCC1	F: CGGAAACCATCCACGACCCTAA R: TCATGAGGAAGTAGGGCCCAAA
ABCG2	ABCG2	F: CAGGTGGAGGCAAARCRRCGT R: ACCCTGTTAATCCGTTCGTTTT
ATP7B	ATP7B	F: ATATTGAGCGGTTACAAAGCACT R: TGCCCCAAGGTCTCAGAATTA
BAK1	BAK	F: ATGGTCACCTTACCTCTGCAA R: TCATAGCGTCGGTTGATGTCG
CDKN1A	p21	F: TGTCCGTCAGAACCCATGC R: AAAGTCGAAGTTCCATCGCTC
FDXR	FDXR	F: CAGCATTGGGTATAAGAGCCG R: GGCCTGGCACATCCATAACC
MDM2	MDM2	F: CAGTAGCAGTGAATCTACAGGGA R: CTGATCCAACCAATCACCTGAAT
PCNA	PCNA	F: GCGTGAACCTCACCAGTATGT R: TCTTCGGCCCTTAGTGTAATGAT
EPITHELIAL-MESENCHYMAL TRANSITION		
CDH1	E-cadherin	F: AAGGTGACAGAGCCTCTGGAT R: CGTCTGTGGCTGTGACCT
CDH2	N-cadherin	F: TGCGGTACAGTGTAACTGGG R: GAAACCGGGCTATCTGCTCG

FN1	Fibronectin	F: TACGATGATGGGAAGACATAC R: CTCTGAGAATACTGGTTGTAG
SNAI1	SNAIL	F: ATCGGAAGCCTAACTACAGCGAG R: CTTCCCACTGTCCTCATCTGACA
SNAI2	SLUG	F: TGTTGCAGTGAGGGCAAGAA R: GACCCTGGTTGCTTCAAGGA
TWIST1	TWIST	F: GGAGTCCGCAGTCTTACGAG R: TCTGGAGGACCTGGTAGAGG
VIM	Vimentin	F: TCTACGAGGAGGAGATGCGG R: GTCAAGACGTGCCAGAGAC
ZEB1	ZEB1	F: GCACCTGAAGAGGACCAGAG R: TGCATCTGGTGTTCCATTTT
IMMUNITY		
ARG1	Arginase 1	F: GGCAAGGTGATGGAAGAAAC R: GGCAAGGTGATGGAAGAAAC
CCL1	CCL1	F: AATACCAGCTCCATCTGCTCCA R: GAACCCATCCAACTGTGTCCAAG
CCL2	CCL2	F: CAGCCAGATGCAATCAATGCC R: TGGAATCCTGAACCCACTTCT
CCL3	CCL3	F: CAGAATTTCATAGCTGACTACTTTGAG R: GCTTCGCTTGGTTAGGAAGA
CCL4	CCL4	F: CTTCCTCGCAACTTTGTGGT R: CAGCACAGACTTGCTTGCTT
CCL5	CCL5	F: CCATGAAGGTCTCCGCGGCAC R: CCTAGCTCATCTCCAAAGAG
CCL11	CCL11	F: CCCCTTCAGCGACTAGAGAG R: TCTTGGGGTCGGCACAGAT
CCL17	CCL17	F: GGCTTCTCTGCAGCACATC R: GGAATGGCTCCCTTGAAGTA
CCL20	CCL20	F: TGCTGTACCAAGAGTTTGCTC R: CGCACACAGACAACTTTTTCTTT
CCL22	CCL22	F: ATCGCCTACAGACTGCACTC R: GACGGTAACGGACGTAATCAC
CD4	CD4	F: TGCCTCAGTATGCTGGCTCT R: GAGACCTTTGCCTCCTTGTTC
CD8A	CD8	F: ACTTGTGGGGTCCTTCTCCT R: GTCTCCCGATTTGACCACAG
CD27	CD27	F: AGGGACAAGGAGTGCACCGAGT R: TGCTTCCCACTCTCCACCTCATC
CD40L	CD40L	F: CTGCAAGGTGACACTGTTC R: CACAGCATGATCGAAACATAC
CD68	CD68	F: TGGGGCAGAGCTTCAGTTG R: TGGGGCAGGAGAAACTTTGC
CD86	CD86	F: CTGCTCATCTATACACGGTTACC R: GGAAACGTCGTACAGTTCTGTG
CD163	CD163	F: CGAGTTAACGCCAGTAAGG R: GAACATGTCACGCCAGC
CD274	CD274	F: TATGGTGGTGCCGACTACAA R: TGGCTCCCAGAATTACCAAG
CLEC7A	Dectin	F: TCTTTCCAGCCCTTGTCCTC R: CCAGTTGCCAGCATTGTCTT
CSF2	GM-CSF	F: CACTGCTGCTGAGATGAATGAAA R: GTCTGTAGGCAGGTCGGCTC
CSF3	G-CSF	F: CCTGGAGCTGAGAACTACCG R: TCCCGGCTGAGTTATAGG

CTLA4	CTLA-4	F: TGCAGCAGTTAGTTCGGGGTTGTT R: CTGGCTCTGTTGGGGGCATTTTC
CXCL1	CXCL1	F: GCCAGTGCTTGCAGACCCT R: GGCTATGACTTCGGTTTGGG
CXCL5	CXCL5	F: AGCTGCGTTGCGTTTGTTTAC R: TGGCGAACACTTGCAGATTAC
CXCL8	IL-8	F: ATAAAGACATACTCCAAACCTTTCCAC R: AAGCTTTACAATAATTTCTGTGTTGGC
CXCL9	CXCL9	F: CCAGTAGTGAGAAAGGGTCGC R: AGGGCTTGGGGCAAATTGTT
CXCL10	CXCL10	F: AAGGATGGACCACACAGAGG R: ACCCTTGGAAGATGGGAAAG
CXCL11	CXCL11	F: ATGAGTGTGAAGGGCATGGC R: TCACTGCTTTTACCCCAGGG
EOMES	EOMES	F: AGCTCTCCAAGGAGAAAGTG R: GCCTTCGCTTACAAGCACTG
FCGR2A	CD32	F: TTTGAGATGAGTAATCCCAGCCA R: TCAGGCCCAGTCTCCATTTTA
FOXP3	FOXP3	F: GAACGCCATCCGCCACAACCTGA R: CCCTGCCCCCACCACCTCTGC
GZMB	Granzyme B	F: GAAACGCTACTAACTACAGG R: CCACTCAGCTAAGAGGT
HLA-DRA	MHC II	F: CAGGGATCCGCAGAGAATTAC R: GTCCTGCAGTCACTCACCTCGGCG
ICAM1	ICAM-1	F: GGCCGGCCAGCTTATACAC R: TAGACACTTGAGCTCGGGCA
IDO1	IDO	F: GGCAAAGGTCATGGAGATGT R: CAGGACGTCAAAGCACTGAA
IFNG	IFNγ	F: TGGAAAGAGGAGAGTGACAGAA R: TCTTTTGGATGCTCTGGTCAT
IL1A	IL-1α	F: AGTAGCAACCAACGGGAAGG R: TGGTTGGTCTTCATCTTGGG
IL1B	IL-1β	F: ATGATGGCTTATTACAGTGGCAA R: GTCGGAGATTCGTAGCTGGA
IL6	IL-6	F: GTAGCCGCCCCACACAGA R: CATGTCTCCTTTCTCAGGGCTG
IL10	IL-10	F: GACTTTAAGGGTTACCTGGGTTG R: TCACATGCGCCTTGATGTCTG
IL18	IL-18	F: GCTTGAATCTAAATTATCAGTC R: CAAATTGCATCTTATTATCATG
NOS2	iNOS	F: ACAAGCTGGCCTCGCTCTGGAAAGA R: TCCATGCAGACAACCTTGGGGTTGAAG
MARCO	MARCO	F: CTGGTGGTCCAAGTTCTGAATCT R: TCAGCCGCCAGAGTGTCA
MRC1	CD206	F: CCTCTGGTGAACGGAATGAT R: AGGCCAGCACCCGTTAAAAT
PDCD1	PD-1	F: ACCCTGGTCATTCACTTGGG R: CATTTGCTCCCTCTGACACTG
PRF1	Perforin	F: CGCCTACCTCAGGCTTATCTC R: CCTCGACAGTCAGGCAGTC
PSMB9	PSMB9	F: GCACCAACCGGGGACTTAC R: CACTCGGGAATCAGAACCCAT
PTGS2	COX2	F: CTGGCGCTCAGCCATACAG R: CGCACTTATACTGGTCAAATCCC
SERPINE1	PAI-1	F: TGCTGGTGAATGCCCTCTACT R: CGGTCATTCCCAGGTTCTCTA
STAT1	STAT1	F: AACAGAAAAATGCTGGCACC R: AGAGGTCGTCTCGAGGTCAA

TAP1	TAP1	F: TGCCCCGCATATTCTCCCT R: CACCTGCGTTTTCGCTCTTG
TAP2	TAP2	F: TGGACGCGGCTTTACTGTG R: GCAGCCCTCTTAGCTTTAGCA
TIGIT	TIGIT	F: TCTGCATCTATCACACCTACC R: CCACCACGATGACTGCTGT
TNF	TNFα	F: CCTCTCTCTAATCAGCCCTCTG R: GAGGACCTGGGAGTAGATGAG
REACTIVE STROMA		
MS4A4A	MS4A4	F: ACCATGCAAGGAATGGAACAG R: TTCCCATGCTAAGGCTCATCA
FAP	FAP	F: TGAACGAGTATGTTTGCAGTGG R: GGTCTTTGGACAATCCCATGT
LOXL1	LOXL	F: CCACTACGACCTACTGGATGC R: GTTGCCGAAGTCACAGGTG
COL5A1	Collagen V	F: GCCCGGATGTCGCTTACAG R: AAATGCAGACGCAGGGTACAG
MMP9	MMP9	F: AGACCTGGGCAGATTCCAAAC R: CGGCAAGTCTTCCGAGTAGT
MMP3	MMP3	F: CTGGACTCCGACACTCTGGA R: CAGGAAAGGTTCTGAAGTGACC
POSTN	Periostin	F: GCTATTCTGACGCCTCAAAACT R: AGCCTCATTACTCGGTGCAAA
TDO2	TDO	F: AAGGTTGTTTCTCGGATGCAC R: TGTCATCGTCTCCAGAATGGAA
STEMNESS		
AFP	AFP	F: AGTGAGGACAAACTATTGGCCT R: ACACCAGGGTTTACTGGAGTC
CTNNB	β-catenin	F: TGGATGGGCTGCCTCCAGGTGAC R: ACCAGCCCACCCCTCGAGCCC
FOXA2	Forkhead box A2	F: CTTCAAGCACCTGCAGATTC R: AGACCTGGATTTCACCGTGT
NANOG	NANOG	F: ACCAGAACTGTGTTCTCTTCCACC R: CCATTGCTATTCTTCGGCCAGTTG
NOTCH1	NOTCH1	F: TTGCTGCTGGTCATTCTCG R: TCCTCTTCAGTTGGCATTGG
OTX2	OTX2	F: GACCACTTCGGGTATGGACT R: TGGACAAGGGATCTGACAGT
POU5F1	OCT3/4	F: AGCAAAACCCGGAGGAGT R: CCACATCGGCCTGTGTATATC
ROR1	ROR1	F: CAACAAGAAGCCTCCCTAATGG R: CCTGAGTGACGGCACCTAGAA
SOX2	SOX-2	F: TTGCTGCCTCTTTAAGACTAGGA R: CTGGGGCTCAAACTTCTCTC

Appendix 2. List of antibodies used for flow cytometry. All antibodies were mouse anti-human.

Antigen	Fluorochrome	Manufacturer	Catalog no.	Dilution
CD3	AF488	BD Bioscienes	557694	1:10
CD4	BV510	BD Biosciences	562970	1:10
CD14	V450	BD Biosciences	560349	1:20
CD11c	APC-Cy7	BioLegend	337217	1:100
CD25	PE-Cy7	BD Biosciences	557741	1:10
CD68	APC	BioLegend	333810	1:200
CD69	PE	Santa Cruz	sc-18880	1:100
CD80	FITC	BD Biosciences	557226	1:10
CD80	V450	BD Biosciences	560444	1:20
CD83	BV510	BD Biosciences	563223	1:20
CD85k	APC	BioLegend	333015	1:100
CD86	FITC	EXBIO	1F-531-T025	1:10
CD127	BV421	BioLegend	562436	1:100
CD195	APC	BD Biosciences	550856	1:20
CD197	PE-Cy7	BD Biosciences	557648	1:10
CD197	AF647	BioLegend	353418	1:200
CD206	BV421	BioLegend	321126	1:200
CD274	PE	BD Biosciences	557924	1:20
FoxP3	APC	eBiosciences	77-5774-40	1:10
HLA-DR	APC	BioLegend	307610	1:400